Saturated Boundary Stabilization of Partial Differential Equations Using Control-Lyapunov Functions

Hugo Lhachemi, Christophe Prieur

Chapter 1

Saturated boundary stabilization of partial differential equations using control-Lyapunov functions

Hugo Lhachemi

Université Paris-Saclay, CNRS, CentraleSupélec, Laboratoire des signaux et systèmes, 91190, Gif-sur-Yvette, France
hugo.lhachemi@centralesupelec.fr

Christophe Prieur*

Université Grenoble Alpes, CNRS, Grenoble-INP, GIPSA-lab, F-38000, Grenoble, France
christophe.prieur@gipsa-lab.fr

This chapter reviews some recent results on the boundary stabilization of different classes of partial differential equations. In order to provide a self-content chapter with consistent control objectives and notation, we first review the finite-dimensional case. Controllability and observability conditions for linear ordinary differential equations are recalled together with some basic Lyapunov theory for the stability analysis and the design of saturated controllers. Then we address the boundary control problem for the stabilization of a reaction-diffusion equation by means of numerically tractable design methods while considering different norms and possible constraints on the amplitude of the inputs. Finally similar control design problems will be studied for the stabilization of the Korteweg–de-Vries equation and the wave equation.

*This work has been partially supported by MIAI@Grenoble Alpes (ANR-19-P3IA-0003).

1. Introduction

The goal of this chapter is to review some recent results on boundary stabilization of distributed parameter systems as those modeled by parabolic partial differential equations or hyperbolic partial differential equations. No prerequisite on control theory will be necessary, only basic knowledge on control objectives. However, background in nonlinear dynamical systems and essentials on partial differential equations (PDEs) would be helpful, even if some references will be given throughout the text.

The topics covered in this chapter embrace different potential applications such as control and stability theory of reaction-diffusion phenomenon as those modeled by parabolic PDEs. Some control techniques presented in this chapter will be useful for stability theory of physical dynamics described by balance laws and modeled by hyperbolic partial differential equation. Different control objectives will be studied and solved such as the design of stabilizing control laws ensuring that all the trajectories of the closed-loop systems converge to a given equilibrium. Different control schemes are considered, covering in-domain control (the control input appears directly in the main part of the PDE) and boundary control (the control input applies at the boundary of the domain as it appears through the boundary conditions). Moreover, when possible, the described control laws will be designed based on the only knowledge of a prescribed and limited part of the state, the so-called output.

For each of the different numerical illustrations reported in this chapter, the Python code of the numerical simulations is provided, allowing the readers to easily modify the control objectives and further experience the control theory of the considered dynamical systems.

The outline of this chapter is as follows. First finite-dimensional control systems will be considered and some basic definitions will be given on stability, attractivity, etc., providing a sharp introduction to basics of control systems theory. Then in Section 3, parabolic PDEs are considered for the design of finite-dimensional output-feedback controllers towards saturated control schemes. Section 4 is devoted to the wave and Korteweg–de-Vries equation, and the use of finite-dimensional controllers to solve the stabilization problems. In these both sections, linear feedback laws and also cone-bounded controllers are designed. Section 5 contains a concluding discussion on current research activities and presents some possible research directions emanating from this chapter.

This chapter has been written following an online course given in

LIASFMA school by the second author in April 2021. We would like to thank the Organizing Committee of this school that was composed of Jean-Michel Coron (Sorbonne Université), Tatsien Li (Fudan University), and Zhiqiang Wang (Fudan University). The help of Xinyue Feng has been very much appreciated.

Notation used in this chapter

Spaces $\mathbb{R}^n$ are endowed with the Euclidean norm denoted by $\|\cdot\|$. The associated induced norms of matrices are also denoted by $\|\cdot\|$. Given two vectors X and Y, $\mathrm{col}(X,Y)$ denotes the vector $[X^\top, Y^\top]^\top$. $L^2(0,1)$ stands for the space of square integrable functions on $(0,1)$ and is endowed with the inner product $\langle f, g\rangle = \int_0^1 f(x)g(x)\,\mathrm{d}x$ with associated norm denoted by $\|\cdot\|_{L^2}$. For an integer $m \geq 1$, the m-order Sobolev space is denoted by $H^m(0,1)$ and is endowed with its usual norm denoted by $\|\cdot\|_{H^m}$. For a symmetric matrix $P \in \mathbb{R}^{n\times n}$, $P \succeq 0$ (resp. $P \succ 0$) means that P is positive semi-definite (resp. positive definite) while $\lambda_M(P)$ (resp. $\lambda_m(P)$) denotes its maximal (resp. minimal) eigenvalue. For a symmetric matrix, $\star$ stands for the symmetric term. For instance, $\begin{bmatrix} A & B \\ \star & C \end{bmatrix}$ stands for $\begin{bmatrix} A & B \\ B^\top & C \end{bmatrix}$.

For any Hilbert basis $\{\phi_n,\ n \geq 1\}$ of $L^2(0,1)$ and any integers $1 \leq N < M$, we define the operators of projection $\pi_N : L^2(0,1) \to \mathbb{R}^N$ and $\pi_{N,M} : L^2(0,1) \to \mathbb{R}^{M-N}$ by setting $\pi_N f = \big[\langle f,\phi_1\rangle \dots \langle f,\phi_N\rangle\big]^\top$ and $\pi_{N,M} f = \big[\langle f,\phi_{N+1}\rangle \dots \langle f,\phi_M\rangle\big]^\top$. We also define $\mathcal{R}_N : L^2(0,1) \to L^2(0,1)$ by $\mathcal{R}_N f = f - \sum_{n=1}^N \langle f,\phi_n\rangle\,\phi_n = \sum_{n\geq N+1} \langle f,\phi_n\rangle\,\phi_n$.

2. Finite-dimensional systems

2.1. *Stability notions of nonlinear finite-dimensional systems*

This section is devoted to the introduction of control theory for finite-dimensional systems, as those described by nonlinear dynamics. To be more specific, let us consider the following dynamical system:

$$\dot{z}(t) = f(z(t)) \tag{1}$$

where the state $z(t)$ is a vector from a finite-dimensional state-space $\mathbb{R}^n$ and f is a nonlinear function from $\mathbb{R}^n$ to $\mathbb{R}^n$. Under suitable regularity assumptions, such as locally Lipchitz continuity of f with respect to z, for any given initial condition $z_0 \in \mathbb{R}^n$ there exists a unique solution $x : [0, T) \to \mathbb{R}^n$ to the Cauchy problem:

$$\begin{aligned} &\dot{z}(t) = f(z(t)), \quad t > 0 \\ &z(0) = z_0 \end{aligned} \tag{2}$$

defined on a maximal interval of existence $[0, T)$ for some $T > 0$ (which depends on z_0). See e.g. [30, Theorem 3.1] for such a existence and uniqueness result. The value z_0 is called the initial condition and, at any time $t \in [0, T)$, the value $z(t)$ is called the state at time t.

Assume further that $f(0) = 0$. This implies that the constant trajectory $z(t) = 0$, for all $t \geq 0$, is a particular solution to (1) associated with the initial condition $z_0 = 0$. The point $0 \in \mathbb{R}^n$, sometimes referred to as the origin, is called an equilibrium for (1). In control theory, the nature of an equilibrium is characterized by certain "stability" properties. Some basic definitions related to the concept of "stability" are introduced in the following definition.

Definition 1. Assume that $f(0) = 0$. Then the equilibrium 0 of (1) is said to be

- $s$table if for any $\varepsilon > 0$, there exists $\delta > 0$ such that
$$|z(0)| \leq \delta \Rightarrow |z(t)| \leq \varepsilon \ , \ \forall t \geq 0 \ .$$
- $a$ttractive if there exists $\delta > 0$ such that
$$|z(0)| \leq \delta \Rightarrow z(t) \to_{t \to +\infty} 0 \ .$$
- $a$symptotically stable if it is both stable and attractive.

In the previous definition, it is implicitly required that the solutions exist, are unique, and are well defined for all $t \geq 0$. Even implicit, these requirements are of primary importance. Some of them can be difficult to check in practice depending upon the nature of the studied system.

Assuming that 0 is an attractive equilibrium of (1), an important concept is the notion of *basin of attraction*. This is defined as the set of all initial conditions $z_0 \in \mathbb{R}^n$ such that the solution to (2) tends to 0 as $t \to \infty$. In addition, we say that the equilibrium is *globally attractive* if it is attractive and the basin of attraction coincides with the whole state-space $\mathbb{R}^n$. When 0 is not globally attractive, we often write that 0 is *locally asymptotically stable* (LAS) to emphasize the "local" nature of the property. Finally, we say that 0 is *globally asymptotically stable* (GAS) if it is asymptotically stable and globally attractive. It is worth being noted that the notions of attractivity and stability are disconnected. More specifically, there exist systems for which 0 is stable but not attractive (the most simple example being $\dot{z} = 0$) while there are also systems such that 0 is attractive but not stable (see for instance the example of [24, Paragraph 40]).

Instead of (1), let us now consider the case where the dynamics depends on an external signal, called the *control* or the *input*. More specifically, consider the dynamics described by

$$\dot{z}(t) = f(z(t), u(t)) \tag{3}$$

where $u(t)$ is a vector of $\mathbb{R}^m$. The input u is seen as a way to influence the dynamics of the system, which can significantly vary depending on the choice of the control. As an example, consider the following control system described by

$$\dot{z}(t) = u(t)z(t) \tag{4}$$

with $u(t) \in \mathbb{R}$. If $u(t) = u \in \mathbb{R}$ is constant control, the trajectories of the system stating at time $t = 0$ from the initial condition $z_0 \in \mathbb{R}^n$ can be expressed as $z(t) = e^{ut}z_0$ for all $t \geq 0$. For $u = -1$ (more generally for any constant control $u < 0$), the equilibrium 0 is globally asymptotically stable. For $u = 0$, any point of $\mathbb{R}^n$ is an equilibrium (they are stable but not attractive). For $u = 1$ (more generally for any constant control $u > 0$), all solutions to (4) with non zero initial condition $z_0 \neq 0$ diverges to infinity (the equilibrium 0 is neither stable nor attractive).

In the more general setting of a time-varying control, i.e., $u = u(t)$ for a suitable function u of the time, (3) is a time-varying system. This implies that the solution starting from an initial condition z_0 at time t_0 differs, in

general, from the trajectory starting from the same initial condition z_0 but at a different time $t_1 \neq t_0$. The behavior of these different solutions can be very different.

Assuming that f in (1) is linear, the system dynamics reduces to

$$\dot{z}(t) = Az(t) \tag{5}$$

where A is a matrix in $\mathbb{R}^{n\times n}$. In this case, the stability of the origin is intimately related to the position of the eigenvalues of the matrix A in the complex plane (see [26, theorem 6.1]). More specifically, it can be proven that the origin of (5) is stable if and only if (i) all eigenvalues of A have a non-positive real part and (ii) for all eigenvalues with a zero real part, their algebraic multiplicity (exponent associated with the eigenvalue when computing the characteristic polynomial) coincides with their geometric multiplicity[a] (dimension of the eigenspace associated with the eigenvalue). Moreover, the origin of (5) is asymptotically stable if and only if all eigenvalues of A have a negative real part. In that case we say that the matrix A is Hurwitz. Finally, for such linear systems, the attractivity of the origin of (5) implies that the origin is stable and also asymptotically stable.

In this lecture notes, we will first study finite-dimensional control systems, and then dynamical control systems described by linear partial differential equations (PDEs) for which some nonlinear control problems will be solved.

2.2. *Control systems: a basic tour*

We focus in the the first part of this section on systems described by

$$\dot{z} = Az + Bu \tag{6}$$

where $z \in \mathbb{R}^n$ is the state, $u \in \mathbb{R}^m$ is the control, A, B are two matrices of appropriate dimensions. One natural question is the design of a so-called stabilizing state feedback law. That is, can we compute state-feedback law $z \mapsto u(z)$ so that the resulting closed-loop system

$$\dot{z} = Az + Bu(z) \tag{7}$$

is asymptotically stable? In this context, due to the linearity of the system, it is natural to try to determine a state-feedback law $z \mapsto u(z)$ that is also linear, i.e., which tales the form $u = Kz$ where K is a matrix that is referred

[a]Condition (ii) is crucial as it can be seen by considering the case $A = \begin{bmatrix} 0 & 1 \\ 0 & 0 \end{bmatrix}$

to as the feedback gain. In this setting, the closed-loop system dynamics reads

$$\dot{z} = (A + BK)z \tag{8}$$

Consequently the stability properties of the closed-loop system are fully characterized by the spectrum of the closed-loop matrix $A + BK$. The question is: can we compute a matrix K in order to impose the spectrum of $A + BK$ to ensure stability properties for the closed-loop system?

For linear finite-dimensional systems, the control theory is complete and the design of stabilizing state feeback laws is fully solved.[1,26] More specifically, assuming the following *Kalman rank condition* (for controllability)

$$\operatorname{rank}\left[B,\ AB, \ldots,\ A^{n-1}B\right] = n\ ,$$

there exists a matrix K so that $u(z) = Kz$ makes the system (7) asymptotically stable. Furthermore, the matrix gain K can be selected to impose any arbitrary spectrum assignment for the closed-loop matrix $A + BK$. This result is not only an existence result, but it is also a practical design method. Indeed, it is the base of efficient numerical algorithms to compute the control matrix K. This is the so-called pole-shifting theorem (see[73] for an existence result and[71] for a constructive algorithm), which is stated in the next result.

Theorem 1. *Under the Kalman rank condition assumption, for any polynomial* Π *of degree* n *and with unit dominant coefficient, there exists a matrix* K *such that the characteristic polynomial of* $A + BK$ *is* Π.

With the previous result, computing a matrix K so that the linear state feedback law $z \mapsto Kz$ renders the origin of the closed-loop system (8) asymptotically stable is numerically tractable.

Example 1. Let us see how to solve this control problem in practice using the programming language Python. In the next lines, with dimension $n = 3$, first a randomly chosen control system is selected (lines 7-8), the controllability condition is checked and a pole-placement controller is computed using the *Python Control Systems Library* (lines 10-18). Then the differential equation is integrated numerically and the phase-portrait of the solution is plotted (lines 27-33). This givea Figure 1 where it can be checked that a solution converges to the equilibrium 0 in $\mathbb{R}^3$.

```
1 import numpy as np
2 import control
3 from scipy.integrate import odeint
```

```
import matplotlib as mpl
import matplotlib.pyplot as plt

n= 3 # dimension of the state space
A= np.random.random([n,n])
B= np.random.random([n,1])
CtrbMatrix= control.ctrb(A,B) # compute the controlability
    matrix

if np.linalg.matrix_rank(CtrbMatrix)== n:
    print('controllable system')
else:
    print('uncontrollable system')

p= np.linspace(-n,-1,n) # choice of the eigenvalues of the
    closed-loop system
K=-control.place(A,B,p)

def ode(z,t):
    return np.dot((A+np.dot(B,K)),z)

z0=np.random.random([n,1]); z0=z0.reshape(n,)
t=np.linspace(0,10,1000)
sol=odeint(ode,z0,t)

if n==3: # plot3D
    from mpl_toolkits.mplot3d import Axes3D
    mpl.rcParams['legend.fontsize'] = 10
    fig = plt.figure(); ax = fig.gca(projection='3d')
    x, y, z =sol.T
    ax.plot(x, y, z, label='solution'); ax.legend()
    plt.savefig('solution.png',bbox_inches='tight')
```

We repeat the same procedure for 10 randomly chosen initial conditions. See the lines 35-41 of the code and the corresponding Figure 1.

```
fig = plt.figure(); ax = fig.gca(projection='3d')
for i in range(10):
    z0=np.random.random([n,1]); z0=z0.reshape(n,)
    sol=odeint(ode,z0,t)
    x, y, z =sol.T
    ax.plot(x, y, z, label='solution'+str(i));
ax.legend()

plt.savefig('solutions.png',bbox_inches='tight')
```

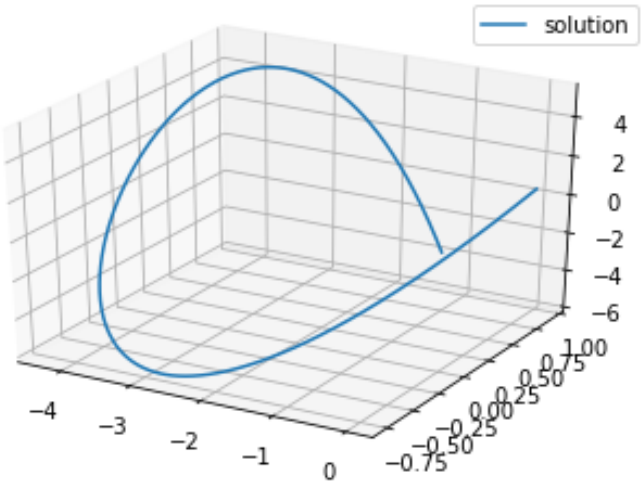

Fig. 1. Time-evolution of a particular solution to (7) with $u = Kz$

2.3. *Lyapunov direct method*

The first part of this section was devoted to linear systems for which the situation is relatively simple as the stability of the origin is fully characterized by the spectrum of the matrix A. When considering general nonlinear systems such as (1), the situations becomes much more complex. Here we need tools that allow studying the stability properties of an equilibrium condition without being able to write down the system trajectories in closed form (in general, very few nonlinear systems can be analytically integrated to obtain the closed form of the trajectories). In this context, an important tool to prove the attractivity of the equilibrium is the so-called *Direct Lyapunov method* which relies on the concept of *Lyapunov functions*. To explain this method, let us come back to the nonlinear system described by (1). The so-called Lyapunov stability theorem can be stated as follows (see [30, Theorem 4.1] for a proof.)

Theorem 2. *Assume that* $f(0) = 0$ *and let* D *be an open and connected subset of* $\mathbb{R}^n$ *containing* 0. *Assume that* $V : D \to \mathbb{R}$ *is a* $\mathcal{C}^1$ *function such that*

$$V(0) = 0 \text{ and } V(z) > 0 \ , \ \forall z \in D \setminus \{0\}$$
$$\tfrac{\partial V}{\partial z}(z) \cdot f(z) \leq 0 \ , \ \forall z \in D \ .$$

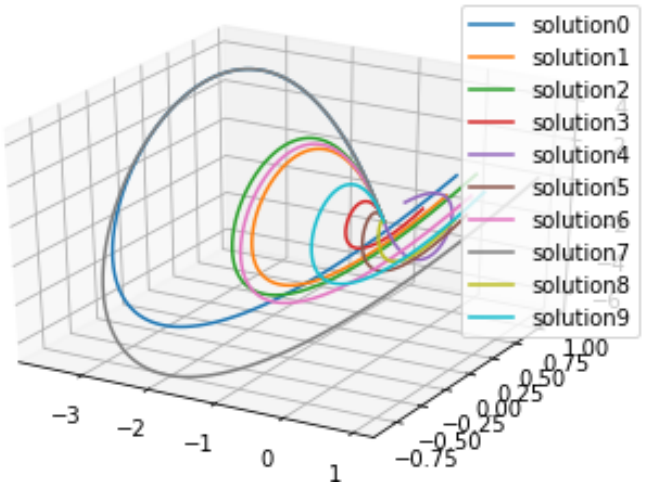

Fig. 2. Time-evolution of solutions to (7) with $u = Kz$ for 10 randomly chosen initial conditions

Then $z = 0$ is stable. Moreover, if we have

$$\frac{\partial V}{\partial z}(z) \cdot f(z) < 0 \ , \ \forall z \in D \setminus \{0\} \ ,$$

then $z = 0$ is locally asymptotically stable.

We often denote

$$\dot{V} = \frac{\partial V}{\partial z}(z) \cdot f(z)$$

since $\frac{\partial V}{\partial z}(z(t)) \cdot f(z(t))$ is the time-derivative of $V(z(t))$ along the solutions to (1).

If the Lyapunov theorem applies with the domain D specified as

$$D = \{z, \ V(z) < r\}$$

for some given $r > 0$, then the level set $\{z, \ V(z) < r\}$ is contained in the basin of attraction. Hence V can be used in order to estimate the basin of attraction while trying to maximize the value of $r > 0$ such that Theorem 2 applies with $D = \{z, \ V(z) < r\}$.

It is worth noting that, for finite-dimensional systems as the ones that are considered in this section, all norms are equivalent and, somehow, V is "equivalent" to any norm (say, e.g., the Euclidian norm). Thus establishing a stability by considering a particular norm is actually the same as

establishing a stability by considering any other norm. Such an equivalence fails in infinite-dimension, which will be the topic of the next sections.

As we saw, Lyapunov functions are very convenient to prove asymptotic stability since all we need is to consider a suitable Lyapunov function candidate $V : D \to \mathbb{R}$, that is a $\mathcal{C}^1$ function such that

$$V(0) = 0 \text{ and } V(z) > 0 \ , \ \forall z \in D \setminus \{0\}$$

and then compute the following vectors in $\mathbb{R}^n$:

$$\frac{\partial V}{\partial z}(z) \cdot f(z) \ , \ \forall z \in D \setminus \{0\} \ .$$

and evaluate its sign. Obviously, finding such functions V highly depends on the nature of the studied nonlinear system and can be very complex in practice. Some basic techniques for finding such functions will be reviewed in this notes, as well as associated numerically tractable methods.

In the context of linear systems as described by (5), the Lyapunov theorem is rewritten as follows. Using the Lyapunov function candidate $V(z) = z^\top P z$ for some symmetric positive definite matrix P, and computing its time derivative along the system trajectories, the origin of (5) is asymptotically stable if and only if there exists such a symmetric positive definite matrix P such that

$$A^\top P + P A^\top \preceq -I$$

Let us emphasize the "if and only if" condition from the previous statement, as well as the class of quadratic function $V(z) = z^\top P z$ as sufficient Lyapunov function candidates. In other words, for linear systems, there is not need to consider other class of Lyapunov function candidates. This result is one of so-called *converse Lyapunov theorems*. Such converse results of the direct method also exist for nonlinear systems under certain regularity conditions on the function f (see e.g. [2, Theorem 2.4]). Note however that converse Lyapunov theorems can hardly be applied to actually find Lyapunov function candidates since these converse results are generally not constructive (even if some design methods exist as reviewed in particular in the references[14,63]).

Example 2. (Example 1 continued) In this extension of Example 1, we compute the eigenvalues of the previous closed-loop system (see line 45) and we compute a Lyapunov matrix P.

```
45 AA=A+np.dot(B,K); e, v= np.linalg.eig(AA) # eigen-values, -
       vectors
46 m=max(e.real)
```

```
print('Largest real part for the closed-loop system:',"{:.2f}".
    format(m))

P=control.lyap(AA.T,np.eye(n))
```

2.4. *Separation principle for linear systems*

Up to now we only considered the control problem of dynamical systems such as the ones described by (3). In this context, we made the implicit assumption that the full state $z(t)$ is known in real time at any time $t \geq 0$ so that we can use this information to implement the control law $z \mapsto u(z)$. We say that this control strategy takes the form of a state-feedback. However in many applications the full state is not available in real-time. Only partial information are available under the form of sensor measurements $y(t) \in \mathbb{R}^p$ which are somehow related to the state $x(t) \in \mathbb{R}^n$ of the system. For control linear system described by (6), the relation between the output y and the state x generally takes the form:

$$y = Cz \tag{9}$$

where C is a matrix of appropriate dimensions. We say that y is the output of the system. This output represents the measurements that are assumed to be available at each time instant. In this context, a natural question is whether the knowledge of the system (i.e., the matrices A, B, and C), of the control $u(t)$, and of the measurements $y(t)$, is sufficient to asymptotically estimate the state $z(t)$. This problem is a so-called observation problem. For linear systems, this problem is also fully solved and is strongly connected to the so-called *Kalman rank condition for observability*, which is written as

$$\operatorname{rank} \begin{bmatrix} C \\ \vdots \\ CA \\ CA^{n-1} \end{bmatrix} = n.$$

Note that this assumption is equivalent to the controllability of the pair $(A^\top, C^\top)$. This is why observability and controllability properties are said to be dual properties.

Consider now the dynamics described by

$$\dot{\hat{z}} = A\hat{z} + Bu + L(C\hat{z} - y) \tag{10}$$

where L is a matrix with suitable dimensions. We say that (10) is an observer for (6). The observer mimics the dynamics of the system (6) while

adding an extra term used to correct the dynamics of the observation in function of the error between the actual measurement $y(t)$ and its estimation $\hat{y}(t) = C\hat{x}(t)$ obtained from the observer. Introducing the error of observation $e = z - \hat{z}$, this error satisfies the dynamics described by

$$\dot{e} = (A + LC)e. \tag{11}$$

Under the abovementionned observability assumption, there exists a matrix L so that $A + LC$ is Hurwitz. Selecting this way the observer gain L, the origin of (11) is asymptotically stable, meaning that the observation error $e(t) = z(t) - \hat{z}(t)$ asymptotically converges to zero. In other words, the state of the observer $\hat{z}(t)$ "asymptotically observes" the actual (unmeasured) stated of the system $z(t)$. We say that (10) is an observer for (6).

So far, we detailed (i) how an state feedback $u = Kz$ can be designed to stabilize the linear system (6) and (ii) how an observer of the form (10) can be designed in order to compute $\hat{z}$ an estimate of the state z of the system (6) from its outputs y given by (9). A natural question is whether we can reunite these two approaches to obtain a stabilizing output feedback. In other words, under the controllability assumption of (A, B) and the observability assumption of (A, C), can we separately design a feedback gain K and an observer gain L so that the origin of the system (6) in closed-loop with $u = K\hat{z}$ where the dynamics of $\hat{z}$ is given by (10) is asymptotically stable? The answer to this question is positive and is referred to as the *separatation principle* for linear finite-dimensional systems.

Theorem 3. *Let us consider the dynamics:*

$$\begin{aligned} \dot{z} &= Az + Bu \\ y &= Cz \end{aligned} \tag{12}$$

where $z \in \mathbb{R}^n$, $y \in \mathbb{R}^p$ and A, B, C are matrices with suitable dimensions. Assume that the pair (A, B) is controllable and the pair (A, C) is observable. Then for any matrices K and L such that $A+BK$ and $A+LC$ are Hurwitz, the equilibrium $(0, 0)$ of

$$\begin{aligned} \dot{z} &= Az + BK\hat{z} \\ \dot{\hat{z}} &= (A + BK)\hat{z} + L(C\hat{z} - y) \end{aligned} \tag{13}$$

is asymptotically stable.

This theorem provides a design method for a stabilizing dynamic output feedback controller whose architecture is described by

$$\begin{aligned} \dot{\hat{z}} &= A\hat{z} + Bu + L(C\hat{z} - y) \\ u &= K\hat{z} \end{aligned}$$

Proof of Theorem 3. For proving Theorem 3, it is convenient not to study the asymptotic stability of the origin of (13) in the coordinates $(z, \hat{z})$, but rather in the coordinates $(\hat{z}, e)$ which give

$$\begin{aligned} \dot{\hat{z}} &= (A + BK)\hat{z} + L(y - C\hat{z}) \\ \dot{e} &= (A + LC)e \end{aligned} \tag{14}$$

Since $A + LC$ is Hurwitz, there exists a symmetric positive definite matrix Q such that

$$(A + LC)^\top Q + Q(A + LC)^\top \preceq -I \tag{15}$$

and so $W(e) = e^\top Qe$ satisfies

$$\dot{W} \leq -e^\top e$$

along the trajectories of $\dot{e} = (A + LC)e$. Hence the e-component of (14) converges to 0 as time goes to $+\infty$. Now pick a symmetric positive definite matrix P such that

$$(A + BK)^\top P + P(A + BK)^\top \preceq -I. \tag{16}$$

Letting $V(\hat{z}) = \hat{z}^\top P\hat{z}$ we have

$$\dot{W} \leq -\hat{z}^\top \hat{z} + 2\hat{z}LCe$$

along the trajectories of $\dot{\hat{z}} = A\hat{z} + BK\hat{z} + L(y - C\hat{z})$. Invoking now Young inequality and the fact that $e(t) \to 0$ gives that $\hat{z}(t)$ goes to 0 as well when time goes to $+\infty$. Therefore, the origin of the linear system (14) is attractive and thus asymptotically stable.

Note that another proof of the asymptotic stability of the origin of (14) is based on proving that $V + 4\|PLC\|^2 W$ is actually a Lyapunov function. To do that denote $\mathcal{V}(\hat{z}, e) = V(\hat{z}) + 4\|PLC\|^2 W(e)$ and compute the time derivative of $\mathcal{V}$ along the solutions to (14):

$$\begin{aligned} \dot{\mathcal{V}} &= \hat{z}^\top((A + BK)^\top P + P(A + BK))\hat{z} + 2\hat{z}^\top PLCe \\ &\quad +4\|PLC\|^2 e^\top((A + LC)^\top Q + (A + LC)Q)e \\ &\leq -\frac{1}{2}\|\hat{z}\|^2 + 2\|PLCe\|^2 - 4\|PLC\|^2\|e\|^2 \,, \end{aligned}$$

where Young inequality, (15) and (16) have been used for the previous inequality. Therefore $\dot{\mathcal{V}} \preceq -\frac{1}{2}I$, and $\mathcal{V}$ is a Lyapunov function for (14). □

The computation done in the proof of Theorem 3 will be generalized for PDEs in the next sections.

Example 3. (Example 1 continued) In this part of the example, we first select a ramdomnly chosen matrix, and we check the Kalman rank condition for observability (lines 54-57). Then we compute a matrix L by placing the eigenvalues of the matrix $A + LC$ (line 60), and finally we plot solutions of (13) for 10 ramdomnly chosen initial conditions (lines 72-79).

```
C= np.random.random([1,n])
ObsvMatrix= control.obsv(A,C) # compute the observability
    matrix

if np.linalg.matrix_rank(ObsvMatrix)== n:
    print('observable system')
else:
    print('unobservable system')

q= np.linspace(-n-1,-2,n) # choice of the eigenvalues of the
    closed-loop system
L=-control.place(A.T,C.T,q).T

def ode2(ztot,t):
    z=ztot[:n]; zhat=ztot[n:]
    u= np.dot(np.dot(B,K),zhat)
    return np.concatenate((np.dot(A,z)+u ,np.dot(A,zhat)+u-np.
    dot(L,np.dot(C,z)-np.dot(C,zhat))))

# set up a figure twice as wide as it is tall
fig = plt.figure(figsize=plt.figaspect(0.5))
ax0 = fig.add_subplot(1, 2, 1, projection='3d')
ax1 = fig.add_subplot(1, 2, 2, projection='3d')

for i in range(10):
    z0=np.random.random([n,1]); z0=z0.reshape(n,)
    zhat0=np.random.random([n,1]); zhat0=zhat0.reshape(n,)
    ztot0=np.concatenate((z0,zhat0))
    sol=odeint(ode2,ztot0,t)
    ztot =sol.T; z=ztot[:n]; zhat=ztot[n:];
    ax0.plot(z[0], z[1], z[2]);
    ax1.plot(zhat[0], zhat[1], zhat[2]);

ax0.set_title('z'); ax1.set_title('$\hat z$')
plt.savefig('solutions2.png',bbox_inches='tight')
```

Figure 3 presents several solutions to (14) for ranmdonly chosen initial conditions $(z(0), \hat{z}(0))$, and confirms the attractivity of the origin for this system.

The Lyapunov function that is considered at the end of the proof of Theorem 3 is computed on lines 49, 85 and 86. It is checked on Figure 3 that this function decreases and converge to 0 along the solutions to (14) for the initial conditons used for Figure 3.

```
AE=A+np.dot(L,C);
Q=control.lyap(AE.T,np.eye(n))
M= 4*np.linalg.norm(np.dot(P,np.dot(L,C)))**2

fig , ax= plt.subplots()
```

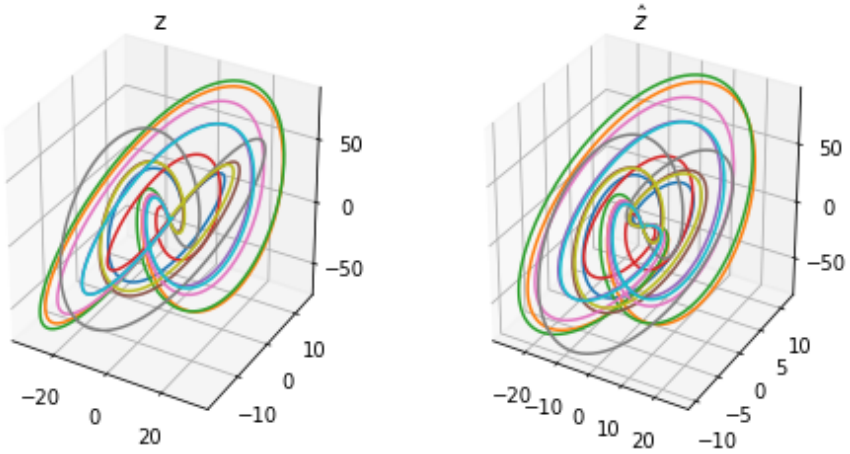

Fig. 3. Time-evolution of solutions to (13) for 10 randomnly chosen initial conditions

```
ax.set_title('Lyapunov function')

for i in range(10):
    z0=np.random.random([n,1]); z0=z0.reshape(n,)
    zhat0=np.random.random([n,1]); zhat0=zhat0.reshape(n,)
    ztot0=np.concatenate((z0,zhat0))
    sol=odeint(ode2,ztot0,t)
    ztot=sol.T; z=ztot[:n]; zhat=ztot[n:]; e=z-zhat; lyapu=[]
    for tt in range(len(t)):
        lyapu.append(np.dot(np.dot(zhat[:,tt].T,P),zhat[:,tt])+
    M*np.dot(np.dot(e[:,tt].T,Q),e[:,tt]))
    ax.plot(t,lyapu)
plt.savefig('lyapu2.png',bbox_inches='tight')
```

2.5. *Saturated control*

For many applications of control problems, the input values are limited in amplitude. Instead of applying $u = Kz$, only

$$u = \mathtt{sat}(Kz)$$

can actually be applied, where $\mathtt{sat}\colon \mathbb{R}^m \to \mathbb{R}^m$ is the saturation map defined componentwise by, for all $i = 1, \dots, m$,

$$\mathtt{sat}_i(\sigma_i) = \begin{cases} \sigma_i & \text{if } |\sigma_i| < s_i \\ \mathtt{sign}(\sigma_i) s_i \ , & \text{else} \end{cases} , \tag{17}$$

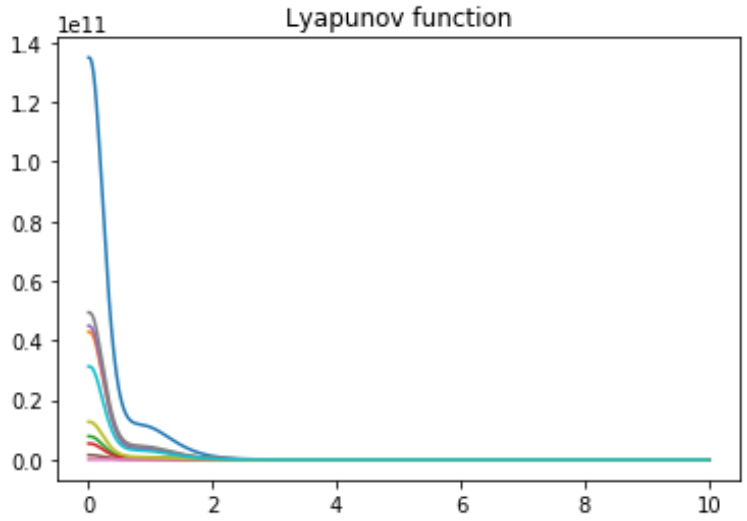

Fig. 4. Time-evolution of the designed Lyapunov function along several solutions to (14)

for a fixed vector s in $\mathbb{R}^m$ with positive components $s_i > 0$. Such function is a decentralized nonlinear map that makes the closed-loop system as follows:

$$\dot{z} = Az + B\mathtt{sat}(Kz) \tag{18}$$

In the presence of a saturation, system (18) can exhibit various behaviors. Even if the matrix $A + BK$ is Hurwitz, there may exist several equilibrium points, some limit cycle may appear, and there may exist diverging trajectories. See[70,74] for introductory references on stability of such dynamical systems.

Example 4. As an example, consider

$$\dot{z} = Az + B\mathtt{sat}(Kz) \tag{19}$$

with $A = \begin{pmatrix} 0 & 1 \\ 1 & 0 \end{pmatrix}$, $B = \begin{pmatrix} 0 \\ -1 \end{pmatrix}$, $K = \begin{pmatrix} 13 & 7 \end{pmatrix}$, and $s = 5$ as saturation level. The matrix A is unstable (eigenvalues located at -1 and $+1$), and the matrix $A + BK$ is Hurwitz (eigenvalues located at -1 and -13). As noted in [70, Example 1.1], the nonlinear system (19) exhibits several equilibriums and presents different behaviors depending on the initial condition. These behaviors are illustrated on Figure 21 based on different initial conditions. The first trajectory converges to 0 in $\mathbb{R}^2$, the second trajectory converges

to the non zero equilibrium point $\begin{pmatrix} -5 \\ 0 \end{pmatrix}$, and the last trajectory diverges as the time increases.

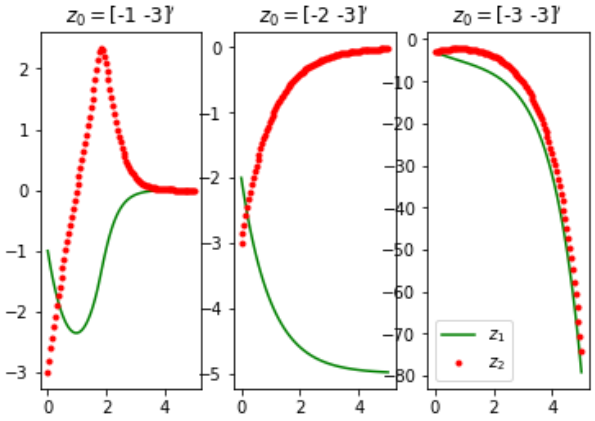

Fig. 5. Time-evolutions of three solutions to (19) for three different initial conditions

The simulation code is given below.

```
import numpy as np
import control
from scipy.integrate import odeint
import matplotlib as mpl
import matplotlib.pyplot as plt

n= 3 # dimension of the state space
A= np.random.random([n,n])
B= np.random.random([n,1])
CtrbMatrix= control.ctrb(A,B) # compute the controlability
    matrix

if np.linalg.matrix_rank(CtrbMatrix)== n:
    print('controllable system')
else:
    print('uncontrollable system')

p= np.linspace(-n,-1,n) # choice of the eigenvalues of the
    closed-loop system
K=-control.place(A,B,p)

def ode(z,t):
    return np.dot((A+np.dot(B,K)),z)
```

```
22
23 z0=np.random.random([n,1]); z0=z0.reshape(n,)
24 t=np.linspace(0,10,1000)
25 sol=odeint(ode,z0,t)
26
27 if n==3: # plot3D
28     from mpl_toolkits.mplot3d import Axes3D
29     mpl.rcParams['legend.fontsize'] = 10
30     fig = plt.figure(); ax = fig.gca(projection='3d')
31     x, y, z =sol.T
32     ax.plot(x, y, z, label='solution'); ax.legend()
33     plt.savefig('solution.png',bbox_inches='tight')
34 # for 10 randomnly chose initial conditions
35 fig = plt.figure(); ax = fig.gca(projection='3d')
36 for i in range(10):
37     z0=np.random.random([n,1]); z0=z0.reshape(n,)
38     sol=odeint(ode,z0,t)
39     x, y, z =sol.T
40     ax.plot(x, y, z, label='solution'+str(i));
41 ax.legend()
42
43 plt.savefig('solutions.png',bbox_inches='tight')
```

To analyze the stability of the equilibrium 0 of (18), let us consider the following Lyapunov function candidate $V : z \mapsto z^\top P z$, where $P \in \mathbb{R}^{n\times n}$ is a symmetric definite positive matrix. The computation of its time derivative along the solutions of (18) gives

$$\dot{V} = z^\top (A^\top P + PA) z + 2 z^\top P B \mathtt{sat}(Kz)\,.$$

To ease the comparison of the dynamics of (19) and of (18), we introduce the deadzone function ϕ defined by

$$\phi(\sigma) = \mathtt{sat}(\sigma) - \sigma \ , \ \forall \sigma \in \mathbb{R}^m \ . \tag{20}$$

Using this notation we get

$$\begin{aligned}\dot{V} &= z^\top ((A+BK)^\top P + P(A+BK)) z + 2 z^\top P B \phi(Kz) \\ &= \begin{pmatrix} z \\ \phi(Kz) \end{pmatrix}^\top \begin{pmatrix} (A+BK)^\top P + P(A+BK) & PB \\ \star & 0 \end{pmatrix} \begin{pmatrix} z \\ \phi(Kz) \end{pmatrix}\end{aligned}$$

Note that the matrix $\begin{pmatrix} (A+BK)^\top P + P(A+BK) & PB \\ \star & 0 \end{pmatrix}$ can not be in general negative semidefinite (except, e.g., for the trivial case $B = 0$). Consequently, in order to use the Lyapunov function candidate V to analyze the stability of the origin of (18), we need to find a relation between z and $\mathtt{sat}(Kz)$. This can be done by using the geometric conditions of

the saturation map, as described by the so-called local and global sector conditions.

As introduced in,[23] for any given $G \in \mathbb{R}^{m\times n}$ and any given diagonal positive definite matrix $T \in \mathbb{R}^m$, the following *local sector condition* holds:

$$(\mathtt{sat}(Kz)-Kz)T(\mathtt{sat}(Kz)-(K-G)z) \leq 0\ ,\ \forall z \text{ such that } |((K-G)z)_i| \leq s_i, \tag{21}$$

where $(K-G)_{(i)}$ denotes the ith row of $K-G$.

Letting in particular $G = K$ in (21), the following *global sector condition* holds for any diagonal positive definite matrix T

$$(\mathtt{sat}(Kz) - Kz)T\mathtt{sat}(Kz) \leq 0\ ,\ \forall z \in \mathbb{R}^m \tag{22}$$

From the local sector condition, we obtain that for any $G \in \mathbb{R}^{n\times m}$ and any diagonal positive definite matrix T, as long as $|((K-G)z)_i| \leq s_i$,

$$\begin{aligned}\dot{V} &\leq z^\top((A+BK)^\top P + P(A+BK))z + 2z^\top PB\phi(Kz)\\ &\quad -2\phi(Kz)^\top T(\phi(Kz)+Gz)\\ &\leq \begin{pmatrix} z \\ \phi(Kz)\end{pmatrix}^\top \begin{pmatrix} (A+BK)^\top P + P(A+BK) & PB-G^\top T \\ \star & -2T\end{pmatrix}\begin{pmatrix} z \\ \phi(Kz)\end{pmatrix}\end{aligned}$$

Considering the special case where $G = K$, we obtain the following theorem.

Theorem 4. *If there exist a symmetric definite matrix P in $\mathbb{R}^{n\times n}$ and a diagonal positive definite matrix T in $\mathbb{R}^m$ such that*

$$\begin{pmatrix} (A+BK)^\top P + P(A+BK) & PB - K^\top T \\ \star & -2T\end{pmatrix} \prec 0$$

then the origin of (19) is globally asymptotically stable.

Remark 1. Some observations are in order.

Checking the existence of such matrices P and T is numerically tractable. This is a convex problem that could be solved using different solvers and method as interior-point method,[22] or a primal/dual method.[21] See also.[6]

As discussed in,[67] the existence of a globally stabilizing saturating control is subject to a number of strong conditions such as: (i) A has no eigenvalues with positive real part, and (ii) the pair (A, B) is stabilizable in the ordinary sense, that there exists a matrix K such that $A + BK$ is asymptotically stable.

Setting $G = K$ is generally restrictive since global asymptotic stability is generally a too strong property for saturated systems. To derive a sufficient condition for the weaker property of local asymptotic stability, we use the local sector condition (21). To ensure the condition $|((K-G)z)_i| \leq s_i$, we note that $\{z,\ z^\top Pz \leq 1\} \subset \{z,\ |((K-G)z)_i| \leq s_i\}$ provided the LMI condition

$$\begin{pmatrix} P & (K-G)_{(i)}^\top \\ \star & s_i^2 \end{pmatrix} \succeq 0$$

holds. This result is a direct consequence of the Schur complement (see [6, Page 7]). Returning now to the LMI

$$\begin{pmatrix} (A+BK)^\top P + P(A+BK) & PB - G^\top T \\ \star & -2T \end{pmatrix} \prec 0$$

we note that there is a product $G^\top T$ of unknown variables, making the problem nonlinear. Nevertheless, the problem can be made linear by introducing a simple change of variable. Indeed, using the change of variables $S = T^{-1}$, $W = P^{-1}$, and $H = GP^{-1}$, we obtain the equivalent condition

$$\begin{pmatrix} W(A+BK)^\top + (A+BK)W & BS - H^\top \\ \star & -2S \end{pmatrix} \prec 0$$

We have thus proven the following sufficient condition for local asymptotic stability of (19).

Theorem 5. *If there exist $W = W^\top > 0$, S diagonal definite positive and G such that*

$$\begin{pmatrix} W & WK_{(i)}^\top - H_{(i)}^\top \\ \star & s_i^2 \end{pmatrix} \succeq 0 \tag{23}$$

$$\begin{pmatrix} W(A+BK)^\top + (A+BK)W & BS - H^\top \\ \star & -2S \end{pmatrix} \prec 0 \tag{24}$$

then the origin of (19) locally asymptotically stable with a basin of attraction containing $\{z,\ z^\top W^{-1} z \leq 1\}$.

Remark 2. Checking the condition of Theorem 5 reduces to solving a convex problem. Different optimization criterion can be considered in order to maximize the estimation of the basin of attraction, as e.g., maximizing the trace of the matrix W. This idea is illustrated in Example 5 below.

Note that this sufficient condition for local asymptotic stability of the closed-loop system can also be used in order to compute the matrix of feedback gain K. See [70, Chapter 3] and in the next sections for infinite-dimensional dynamics.

Example 5. (Example 4 continued) Solving the matrix inequalities of Theorem 5 is done with the code below, where the *Python cvxpy Library* has been used to write the matrix conditions in lines 52-64 with the unknown variables introduced in lines 46-48. The optimization problem

$$\max_{W,S,H} \texttt{trace}(W) \text{ such that (23) and (24) hold}$$

is solved in line 56, using the default solver.

```
44 n=len(A); m= 1
45
46 W=cp.Variable((n,n),PSD=True)
47 S=cp.Variable((m,m),diag=True)
48 H=cp.Variable((m,n))
49 B=B.reshape(2,1)
50 K=K.reshape(1,2)
51
52 M11=W @ (np.transpose(A+np.dot(B,K)))
53 M11=M11+M11.T
54 M12=B @ S - H.T
55 matrixConstr1 = cp.bmat([[ M11 , M12],
56                           [M12.T, -2 *S]])
57 M22= W @ K.T  - H.T
58 matrixConstr2 = cp.bmat([[W,     M22    ],
59                           [M22.T ,s0 ** 2*np.array([[1]])]])
60
61 constr =  [S >> 0]
62 constr += [matrixConstr1<<0] + [matrixConstr2>>0]
63 prob = cp.Problem(cp.Maximize(cp.trace(W)),constr)
64 prob.solve()
65
66 P=np.linalg.inv(W.value)
67 z0=z0tot[0]
68 print("z0^T P z0 is "+str(np.dot(np.dot(z0.T,P),z0)))
```

It gives

$$P = \begin{pmatrix} 0.19727007 & 0.11506782 \\ \star & 0.08307019 \end{pmatrix}$$

for which, due to Theorem 5, $\{z,\ z^\top P z \leq 1\}$ is included in the basin of attraction.

For the first initial condition of Figure 4, that is with $z_0 = [-1\ -3]^\top$, we have

$$z_0^\top P z_0 = 0.99 < 1.$$

Thus z_0 is indeed in the basin of attraction, as confirmed by the time-evolution of the first solution in Figure 4.

2.6. *Section conclusion*

This section was devoted to finite-dimensional control systems by recalling some basic definitions and techniques for the stability analysis of equilibrium of such dynamical systems. In particular we reviewed the direct Lyapunov method for the asymptotic stability analysis. The control systems with saturated inputs have been also considered, and some sufficient conditions for the local (and global) asymptotic stability of the origin have been recalled. The next section will develop these techniques for the boundary stabilization of parabolic and hyperbolic systems.

3. Parabolic equations

3.1. *Introduction*

This section considers parabolic partial differential equations modeling reaction-diffusion phenomenon. This class of dynamical systems may be unstable in open loop. We focus on 1D parabolic equations for which spectral decomposition can be easily handled since the eigenvalues are simple and the eigenfunctions form a Hilbert basis of the state-space. For further studies on abstract parabolic PDEs in several dimensional spaces, see[7] in particular for controllability properties of such systems.

Based on the basic tools presented in the previous section, we present design methods for the design of output-feedback laws rendering the equilibrium asymptotically stable. The approach is based on modal approximation methods that have been shown to be efficient for other control problems related to parabolic PDEs; see[61] as well as more recent references including.[15,16,37,43,50,57] The rationale behind the design method presented in this section is split into several steps. First a finite-dimensional state-feedback is computed only with a finite number of selected modes of the model. Then a finite-dimensional observer is designed in a separate fashion in order to estimate a finite number of modes that include in particular the modes used for the state-feedback design. Such a control design approach roots back to the pioneer papers[3,18,25,62] which essentially rely on small gain arguments. Taking advantage of the controller architecture reported in,[62] the possibility to recast this control design problem into a LMI framework was shown in[29] for a particular set of input/output maps and specific norms for the asymptotic stability estimates. This procedure was enhanced and generalized in a systematic manner in[40,41] for general reaction-diffusion PDEs with Dirichlet/Neumann/Robin boundary control and Dirichlet/Neumann measurement while performing the control design directly with the control input instead of it time derivative (see[17] for an introduction to boundary control systems). This generalized and systematic approach has been shown to be key and very efficient for the predictor-based compensation of arbitrarily long input and output delays,[38,42] the domination of state-delays,[44] the local output feedback stabilization of linear reaction-diffusion PDEs in the presence of a saturation,[34] the global stabilization of linear-reaction-diffusion PDEs in the presence of a Lipchitz continuous sector nonlinearity in the application of the boundary control,[40] as well as the global stabilization of semilinear reaction-diffusion PDE with

globally Lipchitz nonlinearity.[39]

In this framework, the proof of stability of the closed-loop system (composed of the PDE, the finite-dimensional observer, and the state-feedback) is assessed using the Lyapunov direct method presented in the previous section, but adapted to the distributed nature of the state. This approach can be seen as an alternative output feedback design method for reaction parabolic PDEs to other very efficient tools, such as backstepping transformations for PDEs (see the introductory textbook[31]) for which a form of separation principle between controller and observer designs generally exists. Nevertheless, the infinite-dimensional nature of the observer obtained using backstepping methods implies the necessity to resort to late lumping approximations in order to obtain a finite-dimensional control strategy that is suitable for practical implementation, inducing in general the loss of the stability performance guarantees originally obtained during the synthesis phase. The benefit of the approach reported in this section is that the observer obtained during the synthesis phase is directly finite-dimensional.

The material presented in this Section of the lecture notes is widely inspired from[41] in the linear case and from[34] for the saturated input scenario.

The rest of this section is organized as follows. After introducing a number of notations and properties, the case of Dirichlet boundary control with a bounded observation operator is considered in Section 3.2. The control design procedure is then extended to the cases of a boundary Dirichlet observation in Section 3.3. The case of in-domain control in the presence of an input saturation in discussed in Section 3.4.

Reminders on Sturm Liouville theory

Let us conclude this introduction with some reminders on Sturm Liouville theory for parabolic operators in one space dimension. See[51] for a reference on the mathematical properties that will be extensively used in this section.

Let $\theta_1, \theta_2 \in [0, \pi/2]$, $p \in \mathcal{C}^1([0,1])$, and $q \in \mathcal{C}^0([0,1])$ with $p > 0$ and $q \geq 0$. Consider the Sturm-Liouville operator $\mathcal{A} : D(\mathcal{A}) \subset L^2(0,1) \to L^2(0,1)$ defined by

$$\mathcal{A}f = -(pf')' + qf$$

on the domain

$$\begin{aligned} D(\mathcal{A}) = \{f \in H^2(0,1) \, : \, & \cos(\theta_1)f(0) - \sin(\theta_1)f'(0) = 0, \\ & \cos(\theta_2)f(1) + \sin(\theta_2)f'(1) = 0\}. \end{aligned}$$

The eigenvalues $(\lambda_n)_{n\geq 1}$ of $\mathcal{A}$ are simple, non negative, and form an increasing sequence with $\lambda_n \to +\infty$ as $n \to +\infty$. The associated unit eigenvectors $\Phi_n \in L^2(0,1)$ form a Hilbert basis. The operator $\mathcal{A}$ and its domain can be characterized by there eigenstructures in the sense that

$$\mathcal{A}f = \sum_{n\geq 1} \lambda_n \langle f, \Phi_n \rangle, \quad \forall f \in D(\mathcal{A})$$

and

$$D(\mathcal{A}) = \{f \in L^2(0,1) : \sum_{n\geq 1} |\lambda_n|^2 |\langle f, \Phi_n \rangle|^2 < +\infty\}$$

where $\langle f, g \rangle = \int_0^1 f(x)g(x), \mathrm{d}x$, for any $f, g \in L^2(0,1)$, stands for the inner product of $L^2(0,1)$. Hence, using an integration by parts, it can be seen that, for any $f \in D(\mathcal{A})$,

$$\sum_{n\geq 1} \lambda_n \langle f, \Phi_n \rangle^2 = \langle \mathcal{A}f, f \rangle$$

$$= p(0)f(0)f'(0) - p(1)f(1)f'(1) + \int_0^1 p(x)f'(x)^2 + q(x)f(x)^2 \, \mathrm{d}x.$$

Using the boundary conditions involved in the definition of $D(\mathcal{A})$, we infer the existence of a constant $C_2 > 0$ such that

$$\sum_{n\geq 1} \lambda_n \langle f, \Phi_n \rangle^2 = \langle \mathcal{A}f, f \rangle \leq C_2 \|f\|_{H^1}.$$

Moreover, if either (i) $\theta_1, \theta_2 \in \{0, \pi/2\}$ with $\theta_i = 0$ for at least one $i \in \{0, 1\}$; or (ii) $q > 0$, this implies the existence of a constant $C_1 > 0$ such that

$$C_1 \|f\|_{H^1} \leq \sum_{n\geq 1} \lambda_n \langle f, \Phi_n \rangle^2 = \langle \mathcal{A}f, f \rangle \leq C_2 \|f\|_{H^1}. \tag{25}$$

Hence, for any $f \in D(\mathcal{A})$, the series expansion $f = \sum_{n\geq 1} \langle f, \Phi_n \rangle \Phi_n$ holds in $H^1(0,1)$ norm. Then, using the definition of $\mathcal{A}$ and the fact that it is a Riesz-spectral operator, we obtain that the latter series expansion holds in $H^2(0,1)$ norm. Due to the continuous embedding $H^1(0,1) \subset L^\infty(0,1)$, we obtain that

$$f(0) = \sum_{n\geq 1} \langle f, \Phi_n \rangle \Phi_n(0), \quad f'(0) = \sum_{n\geq 1} \langle f, \Phi_n \rangle \Phi_n'(0).$$

Let $p_*, p^*, q^* \in \mathbb{R}$ be such that $0 < p_* \leq p(x) \leq p^*$ and $0 \leq q(x) \leq q^*$ for all $x \in [0,1]$. Then we have:[51]

$$0 \leq \pi^2(n-1)^2 p_* \leq \lambda_n \leq \pi^2 n^2 p^* + q^* \tag{26}$$

for all $n \geq 1$. If we further assume that $p \in \mathcal{C}^2([0,1])$, we have (see again[51]) that

$$\Phi_n(0) = O_{n\to+\infty}(1), \quad \Phi_n'(0) = O_{n\to+\infty}(\sqrt{\lambda_n}). \tag{27}$$

3.2. *Bounded observation operator*

We first consider the reaction-diffusion system described by

$$z_t(t,x) = (p(x)z_x(t,x))_x + (q_c - q(x))z(t,x) \tag{28a}$$
$$z_x(t,0) = 0, \quad z(t,1) = u(t) \tag{28b}$$
$$z(0,x) = z_0(x) \tag{28c}$$
$$y(t) = \int_0^1 c(x)z(t,x)\,\mathrm{d}x \tag{28d}$$

for $t > 0$ and $x \in (0,1)$. Here $q_c \in \mathbb{R}$ is a constant, $u(t) \in \mathbb{R}$ is the command input, $y(t) \in \mathbb{R}$ with $c \in L^2(0,1)$ is the measurement, $z_0 \in L^2(0,1)$ is the initial condition, and $z(t,\cdot) \in L^2(0,1)$ is the state.

3.2.1. *Spectral reduction*

In (28), the control input u appears in the right boundary condition. Let us transfer the control input from the boundary into the PDE by invoking the change of variable:

$$w(t,x) = z(t,x) - x^2u(t). \tag{29}$$

It has been specifically selected in order to ensure that we still have the left boundary condition $w_x(t,0) = 0$ while enforcing $w(t,0) = 0$. Hence, we have

$$w_t(t,x) = (p(x)w_x(t,x))_x + (q_c - q(x))w(t,x) + a(x)u(t) + b(x)\dot{u}(t) \tag{30a}$$
$$w_x(t,0) = 0, \quad w(t,1) = 0 \tag{30b}$$
$$w(0,x) = w_0(x) \tag{30c}$$
$$\tilde{y}(t) = \int_0^1 c(x)w(t,x)\,\mathrm{d}x \tag{30d}$$

Here $a, b \in L^2(0,1)$ are defined by $a(x) = 2p(x) + 2xp'(x) + (q_c - q(x))x^2$ and $b(x) = -x^2$, respectively, while $\tilde{y}(t) = y(t) - \left(\int_0^1 x^2c(x)\,\mathrm{d}x\right)u(t)$ and $w_0(x) = z_0(x) - x^2u(0)$.

The parabolic equation (30) presents homogeneous boundary conditions (30b) that are much easier to deal with. However, the price of this transfer is the occurrence of the time derivative $\dot{u}$ of the control input u in the PDE (30a). This is why we introduce the auxiliary command input $v(t) = \dot{u}(t)$, that will be used as the control input for control design. In other words,

v will be used as the control input for the design of the control strategy. However, for final implementation of the control strategy, u remains the actual control input of the plant. In this context, the dynamics of the system reads

$$\dot{u}(t) = v(t) \tag{31a}$$

$$\frac{\mathrm{d}w}{\mathrm{d}t}(t,\cdot) = -\mathcal{A}w(t,\cdot) + q_c w(t,\cdot) + au(t) + bv(t) \tag{31b}$$

with $D(\mathcal{A}) = \{f \in H^2(0,1) : f'(0) = f(1) = 0\}$. Introducing the coefficients of projection $w_n(t) = \langle w(t,\cdot), \Phi_n \rangle$, $a_n = \langle a, \Phi_n \rangle$, $b_n = \langle b, \Phi_n \rangle$, and $c_n = \langle c, \Phi_n \rangle$, the projection of the PDE solutions into the Hilbert basis of eigenfunctions $(\Phi_n)_{n\geq 1}$ gives

$$\dot{u}(t) = v(t) \tag{32a}$$

$$\dot{w}_n(t) = (-\lambda_n + q_c)w_n(t) + a_n u(t) + b_n v(t), \quad n \geq 1 \tag{32b}$$

$$\tilde{y}(t) = \sum_{i\geq 1} c_i w_i(t) \tag{32c}$$

Note that (32) has been obtained from (31) by 1) multiplying (31) by Φ_n; 2) integrating on the space domain; and 3) performing two integration by parts why using the boundary conditions coming from the definition of $D(\mathcal{A})$.

3.2.2. *Control design*

We start by fixing an integer $N_0 \geq 1$ and positive real number $\delta > 0$ such that $-\lambda_n + q_c < -\delta < 0$ for all $n \geq N_0 + 1$. Let $N \geq N_0 + 1$ be arbitrary. The general idea, borrowed to,[62] is to compute a stabilizing output-feedback controller in three steps. First an observer to estimate the N first modes of the plant is designed. Secondly the state-feedback is only performed on the N_0 first estimated modes of the plant. Finally a dedicated stability analysis is performed to prove that the origin of the closed-loop is asymptotically stable. In this context, inspired by the controller architecture first reported

in,[62] the adopted control strategy takes the form:

$$\dot{\hat{w}}_n(t) = (-\lambda_n + q_c)\hat{w}_n(t) + a_n u(t) + b_n v(t) + l_n\left(\hat{y}(t) - \tilde{y}(t)\right), \quad 1 \le n \le N_0 \tag{33a}$$

$$\dot{\hat{w}}_n(t) = (-\lambda_n + q_c)\hat{w}_n(t) + a_n u(t) + b_n v(t), \quad N_0 + 1 \le n \le N \tag{33b}$$

$$\hat{y}(t) = \int_0^1 c(x) \sum_{i=1}^{N} \hat{w}_i(t)\Phi_i(x)\,\mathrm{d}x = \sum_{i=1}^{N} c_i \hat{w}_i(t) \tag{33c}$$

$$v(t) = \dot{u}(t) = \sum_{i=1}^{N_0} k_i \hat{w}_i(t) + k_u u(t) \tag{33d}$$

where $k_i, k_u \in \mathbb{R}$ are the feedback gains while $l_n \in \mathbb{R}$ are the observer gains. Signals $\hat{w}_n$ stand for the estimations of the modes w_n for $1 \le n \le N$. These estimations are used for the computation of $\hat{y}$ that represents the estimation of the actual system measurement $\tilde{y}$. Note that the feedback law (33d) is computed only based on the observations $\hat{w}_n$ for $1 \le n \le N_0$. The remaining observations, namely $\hat{w}_n$ for $N_0 + 1 \le n \le N$, are only used in (33c) to improve the estimation $\hat{y}$ of the actual system output $\tilde{y}$. This estimation $\hat{y}$ is used to introduce a correction term in the observation dynamics (33a) related to the mismatch between the estimation $\hat{y}$ and the measurement $\tilde{y}$. Note that no such correction is applied in (33b) for the observed modes associated with $N_0 + 1 \le n \le N$.

In order to study the validity of the control strategy (33), we need to introduce a number of definitions. Introducing

$$W^{N_0}(t) = \begin{bmatrix} w_1(t) \\ \vdots \\ w_{N_0}(t) \end{bmatrix}, \quad B_{0,a} = \begin{bmatrix} a_1 \\ \vdots \\ a_{N_0} \end{bmatrix}, \qquad B_{0,b} = \begin{bmatrix} b_1 \\ \vdots \\ b_{N_0} \end{bmatrix},$$

$$A_0 = \mathrm{diag}(-\lambda_1 + q_c, \ldots, -\lambda_{N_0} + q_c),$$

we have from (32b) that

$$\dot{W}^{N_0}(t) = A_0 W^{N_0}(t) + B_{0,a} u(t) + B_{0,b} v(t). \tag{34}$$

Hence, defining

$$W_a^{N_0}(t) = \begin{bmatrix} u(t) \\ W^{N_0}(t) \end{bmatrix}, \; A_1 = \begin{bmatrix} 0 & 0 \\ B_{0,a} & A_0 \end{bmatrix}, \; B_1 = \begin{bmatrix} 1 \\ B_{0,b} \end{bmatrix},$$

we obtain that

$$\dot{W}_a^{N_0}(t) = A_1 W_a^{N_0}(t) + B_1 v(t).$$

We now define for $1 \leq n \leq N$ the observation error as

$$e_n(t) = w_n(t) - \hat{w}_n(t). \tag{35}$$

With $\zeta(t) = \sum_{i \geq N+1} c_i w_i(t)$, we infer from (33a) that

$$\dot{\hat{w}}_n(t) = (-\lambda_n + q_c)\hat{w}_n(t) + a_n u(t) + b_n v(t) - l_n \sum_{i=1}^{N} c_i e_i(t) - l_n \zeta(t) \tag{36}$$

for $1 \leq n \leq N_0$. Inspired by Section 2, we write the dynamics in coordinates of the observer state and of the error variable. To do so we introduce

$$\hat{W}^{N_0}(t) = \begin{bmatrix} \hat{w}_1(t) \\ \vdots \\ \hat{w}_{N_0}(t) \end{bmatrix}, \quad E^{N_0}(t) = \begin{bmatrix} e_1(t) \\ \vdots \\ e_{N_0}(t) \end{bmatrix}, \quad E^{N-N_0}(t) = \begin{bmatrix} e_{N_0+1}(t) \\ \vdots \\ e_N(t) \end{bmatrix},$$

$$C_0 = \begin{bmatrix} c_1 \ c_2 \ \dots \ c_{N_0} \end{bmatrix}, \quad C_1 = \begin{bmatrix} c_{N_0+1} \ \dots \ c_N \end{bmatrix}, \quad L = \begin{bmatrix} l_1 \\ \vdots \\ l_{N_0} \end{bmatrix}.$$

Hence we have

$$\begin{aligned} \dot{\hat{W}}^{N_0}(t) = {} & A_0 \hat{W}^{N_0}(t) + B_{0,a} u(t) + B_{0,b} v(t) \\ & - L C_0 E^{N_0}(t) - L C_1 E^{N-N_0}(t) - L\zeta(t). \end{aligned} \tag{37}$$

With

$$\hat{W}_a^{N_0}(t) = \begin{bmatrix} u(t) \\ \hat{W}^{N_0}(t) \end{bmatrix}, \quad \tilde{L} = \begin{bmatrix} 0 \\ L \end{bmatrix} \tag{38}$$

we deduce that

$$\dot{\hat{W}}_a^{N_0}(t) = A_1 \hat{W}_a^{N_0}(t) + B_1 v(t) - \tilde{L} C_0 E^{N_0}(t) - \tilde{L} C_1 E^{N-N_0}(t) - \tilde{L}\zeta(t) \tag{39}$$

In view of (33d) we deduce that

$$v(t) = K \hat{W}_a^{N_0}(t), \tag{40}$$

where $K \in \mathbb{R}^{1 \times (N_0+1)}$. Hence we obtain that

$$\dot{\hat{W}}_a^{N_0}(t) = (A_1 + B_1 K)\hat{W}_a^{N_0}(t) - \tilde{L} C_0 E^{N_0}(t) - \tilde{L} C_1 E^{N-N_0}(t) - \tilde{L}\zeta(t) \tag{41}$$

and, using (34) and (37),

$$\dot{E}^{N_0}(t) = (A_0 + L C_0) E^{N_0}(t) + L C_1 E^{N-N_0}(t) + L\zeta(t). \tag{42}$$

Claim 1. *The pair (A_1, B_1) is controllable.*

Proof of Claim 1. Let us compute the Kalman matrix $\mathcal{C}$ for controllability of (A_1, B_1) as introduced in Section 1. Denoting by $\mu_n = -\lambda_n + q_c$, we get

$$\mathcal{C} = \begin{bmatrix} 1 & 0 & \dots & 0 \\ b_1 & a_1 + \mu_1 b_1 & \dots & (a_1 + \mu_1 b_1)\mu_1^{N_0-1} \\ b_2 & a_2 + \mu_2 b_2 & \dots & (a_2 + \mu_2 b_2)\mu_2^{N_0-1} \\ \vdots & \vdots & & \\ b_{N_0} & a_{N_0} + \mu_{N_0} b_{N_0} & \dots & (a_1 + \mu_{N_0} b_{N_0})\mu_{N_0}^{N_0-1} \end{bmatrix}$$

whose determinant is

$$\det(\mathcal{C}) = \Pi_{n=1}^{N_0}(a_n + \mu_n b_n) \begin{vmatrix} 1 & \mu_1 & \dots & \mu_1^{N_0-1} \\ 1 & \mu_2 & \dots & \mu_2^{N_0-1} \\ \vdots & \vdots & & \\ 1 & \mu_{N_0} & \dots & \mu_{N_0}^{N_0-1} \end{vmatrix}.$$

The second determinant appearing in the latter equations is known as the Vandermonde determinant. Since the μ_n are distinct, the Vandermonde determinant is non zero hence the pair (A_1, B_1) is controllable if and only if $\Pi_{n=1}^{N_0}(a_n + \mu_n b_n) \neq 0$. To check this latter condition, let us compute, for each $n = 1, \dots, N_0$, the quantity $a_n + \mu_n b_n$. Recalling $\mu_n = -\lambda_n + q_c$ and from the definitions of the function a and b, we obtain that

$$\begin{aligned} a_n + \mu_n b_n &= \int_0^1 [2p(x) + 2xp'(x) + (q_c - q(x))x^2]\Phi_n(x)\mathrm{d}x \\ &\quad + (-\lambda_n + q_c)\int_0^1 -x^2\Phi_n(x)\mathrm{d}x \\ &= \int_0^1 [(2p(x) + 2xp'(x))\Phi_n(x) - x^2 q(x)\Phi_n(x)]\mathrm{d}x \\ &\quad + \int_0^1 [-x^2(p(x)\Phi_n'(x))' + x^2 q(x)\Phi_n(x)]\mathrm{d}x \\ &= \int_0^1 (2p(x) + 2xp'(x))\Phi_n(x)\mathrm{d}x - \int_0^1 x^2(p(x)\Phi_n'(x))'\mathrm{d}x \\ &= -p(1)\Phi_n'(1). \end{aligned}$$

Recalling that Φ_n is a non-trivial solution to a second order ODE with $\Phi_n(1) = 0$, we must have $\Phi_n'(1) \neq 0$. Therefore $a_n + \mu_n b_n \neq 0$ hence the pair (A_1, B_1) is controllable. □

Claim 2. *Assuming $c_n \neq 0$ for all $1 \leq n \leq N_0$, the pair (A_0, C_0) is observable.*

Proof of Claim 2. Let us compute the Kalman matrix for observation of the pair (A_0, C_0):

$$\begin{bmatrix} c_1 & \dots & c_{N_0} \\ \mu_1 c_1 & \dots & \mu_{N_0} c_{N_0} \\ & \dots & \\ \mu_1^{N_0-1} c_1 & \dots & \mu_{N_0}^{N_0-1} c_{N_0} \end{bmatrix}.$$

Since $n \neq m$ implies $\mu_n \neq \mu_m$, this matrix is full rank if an only if $c_n \neq 0$ for all $n = 1, \dots, N_0$. □

We now define the vectors and matrices:

$$\hat{W}^{N-N_0}(t) = \begin{bmatrix} \hat{w}_{N_0+1}(t) \\ \vdots \\ \hat{w}_N(t) \end{bmatrix}, \quad B_{2,a} = \begin{bmatrix} a_{N_0+1} \\ \vdots \\ a_N \end{bmatrix}, \quad B_{2,b} = \begin{bmatrix} b_{N_0+1} \\ \vdots \\ b_N \end{bmatrix},$$

$$A_2 = \operatorname{diag}(-\lambda_{N_0+1} + q_c, \dots, -\lambda_N + q_c).$$

From (33b) and (40) we obtain that

$$\begin{aligned} \dot{\hat{W}}^{N-N_0}(t) &= A_2 \hat{W}^{N-N_0}(t) + B_{2,a} u(t) + B_{2,b} v(t) \\ &= A_2 \hat{W}^{N-N_0}(t) + \left(B_{2,b} K + \begin{bmatrix} B_{2,a} & 0 \end{bmatrix}\right) \hat{W}_a^{N_0}(t) \end{aligned} \tag{43}$$

and, using in addition (32b) and (35),

$$\dot{E}^{N-N_0}(t) = A_2 E^{N-N_0}(t). \tag{44}$$

Putting together (41-44), we obtain with

$$X(t) = \operatorname{col}(\hat{W}_a^{N_0}(t), E^{N_0}(t), \hat{W}^{N-N_0}(t), E^{N-N_0}(t)) \tag{45}$$

that

$$\dot{X}(t) = FX(t) + \mathcal{L}\zeta(t) \tag{46}$$

where

$$F = \begin{bmatrix} A_1 + B_1 K & -\tilde{L} C_0 & 0 & -\tilde{L} C_1 \\ 0 & A_0 + LC_0 & 0 & LC_1 \\ B_{2,b} K + \begin{bmatrix} B_{2,a} & 0 \end{bmatrix} & 0 & A_2 & 0 \\ 0 & 0 & 0 & A_2 \end{bmatrix}, \quad \mathcal{L} = \begin{bmatrix} -\tilde{L} \\ L \\ 0 \\ 0 \end{bmatrix}. \tag{47}$$

Defining $E = \begin{bmatrix} 1 & 0 & \dots & 0 \end{bmatrix}$ and $\tilde{K} = \begin{bmatrix} K & 0 & 0 & 0 \end{bmatrix}$, we obtain from (38), (40), and (45) that

$$u(t) = EX(t), \quad v(t) = \tilde{K} X(t). \tag{48}$$

Finally, defining $g = \|a\|_{L^2}^2 + \|b\|_{L^2}^2 \|K\|^2$, we can introduce

$$G = \|a\|_{L^2}^2 E^\top E + \|b\|_{L^2}^2 \tilde{K}^\top \tilde{K} \preceq gI. \tag{49}$$

3.2.3. *Stability analysis*

Theorem 6. *Let $p \in \mathcal{C}^1([0,1])$ with $p > 0$, $q \in \mathcal{C}^0([0,1])$ with $q \geq 0$, $q_c \in \mathbb{R}$, and $c \in L^2(0,1)$. Consider the reaction-diffusion system described by (28). Let $N_0 \geq 1$ and $\delta > 0$ be given such that $-\lambda_n + q_c < -\delta < 0$ for all $n \geq N_0 + 1$. Assume that $c_n \neq 0$ for all $1 \leq n \leq N_0$. Let $K \in \mathbb{R}^{1\times(N_0+1)}$ and $L \in \mathbb{R}^{N_0}$ be such that $A_1 + B_1 K$ and $A_0 + LC_0$ are Hurwitz with eigenvalues that have a real part strictly less than $-\delta < 0$. Assume that there exist $N \geq N_0 + 1$, $P \succ 0$, $\alpha > 1$, and $\beta, \gamma > 0$ such that*

$$\Theta = \begin{bmatrix} F^\top P + PF + 2\delta P + \alpha\gamma G & P\mathcal{L} \\ \star & -\beta \end{bmatrix} \preceq 0, \tag{50a}$$

$$\Gamma_{1,N+1} = -\lambda_{N+1} + q_c + \delta + \frac{1}{\alpha} + \frac{\beta\|c\|_{L^2}^2}{2\gamma} \leq 0, \tag{50b}$$

$$\Gamma_{2,N+1} = -\left(1 - \frac{1}{\alpha}\right)\lambda_{N+1} + q_c + \delta + \frac{\beta\|c\|_{L^2}^2}{2\gamma\lambda_{N+1}} \leq 0, \tag{50c}$$

for all $n \geq N + 1$. Then, for the closed-loop system composed of the plant (28) and the controller (33)

(1) the origin is asymptotically stable in L^2-norm, that is there exists $M > 0$ such that, for any $\hat{w}_n(0) \in \mathbb{R}$, any $z_0 \in L^2(0,1)$ and any $u(0) \in \mathbb{R}$, the mild solution of the closed-loop system satisfies

$$u(t)^2 + \sum_{n=1}^{N} \hat{w}_n(t)^2 + \|z(t,\cdot)\|_{L^2}^2 \leq Me^{-2\delta t}\left(u(0)^2 + \sum_{n=1}^{N} \hat{w}_n(0)^2 + \|z_0\|_{L^2}^2\right)$$

for all $t \geq 0$.

(2) the origin is asymptotically stable in H^1-norm, that is there exists $M > 0$ such that, for any $\hat{w}_n(0) \in \mathbb{R}$, any $z_0 \in H^2(0,1)$ and any $u(0) \in \mathbb{R}$ such that $z_0'(0) = 0$ and $z_0(1) = u(0)$, the classical solution of the closed-loop system satisfies

$$u(t)^2 + \sum_{n=1}^{N} \hat{w}_n(t)^2 + \|z(t,\cdot)\|_{H^1}^2 \leq Me^{-2\delta t}\left(u(0)^2 + \sum_{n=1}^{N} \hat{w}_n(0)^2 + \|z_0\|_{H^1}^2\right)$$

for all $t \geq 0$.

Moreover, the above constraints are always feasible for N large enough.

Remark 3. The feasibility problem of Theorem 6 is not linear due to the presence of some terms such as $\alpha\gamma$ and $\frac{1}{\alpha}$ involving the decision variables. However the use of Schur complement allows to rewrite (50b) as follows:

$$\begin{bmatrix} -\lambda_{N+1} + q_c + \delta + \frac{\beta\|c\|_{L^2}^2}{2\gamma} & 1 \\ \star & -\alpha \end{bmatrix} \leq 0,$$

and similarly for (50c). Therefore, as soon as γ is fixed, checking the conditions of Theorem 6 reduces to check linear matrix inequalities (LMIs). Thus, given a desired exponential decay rate $\delta > 0$ and a number of modes $N \geq N_0 + 1$ for the observer, the sufficient conditions of the previous theorem can be recasted as an efficient optimization problem to solve LMIs.

Proof of Theorem 6. Consider the Lyapunov function candidate

$$V(X, w) = X^\top P X + \gamma \sum_{n \geq N+1} \langle w, \Phi_n \rangle^2$$

for $X \in \mathbb{R}^{2N+1}$ and $w \in L^2(0,1)$. The first term accounts for the dynamics of the N first modes of the PDE and the dynamics of the observer, while the series accounts for the dynamics of the modes corresponding to $n \geq N+1$. The computation of the time derivative of V along the system solutions (32b) and (46) gives

$$\begin{aligned}\dot{V} + 2\delta V =& X^\top \left(F^\top P + PF + 2\delta P\right) X + 2X^\top P \mathcal{L} \zeta \\ &+ 2\gamma \sum_{n \geq N+1} (-\lambda_n + q_c + \delta) w_n^2 + 2\gamma \sum_{n \geq N+1} (a_n u + b_n v) w_n.\end{aligned}$$

The use of Young's inequality gives

$$\begin{aligned}2 \sum_{n \geq N+1} a_n w_n u &\leq \frac{1}{\alpha} \sum_{n \geq N+1} w_n^2 + \alpha \|a\|_{L^2}^2 u^2, \\ 2 \sum_{n \geq N+1} b_n w_n(t) v(t) &\leq \frac{1}{\alpha} \sum_{n \geq N+1} w_n^2 + \alpha \|b\|_{L^2}^2 v^2.\end{aligned}$$

for any $\alpha > 0$. From (48-49), we infer that

$$\begin{aligned}\dot{V} + 2\delta V \leq& \begin{bmatrix} X \\ \zeta \end{bmatrix}^\top \begin{bmatrix} F^\top P + PF + 2\delta P + \alpha\gamma G & P\mathcal{L} \\ \star & 0 \end{bmatrix} \begin{bmatrix} X \\ \zeta \end{bmatrix} \\ &+ 2\gamma \sum_{n \geq N+1} \left(-\lambda_n + q_c + \delta + \frac{1}{\alpha}\right) w_n^2.\end{aligned}$$

Recalling the definition $\zeta(t) = \sum_{n \geq N+1} c_n w_n(t)$, we obtain from Cauchy-Schwarz inequality that $\zeta(t)^2 \leq \|c\|_{L^2}^2 \sum_{n \geq N+1} w_n(t)^2$. Hence, for any $\beta > 0$,

$$\beta \|c\|_{L^2}^2 \sum_{n \geq N+1} w_n^2 - \beta \zeta^2 \geq 0. \tag{51}$$

Combining the two latter inequalities, we obtain that

$$\dot{V} + 2\delta V \leq \begin{bmatrix} X \\ \zeta \end{bmatrix}^\top \Theta \begin{bmatrix} X \\ \zeta \end{bmatrix} + 2\gamma \sum_{n \geq N+1} \Gamma_{1,n} w_n^2 \leq 0$$

where $\Gamma_{1,n} = -\lambda_n + q_c + \delta + \frac{1}{\alpha} + \frac{\beta\|c\|_{L^2}^2}{2\gamma} \leq \Gamma_{1,N+1}$ for all $n \geq N+1$. The assumptions (50) imply that $V(t) \leq e^{-2\delta t}V(0)$ for all $t \geq 0$, giving the claimed stability estimate for PDE trajectories evaluated in L^2-norm.

We now address the stability assessment of the system trajectories when evaluated in H^1-norm. To do so, in view of (25), we introduce the Lyapunov functional candidate:

$$V(X, w) = X^\top P X + \gamma \sum_{n\geq N+1} \lambda_n \langle w, \Phi_n\rangle^2 \tag{52}$$

with $X \in \mathbb{R}^{2N+1}$ and $w \in D(\mathcal{A})$. The computation of the time derivative of V along the system solutions (32b) and (46) gives

$$\begin{aligned}\dot V + 2\delta V = X^\top \left(F^\top P + PF + 2\delta P\right) X + 2X^\top P\mathcal{L}\zeta \qquad (53)\\ + 2\gamma \sum_{n\geq N+1} \lambda_n(-\lambda_n + q_c + \delta)w_n^2 + 2\gamma \sum_{n\geq N+1} \lambda_n(a_n u + b_n v)w_n(t).\end{aligned}$$

Using again Young's inequality, we obtain

$$2\sum_{n\geq N+1} \lambda_n a_n w_n u \leq \frac{1}{\alpha}\sum_{n\geq N+1} \lambda_n^2 w_n^2 + \alpha\|a\|_{L^2}^2 u^2 \tag{54a}$$

$$2\sum_{n\geq N+1} \lambda_n b_n w_n v \leq \frac{1}{\alpha}\sum_{n\geq N+1} \lambda_n^2 w_n^2 + \alpha\|b\|_{L^2}^2 v^2 \tag{54b}$$

for any $\alpha > 0$. Hence, owing to (48-49) and (51), we deduce that

$$\dot V + 2\delta V \leq \begin{bmatrix} X \\ \zeta\end{bmatrix}^\top \Theta \begin{bmatrix} X \\ \zeta\end{bmatrix} + 2\gamma \sum_{n\geq N+1} \lambda_n \Gamma_{2,n} w_n^2 \leq 0$$

with $\Gamma_{2,n} = -\lambda_n + q_c + \delta + \frac{\lambda_n}{\alpha} + \frac{\beta\|c\|_{L^2}^2}{2\gamma\lambda_n} \leq \Gamma_{2,N+1}$ for all $n \geq N+1$ where it has been used that $\alpha > 1$. Thus (50) implies that $V(t) \leq e^{-2\delta t}V(0)$ for all $t \geq 0$. The claimed stability estimate in H^1-norm is now obtained from (25), (29), and (52).

We conclude the proof by showing that one can always select the order of the observer $N \geq N_0 + 1$ large enough and find $P \succ 0$, $\alpha > 1$, and $\beta, \gamma > 0$ such that $\Theta \preceq 0$, $\Gamma_{1,N+1} \leq 0$, and $\Gamma_{2,N+1} \leq 0$. Owing to the Schur complement, we have $\Theta \preceq 0$ if and only if $F^\top P + PF + 2\delta P + \alpha\gamma G + \frac{1}{\beta} P\mathcal{L}\mathcal{L}^\top P^\top \preceq 0$. We now note that $A_1 + B_1 K + \delta I$ and $A_0 - LC_0 + \delta I$ are Hurwitz and $\|e^{(A_2+\delta I)t}\| \leq e^{-\kappa_0 t}$ with $\kappa_0 = \lambda_{N_0+1} - q_c - \delta > 0$. Moreover, $\|\tilde L C_1\| \leq \|L\|\|c\|_{L^2}$, $\|LC_1\| \leq \|L\|\|c\|_{L^2}$, and $\|B_{2,b}K + \begin{bmatrix} B_{2,a} & 0\end{bmatrix}\| \leq \|b\|_{L^2}\|K\| + \|a\|_{L^2}$. The right-hand sides of all the previous inequalities are independent of the order of the observer $N \geq N_0 + 1$.

Hence, Lemma 1, which is reported immediately after this proof, applied to $F + \delta I$ shows for any $N \geq N_0 + 1$ the existence of $P \succ 0$ such that $F^\top P + PF + 2\delta P = -I$ with $\|P\| = O(1)$ as $N \to +\infty$. Finally, we have (49) and $\|\mathcal{L}\| = \sqrt{2}\|L\|$ with g and L that are independent of N. Hence, with $\alpha = N^{1/4}$, $\beta = N$, and $\gamma = N^{-1/2}$, we infer from (26) the existence of a sufficiently large integer $N \geq N_0+1$, independent of the initial conditions, such that $\Theta \preceq 0$, $\Gamma_{1,N+1} \leq 0$, and $\Gamma_{2,N+1} \leq 0$. □

A technical lemma

The following lemma generalizes the statement of a result presented in[29] while the proof, reported below, remains essentially identical.

Lemma 1. *Let $n, m, N \geq 1$, $M_{11} \in \mathbb{R}^{n\times n}$ and $M_{22} \in \mathbb{R}^{m\times m}$ Hurwitz, $M_{12} \in \mathbb{R}^{n\times m}$, $M_{14}^N \in \mathbb{R}^{n\times N}$, $M_{24}^N \in \mathbb{R}^{m\times N}$, $M_{31}^N \in \mathbb{R}^{N\times n}$, $M_{33}^N, M_{44}^N \in \mathbb{R}^{N\times N}$, and*

$$F^N = \begin{bmatrix} M_{11} & M_{12} & 0 & M_{14}^N \\ 0 & M_{22} & 0 & M_{24}^N \\ M_{31}^N & 0 & M_{33}^N & 0 \\ 0 & 0 & 0 & M_{44}^N \end{bmatrix}.$$

We assume that there exist constants $C_0, \kappa_0 > 0$ such that $\|e^{M_{33}^N t}\| \leq C_0 e^{-\kappa_0 t}$ and $\|e^{M_{44}^N t}\| \leq C_0 e^{-\kappa_0 t}$ for all $t \geq 0$ and all $N \geq 1$. Moreover, we assume that there exists a constant $C_1 > 0$ such that $\|M_{14}^N\| \leq C_1$, $\|M_{24}^N\| \leq C_1$, and $\|M_{31}^N\| \leq C_1$ for all $N \geq 1$. Then there exists a constant $C_2 > 0$ such that, for any $N \geq 1$, there exists a symmetric matrix $P^N \in \mathbb{R}^{n+m+2N}$ with $P^N \succ 0$ such that $(F^N)^\top P^N + P^N F^N = -I$ and $\|P^N\| \leq C_2$.

Proof of Lemma 1. It is sufficient to show the existence of constants $\tilde{C}_0, \eta > 0$ such that $\|e^{F^N t}\| \leq \tilde{C}_0 e^{-\eta t}$ for all $t \geq 0$ and all $N \geq 1$. Indeed, in that case, $P^N = \int_0^\infty e^{(F^N)^\top t} e^{F^N t}\,\mathrm{d}t$ is well defined and satisfies the claimed properties. We introduce $F^N = F_1^N + F_2^N$ with

$$F_1^N = \begin{bmatrix} M_{11} & M_{12} & 0 & 0 \\ 0 & M_{22} & 0 & 0 \\ 0 & 0 & M_{33}^N & 0 \\ 0 & 0 & 0 & M_{44}^N \end{bmatrix}, \qquad F_2^N = \begin{bmatrix} 0 & 0\,0 & M_{14}^N \\ 0 & 0\,0 & M_{24}^N \\ M_{31}^N & 0\,0 & 0 \\ 0 & 0\,0 & 0 \end{bmatrix}.$$

Then there exist constants $\kappa, \tilde{C}_1, \tilde{C}_2 > 0$ such that $\|e^{F_1^N t}\| \leq \tilde{C}_1 e^{-\kappa t}$ and

$\|F_2^N\| \le \tilde{C}_2$ for all $t \ge 0$ and all $N \ge 1$. One can check that $(F_2^N)^3 = 0$ and

$$(F_1^N)^{n_i} = \begin{bmatrix} \bullet & \bullet & 0 & 0 \\ 0 & \bullet & 0 & 0 \\ 0 & 0 & \bullet & 0 \\ 0 & 0 & 0 & \bullet \end{bmatrix}$$

for any $n_i \ge 0$ and where "$\bullet$" denotes a possibly non zero element, that is not needed in this proof. Hence

$$(F_1^N)^{n_i} F_2^N = \begin{bmatrix} 0 & 0 & 0 & \bullet \\ 0 & 0 & 0 & \bullet \\ \bullet & 0 & 0 & 0 \\ 0 & 0 & 0 & 0 \end{bmatrix}$$

for any $n_i \ge 0$. We deduce that

$$\prod_{i=1}^{3} (F_1^N)^{n_i} F_2^N = \begin{bmatrix} 0 & 0 & 0 & \bullet \\ 0 & 0 & 0 & \bullet \\ \bullet & 0 & 0 & 0 \\ 0 & 0 & 0 & 0 \end{bmatrix}^3 = 0$$

for any $n_i \ge 0$. Therefore,

$$\prod_{i=1}^{3} e^{F_1^N t_i} F_2^N = \sum_{k_1 \ge 0} \sum_{k_2 \ge 0} \sum_{k_3 \ge 0} \frac{t_1^{k_1} t_2^{k_2} t_3^{k_3}}{k_1! k_2! k_3!} \prod_{i=1}^{3} (F_1^N)^{k_i} F_2^N = 0 \qquad (55)$$

for all $t_1, t_2, t_3 \ge 0$. Now we note that[b], for any square matrices A, B, $e^{(A+B)t} = e^{At} + \int_0^t e^{A(t-\tau)} B e^{(A+B)\tau} \, \mathrm{d}\tau$. Hence we have, using the last identity three times consecutively,

$$\begin{aligned} e^{F^N t} &= e^{F_1^N t} + \int_0^t e^{F_1^N (t-t_1)} F_2^N e^{F^N t_1} \, \mathrm{d}t_1 \\ &= e^{F_1^N t} + \int_0^t e^{F_1^N (t-t_1)} F_2^N e^{F_1^N t_1} \, \mathrm{d}t_1 \\ &\quad + \int_0^t \int_0^{t_1} e^{F_1^N (t-t_1)} F_2^N e^{F_1^N (t_1-t_2)} F_2^N e^{F^N t_2} \, \mathrm{d}t_2 \mathrm{d}t_1 \\ &= e^{F_1^N t} + \int_0^t e^{F_1^N (t-t_1)} F_2^N e^{F_1^N t_1} \, \mathrm{d}t_1 \\ &\quad + \int_0^t \int_0^{t_1} e^{F_1^N (t-t_1)} F_2^N e^{F_1^N (t_1-t_2)} F_2^N e^{F_1^N t_2} \, \mathrm{d}t_2 \mathrm{d}t_1 \end{aligned}$$

where the last identity has been obtained by using (55). Recalling that $\|e^{F_1^N t}\| \le \tilde{C}_1 e^{-\kappa t}$ and $\|F_2^N\| \le \tilde{C}_2$ for all $t \ge 0$ and all $N \ge 1$, the claimed conclusion holds. □

[b] $x(t) = e^{(A+B)t} x_0$ is such that $\dot{x}(t) = Ax(t) + u(t)$ with $u(t) = Bx(t)$. The claimed formula follows from $x(t) = e^{At} x_0 + \int_0^t e^{A(t-\tau)} u(\tau) \, \mathrm{d}\tau$.

3.3. *Dirichlet boundary measurement*

We extend the result of the previous section to the case of a reaction-diffusion PDE with Dirichlet boundary observation described by

$$z_t(t,x) = (p(x)z_x(t,x))_x + (q_c - q(x))z(t,x) \tag{56a}$$

$$z_x(t,0) = 0, \quad z(t,1) = u(t) \tag{56b}$$

$$z(0,x) = z_0(x) \tag{56c}$$

$$y(t) = z(t,0) \tag{56d}$$

for $t > 0$ and $x \in (0,1)$. We make throughout this subsection the assumption that $p \in \mathcal{C}^2([0,1])$ in order to use the asymptotic behavior (27).

3.3.1. *Spectral reduction*

The only change compared to the previous subsection is the modification of the nature of the observation operator. Hence, the spectral reduction is conducted identically but the observation (30d) is replaced by $\tilde{y}(t) = w(t,0) = y(t)$. Considering classical solutions for the PDE, we have $w(t,\cdot) \in D(\mathcal{A})$ for all $t \geq 0$. Hence, (32c) is simply replaced by $\tilde{y}(t) = \sum_{i\geq 1} \Phi_i(0) w_i(t)$.

3.3.2. *Control design*

Let $N_0 \geq 1$ and $\delta > 0$ be fixes so that $-\lambda_n + q_c < -\delta < 0$ for all $n \geq N_0 + 1$. Let $N \geq N_0 + 1$ be arbitrary and to be determined later. We proceed as in the previous subsection: we design an observer to estimate the N first modes of the plant while the state-feedback is performed on the N_0 first modes of the plant. Hence, the controller dynamics is described by

$$\dot{\hat{w}}_n(t) = (-\lambda_n + q_c)\hat{w}_n(t) + a_n u(t) + b_n v(t) + l_n\left(\hat{y}(t) - \tilde{y}(t)\right), \quad 1 \leq n \leq N_0 \tag{57a}$$

$$\dot{\hat{w}}_n(t) = (-\lambda_n + q_c)\hat{w}_n(t) + a_n u(t) + b_n v(t), \quad N_0 + 1 \leq n \leq N \tag{57b}$$

$$\hat{y}(t) = \sum_{i=1}^{N} \Phi_i(0)\hat{w}_i(t) \tag{57c}$$

$$v(t) = \dot{u}(t) = \sum_{i=1}^{N_0} k_i \hat{w}_i(t) + k_u u(t) \tag{57d}$$

which is the same as the one described by (33) but with measurement, originally given by (33a), replaced by (57a). In this context, (36) is replaced

by the following, defined for $1 \leq n \leq N_0$,

$$\dot{\hat{w}}_n(t) = (-\lambda_n + q_c)\hat{w}_n(t) + a_n u(t) + b_n v(t) \\ - l_n \sum_{i=1}^{N_0} \Phi_i(0) e_i(t) + l_n \sum_{i=N_0+1}^{N} \frac{\Phi_i(0)}{\sqrt{\lambda_i}} \tilde{e}_i(t) + l_n \zeta(t).$$

Here $\zeta(t)$ is defined by $\zeta(t) = \sum_{i \geq N+1} \Phi_i(0) w_i(t)$ while, following,[41] we introduced the scaled error of observation $\tilde{e}_n(t) = \sqrt{\lambda_n} e_n(t)$ with e_n given by (35). The definitions of C_0 and C_1 are replaced by

$$C_0 = \left[\Phi_1(0) \ \dots \ \Phi_{N_0}(0)\right], \ C_1 = \left[\frac{\Phi_{N_0+1}(0)}{\sqrt{\lambda_{N_0+1}}} \ \dots \ \frac{\Phi_N(0)}{\sqrt{\lambda_N}}\right] \tag{58}$$

and defining

$$\tilde{E}^{N-N_0}(t) = \left[\tilde{e}_{N_0+1}(t) \ \dots \ \tilde{e}_N(t)\right]^\top,$$

we obtain in replacement of (37) and (39) that

$$\dot{\hat{W}}^{N_0}(t) = A_0 \hat{W}^{N_0}(t) + B_{0,a} u(t) + B_{0,b} v(t) \\ - LC_0 E^{N_0}(t) - LC_1 \tilde{E}^{N-N_0}(t) - L\zeta(t) \tag{59}$$

and

$$\dot{\hat{W}}_a^{N_0}(t) = A_1 \hat{W}_a^{N_0}(t) + B_1 v(t) - \tilde{L} C_0 E^{N_0}(t) - \tilde{L} C_1 \tilde{E}^{N-N_0}(t) - \tilde{L}\zeta(t), \tag{60}$$

respectively. In this framework, the command input is still given by (40). Using now (34) and (59), the error dynamics originally given by (42) is now replaced by

$$\dot{E}^{N_0}(t) = (A_0 + LC_0) E^{N_0}(t) + LC_1 \tilde{E}^{N-N_0}(t) + L\zeta(t). \tag{61}$$

Moreover, since $\dot{e}_n(t) = (-\lambda_n + q_c) e_n(t)$, we have $\dot{\tilde{e}}_n(t) = (-\lambda_n + q_c)\tilde{e}_n(t)$ for all $N_0 + 1 \leq n \leq N$. Then (44) is replaced by

$$\dot{\tilde{E}}^{N-N_0}(t) = A_2 \tilde{E}^{N-N_0}(t). \tag{62}$$

Putting together (40), (43), and (60-62), the introduction of

$$X(t) = \mathrm{col}(\hat{W}_a^{N_0}(t), E^{N_0}(t), \hat{W}^{N-N_0}(t), \tilde{E}^{N-N_0}(t)),$$

shows that (46) holds with the different matrices defined by (47).

Remark 4. Based on the arguments of Claim 1 and Claim 2, we have that (A_1, B_1) is controllable and (A_0, C_0) is observable.

3.3.3. *Stability analysis*

We introduce the constant $M_{1,\Phi} = \sum_{n\geq 2} \frac{\Phi_n(0)^2}{\lambda_n}$. Note that this constant is well defined (i.e., finite) when $p \in \mathcal{C}^2([0,1])$ due to (26-27).

Theorem 7. *Let $p \in \mathcal{C}^2([0,1])$ with $p > 0$, $q \in \mathcal{C}^0([0,1])$ with $q \geq 0$, and $q_c \in \mathbb{R}$. Consider the reaction-diffusion system described by (56). Let $N_0 \geq 1$ and $\delta > 0$ be given such that $-\lambda_n + q_c < -\delta < 0$ for all $n \geq N_0 + 1$. Let $K \in \mathbb{R}^{1\times(N_0+1)}$ and $L \in \mathbb{R}^{N_0}$ be such that $A_1 + B_1 K$ and $A_0 - LC_0$ are Hurwitz with eigenvalues that have a real part strictly less than $-\delta < 0$. Assume that there exist $N \geq N_0 + 1$, $P \succ 0$, $\alpha > 1$, and $\beta, \gamma > 0$ such that $\Theta \preceq 0$, where Θ is defined by (50a), and*

$$\Gamma_{3,N+1} = -\left(1 - \frac{1}{\alpha}\right)\lambda_{N+1} + q_c + \delta + \frac{\beta M_{1,\Phi}}{2\gamma} \leq 0. \tag{63}$$

Then the origin of the closed-loop system composed of the plant (56) and the controller (57) is exponentially stable in H^1-norm in the sense that there exists $M > 0$ such that, for any $\hat{w}_n(0) \in \mathbb{R}$, for any $z_0 \in H^2(0,1)$ and any $u(0) \in \mathbb{R}$ such that $z_0'(0) = 0$ and $z_0(1) = u(0)$, the classical solution of the closed-loop system satisfies

$$u(t)^2 + \sum_{n=1}^{N} \hat{w}_n(t)^2 + \|z(t,\cdot)\|_{H^1}^2 \leq M e^{-2\delta t}\left(u(0)^2 + \sum_{n=1}^{N} \hat{w}_n(0)^2 + \|z_0\|_{H^1}^2\right).$$

for all $t \geq 0$. Moreover, the above constraints are always feasible for N large enough.

Remark 5. The previous result deals with the exponential stability of the closed-loop system in H^1-norm. This type of approach can be extended to a number of control design problems such as:

- L^2 stability using the same control strategy;[40]
- Robin boundary conditions;[34,40]
- Neumann boundary observations;[41]
- input/output delayed boundary control;[38,42]
- nonlinearities[34,39,40]
- regulation problems.[37]

Proof. Consider again the Lyapunov function candidate defined by (52). The computation of its time derivative along the system solutions (32b) and (46) gives (53). Since $\zeta(t) = \sum_{n\geq N+1} \Phi_n(0) w_n(t)$, we have by Cauchy-Schwarz inequality that $\zeta(t)^2 \leq M_{1,\Phi} \sum_{n\geq N+1} \lambda_n w_n(t)^2$ hence

$\beta M_{1,\Phi} \sum_{n\geq N+1} \lambda_n w_n(t)^2 - \beta\zeta(t)^2 \geq 0$ for any $\beta > 0$. Using this latter estimate into (53) and invoking Young's inequality as in (54) along with (48-49), we deduce that

$$\dot{V} + 2\delta V \leq \begin{bmatrix} X \\ \zeta \end{bmatrix}^\top \Theta \begin{bmatrix} X \\ \zeta \end{bmatrix} + 2\gamma \sum_{n\geq N+1} \lambda_n \Gamma_{3,n} w_n(t)^2 \leq 0$$

where $\Gamma_{3,n} = -\left(1 - \frac{1}{\alpha}\right)\lambda_n + q_c + \delta + \frac{\beta M_{1,\Phi}}{2\gamma} \leq \Gamma_{3,N+1}$ for all $n \geq N+1$. Hence the assumptions give $V(t) \leq e^{-2\delta t} V(0)$ for all $t \geq 0$. Proceeding as in the previous proof, we obtain the claimed estimate.

To complete the proof, it remains to show that one can always select $N \geq N_0 + 1$ large enough, $P \succ 0$, $\alpha > 1$, and $\beta, \gamma > 0$, such that $\Theta \preceq 0$ and $\Gamma_{3,N+1} \leq 0$. Owing to the Schur complement, $\Theta \preceq 0$ is equivalent to $F^\top P + PF + 2\delta P + \alpha\gamma G + \frac{1}{\beta} P\mathcal{L}\mathcal{L}^\top P^\top \preceq 0$. Applying Lemma 1 to[c] $F + \delta I$, we have for any $N \geq N_0 + 1$ the existence of $P \succ 0$ such that $F^\top P + PF + 2\delta P = -I$ with $\|P\| = O(1)$ as $N \to +\infty$. Moreover, we have (49) and $\|\mathcal{L}\| = \sqrt{2}\|L\|$ with g and L that are independent of N. Hence, setting $\alpha = \beta = \sqrt{N}$ and $\gamma = N^{-1}$, we obtain from (26) the existence of a sufficiently large integer $N \geq N_0 + 1$ such that $\Theta \preceq 0$ and $\Gamma_{3,N+1} \leq 0$. □

Example 6. Consider the Dirichlet boundary measurement setting described by (56). Let $p = 1$, $q = 0$, and $q_c = 3$, giving an unstable open-loop system. To obtain the closed-loop exponential decay rate $\delta = 0.5$, we set $N_0 = 1$. Then we run the following Python code. On lines 14-18, we compute the eigenvalues and eigenvectors of the problem. On lines 26-29, we check whether N_0 is selected adequately.

```
1  import numpy as np
2  import control
3  import scipy.integrate as integrate
4  import cvxpy as cp
5  import matplotlib as mpl
6  import matplotlib.pyplot as plt
7  from mpl_toolkits.mplot3d import Axes3D
8
9  # Parameters of the PDE
10 p = 1
11 q = 3 # this is q_c (q is zero)
12 delta = 0.5
13
14 # Eigenstructures
```

[c]This is possible because, owing to the definition (58) of the matrix C_1, it ensures that $\|C_1\| = O(1)$ as $N \to +\infty$. This remark is key to allow the application of Lemma 1.

```
15 def lam(n):
16     return (n-1/2)**2*np.pi**2*p
17 def phi(n,x):
18     return np.sqrt(2)*np.cos((n-1/2)*np.pi*x)
19
20 # Equivalent bounded input operators
21 def input_a(x):
22     return 2*p + q*x**2 # case of p constant and q=0
23 def input_b(x):
24     return -x**2
25
26 # Number of modes to be stabilized
27 N0 = 0
28 while ( -lam(N0+1) + q) >= -delta:
29     N0 = N0 + 1;
```

On line 36, we set define the number N of modes for the observer. Then we start building the matrices necessary to check the conditions of Theorem 7 after line 49.

```
30 if N0 == 0:
31     print('All the modes of the open-loop system are < -delta')
32 else:
33     print('The number of modes to be stabilized is N_0='+str(N0
       ))
34
35 # Select the number of modes for the observer
36 N = N0+2
37
38 # Matrices of the truncated model
39 tmp=[]
40 for i in range(1,N+1):
41     #print(i)
42     tmp.append(-lam(i)+q)
43
44 A0  = np.diag(tmp[0:N0])
45 A2  = np.diag(tmp[N0:N+1])
46
47 B0a = []; B0b = []; B2a = []; B2b = []; C0  = []; C1  = []
48
49 for k in range(1,N0+1):
50     def fun(x):
51         return input_a(x)*phi(k,x)
52     y,err= integrate.quad(fun,0,1)
53     B0a.append(y)
54     def fun(x):
55         return input_b(x)*phi(k,x)
56     y,err=integrate.quad(fun,0,1)
57     B0b.append(y)
58     C0.append(phi(k,0))
```

```
59
60 for k in range(1,N-N0+1):
61     def fun(x):
62         return input_a(x)*phi(N0+k,x)
63     y,err=integrate.quad(fun,0,1)
64     B2a.append(y)
65     def fun(x):
66         return input_b(x)*phi(N0+k,x)
67     y,err=integrate.quad(fun,0,1)
68     B2b.append(y)
69
70 for k in range(N0+1,N+1):
71     C1.append(phi(k,0)/np.sqrt(lam(k)))
72
73 B0a = np.array(B0a).reshape((N0,1))
74 B0b = np.array(B0b).reshape((N0,1))
75 B2a = np.array(B2a).reshape((N-N0,1))
76 B2b = np.array(B2b).reshape((N-N0,1))
77 C0  = np.array(C0).reshape((1,N0))
78 C1  = np.array(C1).reshape((1,N-N0))
79
80 A1 = np.vstack((np.zeros((1,N0+1)),np.hstack((B0a,A0))))
81 B1 = np.vstack((np.ones((1,1)),B0b))
```

The control matrix K and the observation matrix L are chosen separately on lines 84 and 88. The feedback gain is $K = \begin{bmatrix}-5.0058 & -2.7748\end{bmatrix}$, and the observer gain is $L = 1.4373$. The matrix inequalities in Theorem 7 are built after line 104. The Schur complement is used to rewrite (63) into a linear matrix inequality in the unknown variables as described in Remark 3.

```
82 # Pole placement for the state feedback
83 Pdes = np.linspace(-N0-1-delta,-1-delta,N0+1)
84 K    = -control.place(A1,B1,Pdes);
85
86 # Pole placement for the  observer
87 Qdes = np.linspace(-N0-delta,-1-delta,N0)
88 L0   = -control.place(A0.T,C0.T,Qdes).T;
89
90 tL0 =  np.vstack((np.zeros((1,1)),L0))
91
92 def hcont(A,B,C,D): # help to build F by concatenate
       horizontally
93     return np.hstack((np.hstack((np.hstack((A,B)),C)),D))
94
95 F1=hcont(A1+np.dot(B1,K),np.dot(tL0,C0),np.zeros((N0+1,N-N0)),
       np.dot(tL0,C1))
96 F2=hcont(np.zeros((N0,N0+1)),A0+np.dot(L0,C0),np.zeros((N0,N-N0
       )),np.dot(L0,C1))
```

```
97  F3=hcont(np.dot(B2b,K)+np.hstack((B2a,np.zeros((N-N0,N0)))),np.
        zeros((N-N0,N0)),A2,np.zeros((N-N0,N-N0)))
98  F4=hcont(np.zeros((N-N0,N0+1)),np.zeros((N-N0,N0)),np.zeros((N-
        N0,N-N0)),A2)
99
100 F = np.vstack((np.vstack((np.vstack((F1,F2)),F3)),F4))
101
102 cL = np.vstack((np.vstack((np.vstack((tL0,L0)),np.zeros((N-N0
        ,1)))),np.zeros((N-N0,1))))
103
104 # LMI conditions
105 gamma = 0.00155 #Fix the decision variable gamma > 0
106 M_phi = 12/(np.pi**2*p)
107 E  = np.hstack((np.ones((1,1)),np.zeros((1,2*N))))
108 tK = np.hstack((K,np.zeros((1,2*N-N0))))
109
110 def fun(x):
111     return input_a(x)**2
112 y,err=integrate.quad(fun,0,1)
113 norm_a = np.sqrt(y)
114
115 def fun(x):
116     return input_b(x)**2
117 y,err=integrate.quad(fun,0,1)
118 norm_b = np.sqrt(y)
119
120 # check Matrix inequalities
121 alpha = cp.Variable()
122 beta  = cp.Variable()
123 P     = cp.Variable((2*N+1,2*N+1),PSD=True)
124
125 # build the constraints
126 constr =  [alpha >= 1]
127 constr += [beta >= 0]
128 M11= (-lam(N+1)+ q +delta+beta*M_phi/(2*gamma))*np.ones((1,1))
129 M12 =np.sqrt(np.abs(-lam(N+1)))*np.ones((1,1))
130 Gamma=cp.bmat([[ M11, M12],
131                [M12.T,-alpha*np.ones((1,1))] ])
132 constr += [Gamma <<0]
133 # build the last constraint
134 G = norm_a**2*(np.dot(E.T,E))+norm_b**2*(np.dot(tK.T,tK))
135 M11=F.T @ P +P @ F+ 2* delta * P + alpha*gamma*G
136 M12=P@ cL
137 matConstr = cp.bmat([[ M11 , M12],
138                      [M12.T, -beta*np.ones((1,1))]])
139 constr +=  [matConstr << 0]
```

The feasability of the convex problem is checked on line 142 using the solver in CVXOPT with cvxpy package. The conditions of Theorem 7 are thus feasible for $N = 3$. Then the values of the unknown variables are

stored, and matrix constraints are checked before line 166.

```
prob = cp.Problem(cp.Maximize(1),constr)
prob.solve(solver='CVXOPT')
print(prob.status)

P=P.value; alpha=alpha.value; beta=beta.value
w,v=np.linalg.eig(P)
# w should be positive as all constraints
m=np.min([alpha-1,np.min([beta,np.min(w)])])
# first matrix inequality
M11= (-lam(N+1)+ q +delta+beta*M_phi/(2*gamma))
M12 =np.sqrt(np.abs(-lam(N+1)))
M1=np.hstack((M11,M12))
M2=np.hstack((M12,-alpha))
M=np.vstack((M1,M2))
w1,v=np.linalg.eig(M) #max w1 should be negative
# second matrix inequality
M11=np.dot(F.T,P)+np.dot(P,F)+ 2*delta*P +alpha*gamma*G
M12=np.dot(P,cL)
M1=np.hstack((M11,M12))
M2=np.hstack((M12.T,-beta*np.ones((1,1))))
M=np.vstack((M1,M2))
w2,v=np.linalg.eig(M) #max w2 should be negative
mm=np.min([m,-np.max(w2),-np.max(w2)])
if mm<0:
    print('Matrix inequalities not satisfied')
else:
    print('Matrix inequalities satisfied')
```

The code to numerically compute the behavior of the closed-loop system associated with the initial condition $z_0(x) = 1 + x^2$, and with zero initial condition for the observer, obtained based on the 50 dominant modes of the plant is given after line 167.

```
# Simulation
# Number of modes for simulation
Nsim = 50;

if Nsim < 2*N:
    print('Number of modes for simulation strictly less than 2*
    N')

tmp=[]
for i in range(1,Nsim+1):
    tmp.append(-lam(i)+q)

# Matrices of the truncated model
Ass   = np.diag(tmp[0:Nsim]) # System used for simulations
    based on Nsim dominant modes
Aobs  = np.diag(tmp[0:N])
```

```
181
182 Bssa  = []; Bssb  = []; Bobsa = []; Bobsb = []; Css = []; Cobs
        = []
183 for k in range(1,Nsim+1):
184    Css.append(phi(k,0))
185    if k<N+1:
186        Cobs.append(phi(k,0))
187
188 Lobs = np.vstack((L0,np.zeros((N-N0,1))))
189 Lobs=Lobs.reshape(N,)
190
191 for k in range(1,Nsim+1):
192     def fun(x):
193         return input_a(x)*phi(k,x)
194     y,err= integrate.quad(fun,0,1)
195     Bssa.append(y)
196     if k<N+1:
197         Bobsa.append(y)
198     def fun(x):
199         return input_b(x)*phi(k,x)
200     y,err=integrate.quad(fun,0,1)
201     Bssb.append(y)
202     if k<N+1:
203         Bobsb.append(y)
204
205 Bssa  = np.array(Bssa).reshape((Nsim,))
206 Bssb  = np.array(Bssb).reshape((Nsim,))
207 Bobsa = np.array(Bobsa).reshape((N,))
208 Bobsb = np.array(Bobsb).reshape((N,))
209
210 # Initial condition (IC)
211 def z0(x):
212     return 1+x**2 # IC of the PDE
213
214 u0 = z0(1) # IC of the control
215
216 def w0(x):
217     return z0(x) - x**2*u0 #IC of the homogeneous Dirichlet
        system
218
219 zsim0=[]
220 for k in range(1,Nsim+1):
221     def fun(x):
222         return w0(x)*phi(k,x)
223     y,err=integrate.quad(fun,0,1)
224     zsim0.append(y) # Coefficients of projection of the IC w0
225
226 zsim0 = np.array(zsim0).reshape((Nsim,1))
227
228 # Check the validity of the projection (graph)
```

```
space  = np.linspace(0,1,100)
check  = np.zeros((len(space),1))

for kx in range(len(space)):
    for k in range(Nsim):
        check[kx,0] = check[kx,0] + zsim0[k,0]*phi(k,space[kx])

fig , ax= plt.subplots()
ax.set_title('To check')

ax.plot(space, w0(space),'g-', label='w0')
ax.plot(space, check,'r.', label='approx')
ax.legend()
# plt.savefig('to_check.png',bbox_inches='tight')

# time discretization
Tsim = 6;

def ode(z,t):
    u=float(z[0])
    zsim=z[1:Nsim+1]
    zhat=z[Nsim+1:]
    whata=np.vstack((u,zhat[0:N0]))
    v=float(np.dot(K,whata))
    udot=v
    zsimdot=np.dot(Ass,zsim)+np.dot(Bssa,u)+np.dot(Bssb,v)
    zhatdot=np.dot(Aobs,zhat)+np.dot(Bobsa,u)+np.dot(Bobsb,v)
    zhatdot+=-Lobs*float(np.dot(Css,zsim)-np.dot(Cobs,zhat))
    zdot=np.hstack((np.hstack((udot*np.ones(1),zsimdot)),
    zhatdot))
    return zdot

t=np.linspace(0,Tsim,60)

# Initial condition of the full state
zhat0=np.zeros((N,1))
z0tot=np.vstack((np.vstack((u0,zsim0)),zhat0))
z0tot=z0tot.reshape(len(z0tot),)
sol=integrate.odeint(ode,z0tot,t)

Mstate_z  = np.zeros((len(space),len(t))) # PDE in original
    coordinates z
Mstate_w  = np.zeros((len(space),len(t))) # PDE in homogeneous
    coordinates w
MstateObs = np.zeros((len(space),len(t))) # State of the
    observer

for k_time in range(len(t)):
    for k_space in range(len(space)):
        for k in range(Nsim):
```

```
            Mstate_w[k_space,k_time] +=  sol[k_time,k+1]*phi(k,space[k_space])
            Mstate_z[k_space,k_time] = Mstate_w[k_space,k_time] + space[k_space]**2*sol[k_time,0]
            for k in range(N):
                MstateObs[k_space,k_time] += MstateObs[k_space,k_time] + sol[k_time,k+1+Nsim]*phi(k,space[k_space])

mpl.rcParams['legend.fontsize'] = 10
fig = plt.figure(); ax = fig.add_subplot(111, projection='3d')
SX, ST = np.meshgrid(space, t)
ax.plot_surface(SX, ST, Mstate_z.T, cmap='jet')
ax.set_xlabel('x')
ax.set_ylabel('t')
ax.set_zlabel('z(t,x)')
ax.view_init(elev=15, azim=20) # adjust view so it is easy to see
plt.savefig('pde-3d.png')

fig = plt.figure(); ax = fig.add_subplot(111, projection='3d')
ax.plot_surface(SX, ST, Mstate_w.T-MstateObs.T, cmap='jet')
ax.set_xlabel('x')
ax.set_ylabel('t')
ax.set_zlabel('$e(t,x)$')
ax.view_init(elev=15, azim=20) # adjust view so it is easy to see
plt.savefig('pde-error.png')
```

Fig. 6 depicts the corresponding solution. The convergence of the state towards 0 can be observed, confirming the predictions of Theorem 7. The observation error is given on the same figure.

The time-evolutions of the control and output variables are given in Figure 7.

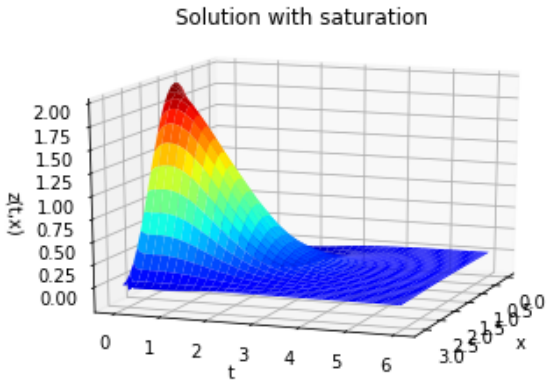

(a) State $z(t, x)$

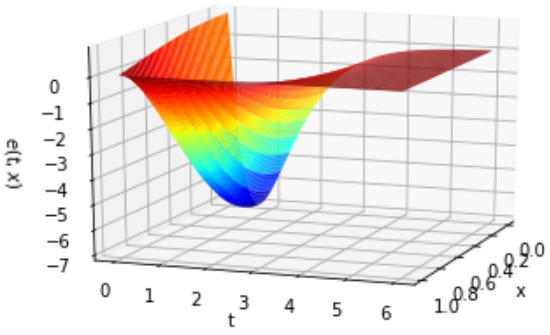

(b) Observation error $e(t, x) = w(t, x) - \sum_{n=1}^{N} \hat{w}_n(t)\Phi_n(x)$

Fig. 6. State z and observation error e in closed-loop with Dirichlet boundary measurement feedback control for the reaction-diffusion system (56)

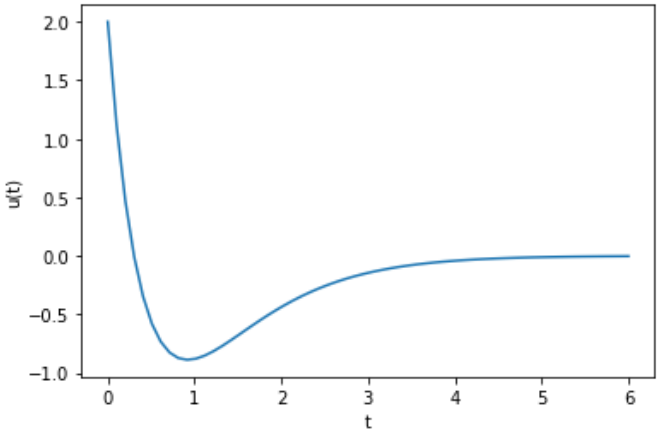

(a) Control $u(t)$

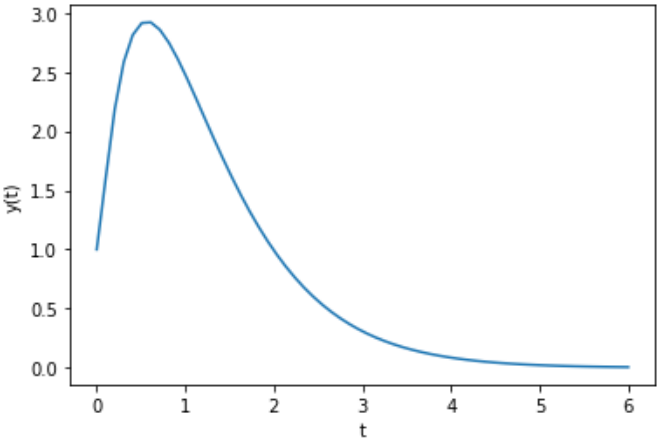

(b) Output $y(t)$

Fig. 7. Control $u(t) = z(t, 1)$ and output $y(t, x) = z(t, 0)$ for the closed-loop system with Dirichlet boundary measurement feedback control for the reaction-diffusion system (56)

3.4. *Saturated control with internal measurement*

In this section we consider the stability analysis of parabolic PDEs when controlled in the presence of input saturations. In this setting, the control inputs apply in the domain by means of a bounded operator while the observation can take the form of either a bounded or an unbounded measurement operator. As in the previous section, the adopted approach relies on spectral-reduction methods. The presence of the input saturation is handled in the stability analysis by invoking the generalized sector condition reported in Section 2. This type of control design problem was reported in[48] in the case of a state-feedback. We consider here the case of an output feedback by combining the Lyapunov-based analysis procedure discussed in the previous sections and the previously generalized sector condition. This allows the derivation of a set of sufficient conditions ensuring the local exponential stability of the origin of the closed-loop system. A subset of the domain of attraction is characterized by the decision variables of the abovementionned sufficient constraints.

Problem description

Let the reaction-diffusion equation with Robin boundary conditions described by

$$z_t(t,x) = (p(x)z_x(t,x))_x - (q(x)-q_c)z(t,x) + \sum_{k=1}^{m} b_k(x)u_{\mathrm{sat},k}(t) \tag{64a}$$

$$\cos(\theta_1)z(t,0) - \sin(\theta_1)z_x(t,0) = 0 \tag{64b}$$

$$\cos(\theta_2)z(t,1) + \sin(\theta_2)z_x(t,1) = 0 \tag{64c}$$

$$z(0,x) = z_0(x) \tag{64d}$$

with measurement equation

$$y(t) = \int_0^1 c(x)z(t,x)\,\mathrm{d}x. \tag{65}$$

Here we have $\theta_1, \theta_2 \in [0, \pi/2]$, $p \in \mathcal{C}^1([0,1])$ with $p > 0$, $q \in \mathcal{C}^0([0,1])$ with $q \geq 0$, $q_c \in \mathbb{R}$, and $b_k \in L^2(0,1)$. The scalar control input $u_{\mathrm{sat},k}(t) \in \mathbb{R}$ act on the system. Hence, (64) can be written as

$$z_t(t,\cdot) = -\mathcal{A}z(t,\cdot) + q_c z(t,\cdot) + \sum_{k=1}^{m} b_k u_{\mathrm{sat},k}(t) \tag{66a}$$

$$z(0,\cdot) = z_0 \tag{66b}$$

where $\mathcal{A}$ is the Sturm-Liouville operator defined at the beginning of this section.

The control input is assumed to be subject to saturations; for a given vector $s = \begin{bmatrix} s_1 & s_2 & \dots & s_m \end{bmatrix}^\top \in (\mathbb{R}_+^*)^m$, we define $\text{sat} : \mathbb{R}^m \to \mathbb{R}^m$ by (17). Hence, the input $u_{\text{sat},k}(t)$ that is applied to the plant is expressed in function of the actual control inputs $u_k(t)$ as

$$u_{\text{sat}}(t) = \text{sat}(u(t)).$$

with $u_{\text{sat}}(t) = \begin{bmatrix} u_{\text{sat},1}(t) & u_{\text{sat},2}(t) & \dots & u_{\text{sat},m}(t) \end{bmatrix}^\top$ and $u(t) = \begin{bmatrix} u_1(t) & u_2(t) & \dots & u_m(t) \end{bmatrix}^\top$.

In this context and similarly to[48] in the case of a state-feedback, the objective is to study the local stabilization of (64) with measurement (65) for the controller architecture studied in the first part of this section but in the presence of the saturating control inputs while estimating the associated domain of attraction.

3.4.1. *Spectral analysis*

Consider again the coefficients of projection $z_n(t) = \langle z(t,\cdot), \Phi_n \rangle$, $b_{n,k} = \langle b_k, \Phi_n \rangle$, and $c_n = \langle c, \Phi_n \rangle$. As done for (31) without saturation, the projection of the system solutions (66) and the output equation (65) into the Hilbert basis $\{\Phi_n : n \geq 1\}$ gives the following representation:

$$\dot{z}_n(t) = (-\lambda_n + q_c) z_n(t) + \sum_{k=1}^{m} b_{n,k} u_{\text{sat},k}(t) \tag{67a}$$

$$y(t) = \sum_{n \geq 1} c_n z_n(t) \tag{67b}$$

Proceeding as in the previous subsection, we consider the feedback law taking the form of a finite-dimensional state-feedback coupled with a finite-dimensional observer. More precisely, let $\delta > 0$ and $N_0 \geq 1$ be such that $-\lambda_n + q_c < -\delta$ for all $n \geq N_0 + 1$. For a given integer $N \geq N_0 + 1$ to be selected later, the controller architecture takes the form:

$$\dot{\hat{z}}_n(t) = (-\lambda_n + q_c)\hat{z}_n(t) + \sum_{k=1}^{m} b_{n,k} u_{\text{sat},k}(t) + L_n \left\{ \sum_{k=1}^{N} c_k \hat{z}_k(t) - y(t) \right\}, \quad 1 \leq n \leq N \tag{68a}$$

$$u_k(t) = \sum_{l=1}^{N_0} K_{k,l} \hat{z}_l(t), \quad 1 \leq k \leq m \tag{68b}$$

with $L_n, K_{k,l} \in \mathbb{R}$ where $L_n = 0$ for $N_0 + 1 \leq n \leq N$.

We define the errors of estimation $e_n(t) = z_n(t) - \hat{z}_n(t)$. As in the previous subsection, we introduce the vectors and matrices defined by $\hat{Z}^{N_0} = \begin{bmatrix}\hat{z}_1 \dots \hat{z}_{N_0}\end{bmatrix}^\top$, $\hat{Z}^{N-N_0} = \begin{bmatrix}\hat{z}_{N_0+1} \dots \hat{z}_N\end{bmatrix}^\top$, $E^{N_0} = \begin{bmatrix}e_1 \dots e_{N_0}\end{bmatrix}^\top$, $E^{N-N_0} = \begin{bmatrix}e_{N_0+1} \dots e_N\end{bmatrix}^\top$, $A_0 = \mathrm{diag}(-\lambda_1+q_c, \dots, -\lambda_{N_0}+q_c)$, $A_1 = \mathrm{diag}(-\lambda_{N_0+1}+q_c, \dots, -\lambda_N+q_c)$, $B_0 = (b_{n,k})_{1\leq n\leq N_0, 1\leq k\leq m}$, $B_1 = (b_{n,k})_{N_0+1\leq n\leq N, 1\leq k\leq m}$, $C_0 = \begin{bmatrix}c_1 \dots c_{N_0}\end{bmatrix}$, $C_1 = \begin{bmatrix}c_{N_0+1} \dots c_N\end{bmatrix}$, $L = \begin{bmatrix}L_1 \dots L_{N_0}\end{bmatrix}^\top$, and $K = (K_{k,l})_{1\leq k\leq m, 1\leq l\leq N_0}$. This leads to

$$\begin{aligned}
\dot{\hat{Z}}^{N_0} &= A_0\hat{Z}^{N_0} + B_0u_{\mathrm{sat}} - LC_0E^{N_0} - LC_1E^{N-N_0} - L\zeta\\
\dot{E}^{N_0} &= (A_0 + LC_0)E^{N_0} + LC_1E^{N-N_0} + L\zeta\\
\dot{\hat{Z}}^{N-N_0} &= A_1\hat{Z}^{N-N_0} + B_1u_{\mathrm{sat}}\\
\dot{E}^{N-N_0} &= A_1E^{N-N_0}\\
u &= K\hat{Z}^{N_0}
\end{aligned}$$

where $\zeta(t) = \sum_{n\geq N+1} c_n z_n(t)$ is the residue of measurement. Owing to the definition of the deadzone nonlinearity (20), we infer that

$$\begin{aligned}
\dot{\hat{Z}}^{N_0} &= (A_0 + B_0K)\hat{Z}^{N_0} - LC_0E^{N_0} - LC_1E^{N-N_0} - L\zeta + B_0\phi(K\hat{Z}^{N_0})\\
\dot{E}^{N_0} &= (A_0 + LC_0)E^{N_0} + LC_1E^{N-N_0} + L\zeta\\
\dot{\hat{Z}}^{N-N_0} &= A_1\hat{Z}^{N-N_0} + B_1K\hat{Z}^{N_0} + B_1\phi(K\hat{Z}^{N_0})\\
\dot{E}^{N-N_0} &= A_1E^{N-N_0}.
\end{aligned}$$

Introducing the state-vector

$$X = \mathrm{col}(\hat{Z}^{N_0}, E^{N_0}, \hat{Z}^{N-N_0}, E^{N-N_0})$$

and the matrices

$$F = \begin{bmatrix} A_0 + B_0K & -LC_0 & 0 & -LC_1\\ 0 & A_0 + LC_0 & 0 & LC_1\\ B_1K & 0 & A_1 & 0\\ 0 & 0 & 0 & A_1 \end{bmatrix}, \quad \mathcal{L} = \begin{bmatrix} -L\\ L\\ 0\\ 0 \end{bmatrix}, \quad \mathcal{L}_\phi = \begin{bmatrix} B_0\\ 0\\ B_1\\ 0, \end{bmatrix}$$

we deduce that

$$\dot{X} = FX + \mathcal{L}\zeta + \mathcal{L}_\phi\phi(K\hat{Z}^{N_0}). \tag{69}$$

We finally define $E = \begin{bmatrix}I\ 0\ 0\ 0\end{bmatrix}$ and $\tilde{K} = \begin{bmatrix}K\ 0\ 0\ 0\end{bmatrix}$, which are such that

$$\hat{Z}^{N_0} = EX, \qquad u = \tilde{K}X.$$

3.4.2. *Stability results*

For $z \in L^2(0,1)$ and $\hat{z} \in \mathbb{R}^N$, we define

$$\Pi(z,\hat{z}) = \begin{bmatrix} \Pi_1(z,\hat{z}) \\ \Pi_2(z,\hat{z}) \\ \Pi_3(z,\hat{z}) \\ \Pi_4(z,\hat{z}) \end{bmatrix}$$

with

$$\Pi_1(z,\hat{z}) = \begin{bmatrix} \hat{z}_1 \\ \vdots \\ \hat{z}_{N_0} \end{bmatrix}, \quad \Pi_2(z,\hat{z}) = \begin{bmatrix} \langle z, \Phi_1 \rangle - \hat{z}_1 \\ \vdots \\ \langle z, \Phi_{N_0} \rangle - \hat{z}_{N_0} \end{bmatrix},$$

and

$$\Pi_3(z,\hat{z}) = \begin{bmatrix} \hat{z}_{N_0+1} \\ \vdots \\ \hat{z}_N \end{bmatrix}, \quad \Pi_4(z,\hat{z}) = \begin{bmatrix} \langle z, \Phi_{N_0+1} \rangle - \hat{z}_{N_0+1} \\ \vdots \\ \langle z, \Phi_N \rangle - \hat{z}_N \end{bmatrix}.$$

Stabilization in L^2 norm Let us now state and prove a result providing a stabilization for (64) in L^2-norm. This result is extracted from.[34]

Theorem 8. *Let $\theta_1, \theta_2 \in [0, \pi/2]$, $p \in \mathcal{C}^1([0,1])$ with $p > 0$, $q \in \mathcal{C}^0([0,1])$ with $q \geq 0$, $q_c \in \mathbb{R}$, and $s \in (\mathbb{R}_+^*)^m$. Let $c \in L^2(0,1)$ and $b_k \in L^2(0,1)$ for $1 \leq k \leq m$. Consider the reaction-diffusion system described by (64) with measured output (65). Let $N_0 \geq 1$ and $\delta > 0$ be given such that $-\lambda_n + q_c < -\delta < 0$ for all $n \geq N_0 + 1$. Assume that 1) for any $1 \leq n \leq N_0$, there exists $1 \leq k = k(n) \leq m$ such that $b_{n,k} \neq 0$; 2) $c_n \neq 0$ for all $1 \leq n \leq N_0$. Let $K \in \mathbb{R}^{m \times N_0}$ and $L \in \mathbb{R}^{N_0}$ be such that $A_1 + B_1 K$ and $A_0 + LC_0$ are Hurwitz with eigenvalues that have a real part strictly less than $-\delta < 0$. Assume that there exist $N \geq N_0 + 1$, a symmetric positive definite $P \in \mathbb{R}^{2N \times 2N}$, $\alpha, \beta, \gamma, \mu, \kappa > 0$, a diagonal positive definite $T \in \mathbb{R}^{m \times m}$, and $G \in \mathbb{R}^{m \times N_0}$ such that*

$$\Theta_1(\kappa) \preceq 0, \quad \Theta_2 \succeq 0, \quad \Theta_3(\kappa) \leq 0 \tag{70}$$

where

$$\Theta_1(\kappa) = \begin{bmatrix} \Theta_{1,1,1}(\kappa) & P\mathcal{L} & -E^\top G^\top T + P\mathcal{L}_\phi \\ \star & -\beta & 0 \\ \star & \star & \alpha\gamma \sum_{k=1}^m \|\mathcal{R}_N b_k\|_{L^2}^2 I - 2T \end{bmatrix}$$

$$\Theta_2 = \begin{bmatrix} P & E^\top (K-G)^\top \\ \star & \mu \operatorname{diag}(s)^2 \end{bmatrix},$$

$$\Theta_3(\kappa) = 2\gamma \left\{ -\lambda_{N+1} + q_c + \kappa + \frac{1}{\alpha} \right\} + \beta \|\mathcal{R}_N c\|_{L^2}^2$$

with $\Theta_{1,1,1}(\kappa) = F^\top P + PF + 2\kappa P + \alpha\gamma \sum_{k=1}^m \|\mathcal{R}_N b_k\|_{L^2}^2 \tilde{K}^\top \tilde{K}$. *Define the ellipsoid*

$$\mathcal{E}_1 = \left\{ (z, \hat{z}) \in L^2(0,1) \times \mathbb{R}^N : \Pi_N(z,\hat{z})^\top P \Pi_N(z,\hat{z}) + \gamma \|\mathcal{R}_N z\|_{L^2}^2 \leq \frac{1}{\mu} \right\}.$$

Then, the origin of the closed-loop system composed of the plant (64) with measured output (65) and the control law (68) is locally exponentially stable in L^2*-norm with exponential decay rate* κ *and with a basin of attraction including* $\mathcal{E}_1$*. More precisely, there exists* $M > 0$ *such that for any initial condition* $(z_0, \hat{z}(0)) \in \mathcal{E}_1$*, the solution satisfies*

$$\|z(t,\cdot)\|_{L^2}^2 + \sum_{n=1}^N \hat{z}_n(t)^2 \leq M e^{-2\kappa t} \left(\|z_0\|_{L^2}^2 + \sum_{n=1}^N \hat{z}_n(0)^2 \right) \tag{71}$$

for all $t \geq 0$*. Moreover, for any fixed* $\kappa \in (0, \delta]$*, the constraints (70) are always feasible for* N *large enough.*

Proof of Theorem 8. Let the Lyapunov function candidate be defined by $V(X,z) = X^\top P X + \gamma \sum_{n \geq N+1} \langle z, \Phi_n \rangle^2$ for $X \in \mathbb{R}^{2N}$ and $z \in L^2(0,1)$. The computation of the time derivative of V along the system solutions to (67) and (69) gives

$$\begin{aligned} \dot{V} + 2\kappa V = {} & X^\top \left(F^\top P + PF + 2\kappa P \right) X + 2X^\top P \mathcal{L}\zeta \\ & + 2X^\top P \mathcal{L}_\phi(K\hat{Z}^{N_0}) + 2\gamma \sum_{n \geq N+1} (-\lambda_n + q_c + \kappa) z_n^2 \\ & + 2\gamma \sum_{n \geq N+1} z_n L_n^b \tilde{K} X + 2\gamma \sum_{n \geq N+1} z_n L_n^b \phi(K\hat{Z}^{N_0}) \end{aligned}$$

where $L_n^b = \begin{bmatrix} b_{n,1} \dots b_{n,m} \end{bmatrix}$. From Young's inequality, we obtain for any $\alpha > 0$ and any $w \in \mathbb{R}^m$ that $2 \sum_{n \geq N+1} z_n L_n^b w \leq \frac{1}{\alpha} \sum_{n \geq N+1} z_n^2 + \alpha \sum_{k=1}^m \|\mathcal{R}_N b_k\|_{L^2}^2 \|w\|^2$. Hence, introducing $\tilde{X} = \mathrm{col}(X, \zeta, \phi(K\hat{Z}^{N_0}))$, we deduce that

$$\begin{aligned} \dot{V} + 2\kappa V \leq {} & \tilde{X}^\top \begin{bmatrix} \Theta_{1,1,1} & P\mathcal{L} & P\mathcal{L}_\phi \\ \star & 0 & 0 \\ \star & \star & \alpha\gamma \sum_{k=1}^m \|\mathcal{R}_N b_k\|_{L^2}^2 I \end{bmatrix} \tilde{X} \\ & + 2\gamma \sum_{n \geq N+1} \left(-\lambda_n + q_c + \kappa + \frac{1}{\alpha} \right) z_n^2. \end{aligned}$$

Since, by definition, $\zeta = \sum_{n \geq N+1} c_n z_n$, we obtain that $\zeta^2 \leq \|\mathcal{R}_N c\|_{L^2}^2 \sum_{n \geq N+1} z_n^2$. Moreover, if $\hat{\tilde{Z}}^{N_0} \in \mathbb{R}^{N_0}$ satisfies $|(K - G)\hat{Z}^{N_0}| \leq s$,

we deduce from (21) that $\phi(K\hat{Z}^{N_0})^\top T(\phi(K\hat{Z}^{N_0})+G\hat{Z}^{N_0}) \leq 0$. Combining the latter estimates, we obtain for all $X \in \mathbb{R}^{2N}$ satisfying $|(K-G)EX| \leq s$ that

$$\dot{V} + 2\kappa V \leq \tilde{X}^\top \Theta_1(\kappa)\tilde{X} + \sum_{n\geq N+1} \Gamma_n z_n^2$$

where $\Gamma_n = 2\gamma\left(-\lambda_n + q_c + \kappa + \frac{1}{\alpha}\right) + \beta\|\mathcal{R}_N c\|_{L^2}^2 \leq \Theta_3(\kappa)$ for all $n \geq N+1$. Hence the assumptions imply that $\dot{V} + 2\kappa V \leq 0$ for all $X \in \mathbb{R}^{2N}$ is such that $|(K-G)EX| \leq s$.

We now need to give a sufficient condition such that $|(K-G)EX| \leq s$ holds. To do so, consider $X \in \mathbb{R}^{2N}$ and $z \in L^2(0,1)$ such that $V(X,z) \leq 1/\mu$. Applying the Schur complement to $\Theta_2 \succeq 0$, we obtain that $P \succeq \frac{1}{\mu}E^\top(K-G)^\top \mathrm{diag}(s)^{-2}(K-G)E$. This implies that $\|\mathrm{diag}(s)^{-1}(K-G)EX\| \leq 1$, giving in particular that $|(K-G)EX| \leq s$ hence $\dot{V} + 2\kappa V \leq 0$.

From now it is easy to show that, for any initial condition selected such that $(z_0, \hat{z}_0) \in \mathcal{E}_1$ with $z_0 \in D(\mathcal{A})$, we have $V(X(t), z(t,\cdot)) \leq 1/\mu$ and $\dot{V}(X(t), z(t,\cdot)) + 2\kappa V(X(t), z(t,\cdot)) \leq 0$ for all $t \geq 0$. The claimed stability estimate (71) follows from the definition of V. The extension of this result to mild solutions associated with any $(z_0, \hat{z}_0) \in \mathcal{E}_1$ follows from a classical density argument [53, Thm. 6.1.2].

The rest of the proof, which concerns the feasibility of the constraints, is reported in.[34] □

Stabilization in H^1 norm The following result deals with the exponential stability of the system trajectories evaluated in H^1-norm.

Theorem 9. *In the context of Theorem 8, we further assume that $q > 0$. Assume that there exist $N \geq N_0 + 1$, a symmetric positive definite $P \in \mathbb{R}^{2N\times 2N}$, $\alpha > 1$, $\beta, \gamma, \mu, \kappa > 0$, a diagonal positive definite $T \in \mathbb{R}^{m\times m}$, and $G \in \mathbb{R}^{m\times N_0}$ such that*

$$\Theta_1(\kappa) \preceq 0, \quad \Theta_2 \succeq 0, \quad \Theta_3(\kappa) \leq 0 \tag{72}$$

where $\Theta_1(\kappa)$ and Θ_2 are defined as in Theorem 8 while

$$\Theta_3(\kappa) = 2\gamma\left\{-\left(1-\frac{1}{\alpha}\right)\lambda_{N+1} + q_c + \kappa\right\} + \frac{\beta\|\mathcal{R}_N c\|_{L^2}^2}{\lambda_{N+1}}.$$

Define the ellipsoid

$$\mathcal{E}_2 = \left\{(z,\hat{z}) \in D(\mathcal{A}) \times \mathbb{R}^N : \Pi(z,\hat{z})^\top P \Pi(z,\hat{z}) + \gamma\|\mathcal{R}_N \mathcal{A}^{1/2} z\|_{L^2}^2 \leq \frac{1}{\mu}\right\}.$$

Then, the origin of the closed-loop system composed of the plant (64) with measured output (65) and the control law (68) is locally exponentially stable in H^1-norm with exponential decay rate κ and with a basin of attraction including $\mathcal{E}_1$. In other words, there exists $M > 0$ such that for any initial condition $(z_0, \hat{z}(0)) \in \mathcal{E}_1$, the solution satisfies

$$\|z(t,\cdot)\|_{H^1}^2 + \sum_{n=1}^{N} \hat{z}_n(t)^2 \leq Me^{-2\kappa t}\left(\|z_0\|_{H^1}^2 + \sum_{n=1}^{N} \hat{z}_n(0)^2\right)$$

for all $t \geq 0$. Moreover, for any fixed $\kappa \in (0, \delta]$, the constraints (72) are always feasible for N large enough.

Proof of Theorem 9. We introduce the Lyapunov functional candidate $V(X,z) = X^\top PX + \gamma \sum_{n\geq N+1} \lambda_n \langle z, \Phi_n\rangle^2$ when $X \in \mathbb{R}^{2N}$ and $z \in D(\mathcal{A})$. The computation of the time derivative of V along the system solutions to (67) and (69) gives

$$\begin{aligned}\dot{V} + 2\kappa V = {} & X^\top \left(F^\top P + PF + 2\kappa P\right) X + 2X^\top P\mathcal{L}\zeta \\ & + 2X^\top P\mathcal{L}_\phi \phi(K\hat{Z}^{N_0}) + 2\gamma \sum_{n\geq N+1} \lambda_n(-\lambda_n + q_c + \kappa) z_n^2 \\ & + 2\gamma \sum_{n\geq N+1} \lambda_n z_n L_n^b \tilde{K} X + 2\gamma \sum_{n\geq N+1} \lambda_n z_n L_n^b \phi(K\hat{Z}^{N_0})\end{aligned}$$

where $L_n^b = \begin{bmatrix} b_{n,1} \dots b_{n,m}\end{bmatrix}$. Invoking Young's inequality, we obtain for any $\alpha > 0$ and any $w \in \mathbb{R}^m$ that $2\sum_{n\geq N+1} \lambda_n z_n L_n^b w \leq \dfrac{1}{\alpha} \sum_{n\geq N+1} \lambda_n^2 z_n^2 + \alpha \sum_{k=1}^m \|\mathcal{R}_N b_k\|_{L^2}^2 \|w\|^2$. Let $\tilde{X} = \mathrm{col}(X, \zeta, \phi(K\hat{Z}^{N_0}))$. Proceeding as in the proof of Theorem 8, we deduce that

$$\dot{V} + 2\kappa V \leq \tilde{X}^\top \Theta_1(\kappa) \tilde{X} + \sum_{n\geq N+1} \lambda_n \Gamma_n z_n^2$$

for all $X \in \mathbb{R}^{2N}$ satisfying $|(K-G)EX| \leq s$ and where $\Gamma_n = 2\gamma\left\{-\left(1 - \frac{1}{\alpha}\right)\lambda_n + q_c + \kappa\right\} + \frac{\beta \|\mathcal{R}_N c\|_{L^2}^2}{\lambda_n} \leq \Theta_3(\kappa)$ for all $n \geq N+1$. The proof now follows similar arguments that the ones employed in the proof of Theorem 8. □

Remark 6. The conditions in Theorem 8 and in Theorem 9 are nonlinear in the unknown variables, due to, in particular the product $G^\top T$. Some nonlinearity could be transformed into linear conditions as for the variable α, as discussed in Remark 3. To deal with the particular case $m = 1$, or to deduce convex constraints from these theorems, see.[34]

3.5. *Section conclusion*

This section has discussed the topic of output feedback stabilization of a reaction-diffusion equation by means of in-domain or boundary control inputs. The controllers that are considered in this section are output feedback laws where the output is defined from a boundary measure or an internal measurement of the state. The control strategy takes the form of a finite-dimensional controller composed of an observer coupled with a finite-dimensional partial state-feedback. The control can be either linear or subject to a saturation map. In the latter scenario, only a local asymptotic stability can be obtained in general along with an estimation of the basin of attraction. The reported stability analysis takes advantage of Lyapunov functionals coupled with the generalized sector condition that has been recalled in Section 2 in the context of finite-dimensional systems. The obtained sets of constraints ensuring the stability of the closed-loop system take an explicit form and have been shown to be feasible when the order of the controller is selected large enough. An explicit subset of the domain of attraction of the closed-loop system has also been derived.

4. Stabilization of wave and KdV equations

Two classes of particular equations are considered in this section: first the wave equation and then the Korteweg–de-Vries (KdV) equation. We particularly focus on the boundary stabilization problem. The interest of the first equation is that it gives a transition towards the boundary control of general hyperbolic systems, whereas the second one allows to show perspectives in terms of stabilization of nonlinear partial differential equations, and give a highlighting example of what could be done for boundary control of other classes of hyperbolic PDEs (as considered e.g. in[55,75]).

For both equations, we solve the common objectives of well-posedness assessment and asymptotic stabilization by means of of distributed or boundary control that can be either linear or subject to a nonlinear map (e.g., a saturation).

This section is organized as follows. First, in Section 4.1, the stabilization of the linear wave equation with linear and with nonlinear in-domain control is presented. The topic of boundary control is then considered for the same equation. Finally the nonlinear KdV equation is considered in Section 4.2 with in-domain control. This result is illustrated with some numerical simulations.

4.1. *Wave equation with a bounded control operator*

Motivated by the illustration depicted in Figure 8, where z stands for the deflection of a membrane with respect to the rest and horizontal axis and that is subject to a distributed force u, we start this section by considering the following wave equation:

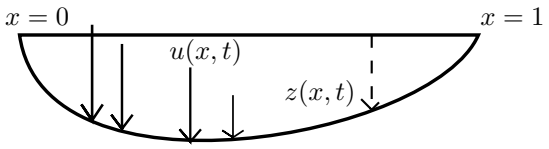

Fig. 8. Wave equation with bounded control operator

$$z_{tt}(t,x) = z_{xx}(t,x) + u(t,x),\ \forall t \geq 0\ ,\ x \in (0,1), \tag{73}$$

We assume that the membrane is clamped at both extremities. This implies the following boundary conditions, for all $t \geq 0$,

$$\begin{aligned} z(t,0) &= 0\ , \\ z(t,1) &= 0\ . \end{aligned} \tag{74}$$

The initial condition are given, for all $x \in (0,1)$, by

$$\begin{aligned} z(0,x) &= z^0(x) \ , \\ z_t(0,x) &= z^1(x) \ , \end{aligned} \tag{75}$$

where z^0 and z^1 stand for the initial deflection and the initial deflection speed, respectively.

Let us note that the function defined by $z(t,x) = 0$, for all (t,x) in $(0,1) \times [0,\infty)$ is a particular solution to (73) and (74) in the uncontrolled scenario ($u = 0$). Hence the orgin is an equilibrium for the studied wave equation. The objective is to render this equilibrium asymptotically stable by designing an adequate feedback control u.

4.1.1. *Internal linear control*

Let us define the linear control by

$$u(t,x) = -az_t(t,x), \ t \geq 0 \ , \ x \in (0,1), \tag{76}$$

and consider

$$V_1 = \frac{1}{2} \int (z_x^2 + z_t^2) \mathrm{d}x. \tag{77}$$

A formal computation gives, along the solutions to (73), (74) and (76),

$$\begin{aligned} \dot{V}_1 &= \textstyle\int_0^1 (z_x z_{xt} - a z_t^2 + z_t z_{xx}) \mathrm{d}x \\ &= - \textstyle\int_0^1 a z_t^2 \mathrm{d}x + [z_t z_x]_{x=0}^{x=1} \\ &= - \textstyle\int_0^1 a z_t^2 \mathrm{d}x \end{aligned}$$

Thus, if $a > 0$, V_1 is a (non strict) Lyapunov function.

Using standard technics, such as Lumer-Phillips thereom for the well-posedness (see e.g., [14, Theorem A.4.]) and Huang-Prüss theorem for the exponential stability (see[27] and[58]), we may prove the following result:

Theorem 10. *For $a > 0$ and $(z^0, z^1) \in H_0^1(0,1) \times L^2(0,1)$, there exists a unique (weak) solution z: $[0,\infty) \to H_0^1(0,1) \times L^2(0,1)$ to (73)-(76). Moreover, the origin of $H_0^1(0,1) \times L^2(0,1)$ is an exponentially stable equilibrium, that is there exist two positive values C and $\mu > 0$ such that, for any initial condition $(z^0, z^1) \in H_0^1(0,1) \times L^2(0,1)$, it holds, for all $t \geq 0$,*

$$\|z\|_{H_0^1(0,1)} + \|z_t\|_{L^2(0,1)} \leq C e^{-\mu t} (\|z^0\|_{H_0^1(0,1)} + \|z^1\|_{L^2(0,1)}).$$

Proof of Theorem 10. Let us first prove the well-posedness. Let A_l be the linear unbounded operator

$$A_l \begin{pmatrix} f \\ g \end{pmatrix} = \begin{pmatrix} g \\ f_{xx} - ag \end{pmatrix}$$

with the domain $D(A_l) = (H^2(0,1) \cap H_0^1(0,1)) \times H_0^1(0,1)$. This domain is dense is $H_0^1(0,1) \times L^2(0,1)$, and the operator A_l is closed. Let us rewrite (73)-(76) as

$$\frac{\partial}{\partial t} \begin{pmatrix} z \\ z_t \end{pmatrix} = A_l \begin{pmatrix} z \\ z_t \end{pmatrix} \ , \ \begin{pmatrix} z \\ z_t \end{pmatrix} (t = 0, \cdot) = \begin{pmatrix} z^0 \\ z^1 \end{pmatrix} \tag{78}$$

Our objective is to prove that A_l generates a contraction semigroup $T_l(t)$, that is the solution of (78) is $T_l(t) \begin{pmatrix} z^0 \\ z^1 \end{pmatrix}$ and satisfies

$$\left\| T_l(t) \begin{pmatrix} z^0 \\ z^1 \end{pmatrix} \right\|^2 \leq \left\| \begin{pmatrix} z^0 \\ z^1 \end{pmatrix} \right\|^2 \ , \ \forall t \geq 0. \tag{79}$$

Informally, one can try to prove (79) by differentiating the right-hand-side with respect to the time. Using $\left\| \begin{pmatrix} z^0 \\ z^1 \end{pmatrix} \right\|^2 = \langle \begin{pmatrix} z^0 \\ z^1 \end{pmatrix}, \begin{pmatrix} z^0 \\ z^1 \end{pmatrix} \rangle$, we get

$$\begin{aligned} \frac{d}{dt} \left\| T_l(t) \begin{pmatrix} z^0 \\ z^1 \end{pmatrix} \right\|^2 &= \langle A_l T_l(t) \begin{pmatrix} z^0 \\ z^1 \end{pmatrix}, \begin{pmatrix} z^0 \\ z^1 \end{pmatrix} \rangle + \langle \begin{pmatrix} z^0 \\ z^1 \end{pmatrix}, A_l T_l(t) \begin{pmatrix} z^0 \\ z^1 \end{pmatrix} \rangle \\ &= 2\mathbb{R}e \langle A_l T_l(t) \begin{pmatrix} z^0 \\ z^1 \end{pmatrix}, \begin{pmatrix} z^0 \\ z^1 \end{pmatrix} \rangle \end{aligned}$$

where $\mathbb{R}e$ denotes the real part. This gives, at time $t = 0$,

$$\frac{d}{dt} \left\| T_l(t) \begin{pmatrix} z^0 \\ z^1 \end{pmatrix} \right\|^2 (t = 0, \cdot) = 2\mathbb{R}e \langle A_l \begin{pmatrix} z^0 \\ z^1 \end{pmatrix}, \begin{pmatrix} z^0 \\ z^1 \end{pmatrix} \rangle$$

This formal computation tends to show that in order to obtain (79), a necessary condition is to have $\mathbb{R}e \langle A_l \begin{pmatrix} z^0 \\ z^1 \end{pmatrix}, \begin{pmatrix} z^0 \\ z^1 \end{pmatrix} \rangle \leq 0$. This condition is one of the two key elements of the Lumer-Phillips theorem which provides a characterization of the unbounded operators generating a contraction semigroup. Specifically, in order to apply the Lumer-Phillips theorem, we need to show that the two following points hold true:

(1) $\mathbb{R}e \langle A_l \begin{pmatrix} z^0 \\ z^1 \end{pmatrix}, \begin{pmatrix} z^0 \\ z^1 \end{pmatrix} \rangle \leq 0$, for all $\begin{pmatrix} z^0 \\ z^1 \end{pmatrix}$ in $D(A_l)$

(2) there exists $\lambda > 0$ such that $\texttt{Ran}(I - \lambda A_l) = H_0^1(0,1) \times L^2(0,1)$, where `Ran` is the range set.

Under these two conditions, the unbounded operator A_l generates a semi-group of contraction and the Cauchy problem (78) is well-posed for strong and weak solutions as considered in Theorem 10.

Even if we do not give here a complete proof of these both properties, note that the interest of the second item is that it replaces the time-dependent Cauchy problem (78) by

$$\forall \begin{pmatrix} f \\ g \end{pmatrix} \in H_0^1(0,1) \times L^2(0,1), \textit{ find } \begin{pmatrix} \tilde{f} \\ \tilde{g} \end{pmatrix} \in D(A_l) \textit{ such that}$$

$$(I - \lambda A_l) \begin{pmatrix} \tilde{f} \\ \tilde{g} \end{pmatrix} = \begin{pmatrix} f \\ g \end{pmatrix}$$

which is a stationary Cauchy problem of a linear ODE with prescribed boundary conditions.

Let us now sketch the proof of the exponential stability. According to Huang-Prüss theorem (see[27] and[58]), it is sufficient to check the two conditions

$$i\mathbb{R} \subset \rho(A), \tag{80}$$

$$\sup_{\beta \in \mathbb{R}} \|(i\beta - A_l)^{-1}\| < \infty. \tag{81}$$

Inspired by,[33] let us prove these both properties succesively. To prove (80), we argue by contradiction, assuming the existence of an eigenvalue of A_l of the form $i\beta$. Pick $\begin{pmatrix} f \\ g \end{pmatrix}$ in $D(A_l) \setminus \{0\}$ such that $(i\beta - A_l) \begin{pmatrix} f \\ g \end{pmatrix} = 0$. Then

$$0 = \langle (i\beta - A_l) \begin{pmatrix} f \\ g \end{pmatrix}, \begin{pmatrix} f \\ g \end{pmatrix} \rangle_{H_0^1(0,1) \times L^2(0,1)}, \tag{82}$$

$$= i\beta \left(\int_0^1 |f|'^2 \mathrm{d}x + \int_0^1 |g|^2 \mathrm{d}x \right) + a \int_0^1 |g|^2 \mathrm{d}x. \tag{83}$$

Thus, inspecting the real part of the previous equation, with $a \neq 0$, we get $g = 0$. Moreover, inspecting the imaginary part, we get $f' = 0$ which gives $f = 0$ using the definition of $D(A_l)$ and the boundary conditions of f. This is a contradiction with $\begin{pmatrix} f \\ g \end{pmatrix} \neq 0$. Therefore (80) holds.

Let us now prove (81), by proceeding again with a contradiction. If 81 is false, then there exists a sequence $(\beta_n)_{n \in \mathbb{N}}$ and a sequence $\begin{pmatrix} f_n \\ g_n \end{pmatrix}_{n \in \mathbb{N}}$ in $D(A_l)$ such that

$$\left\| \begin{pmatrix} f_n \\ g_n \end{pmatrix}_{n \in \mathbb{N}} \right\|_{H_0^1(0,1) \times L^2(0,1)} = 1 \ , \tag{84}$$

$$\beta_n \to_{n \to \infty} +\infty \tag{85}$$

and

$$\left\| \begin{pmatrix} \tilde{f}_n \\ \tilde{g}_n \end{pmatrix} \right\|_{H_0^1(0,1)\times L^2(0,1)} \to_{n\to\infty} 0 \tag{86}$$

where $\begin{pmatrix} \tilde{f}_n \\ \tilde{g}_n \end{pmatrix} = (i\beta_n - A_l) \begin{pmatrix} f_n \\ g_n \end{pmatrix}_{n\in\mathbb{N}}$. We compute

$$\begin{aligned} \langle \begin{pmatrix} \tilde{f}_n \\ \tilde{g}_n \end{pmatrix}, \begin{pmatrix} f_n \\ g_n \end{pmatrix} \rangle_{H_0^1(0,1)\times L^2(0,1)} &= \langle (i\beta_n - A_l) \begin{pmatrix} f_n \\ g_n \end{pmatrix}, \begin{pmatrix} f_n \\ g_n \end{pmatrix} \rangle_{H_0^1(0,1)\times L^2(0,1)} \\ &= i\beta_n (\int_0^1 |f_n|'^2 \mathrm{d}x + \int_0^1 |g_n|^2 \mathrm{d}x) + a\int_0^1 |g_n|^2 \mathrm{d}x. \end{aligned}$$

Therefore, with (84) and (86), inspecting the imaginary part in the last equation,we get

$$\beta_n (\int_0^1 f_n'^2 \mathrm{d}x + \int_0^1 g_n^2 \mathrm{d}x) \to_{n\to\infty} 0 \ ,$$

thus with (84), we get $\beta_n \to 0$ which is a contradiction with (85). Therefore (81) holds. This concludes the proof of the exponential stability and of the proof of Theorem 10. □

4.1.2. *Internal saturating control*

We now study the nonlinear control

$$u(t,x) = -\mathtt{sat}(az_t(t,x)),\ x \in (0,1),\ \forall t \geq 0, \tag{87}$$

where `sat` is the nonlinear function defined in (17) with $m = 1$ and level s_0. Following the terminology of,[45] we call this nonlinearity the localized saturated map. The wave equation (73) in closed loop with the control (87) gives the dynamics

$$z_{tt} = z_{xx} - \mathtt{sat}(az_t) \tag{88}$$

A formal computation of the time derivative of V_1 defined by (77) along the solutions to the wave PDE (88) with boundary conditions (74) gives

$$\dot{V}_1 = -\int_0^1 z_t \mathtt{sat}(az_t) \mathrm{d}x.$$

Hence, in order to conclude on the possible stability of the closed-loop system, one needs to handle the nonlinearity $z_t\mathtt{sat}(az_t)$.

Note that other choices of saturation mechanisms can also be considered instead of the *localized* saturation studied in (87). For instance, papers[66]

and[32] deal with the L^2 saturation denoted by $\mathtt{sat}_{L2}$ and defined for any $\sigma \in L^2(0,1)$ by

$$\mathtt{sat}_{L2}(\sigma)(x) = \begin{cases} \sigma(x) & \text{if } \|\sigma\|_{L^2(0,1)} < 1 \\ \frac{\sigma(x)}{\|\sigma\|_{L^2(0,1)}} , & \text{else} \end{cases} \tag{89}$$

Even if all the different saturation mechanisms are of interest, we focus here on the localized saturation used in (87), which is generally more relevant from a physical point of view and in practical applications.

The well-posedness of the nonlinear PDE (88), which is borrowed from,[56] is assessed by the following theorem.

Theorem 11. *For all $a \geq 0$ and (z^0, z^1) in $(H^2(0,1) \cap H_0^1(0,1)) \times H_0^1(0,1)$, there exists a unique solution z: $[0,\infty) \to H^2(0,1) \cap H_0^1(0,1)$ to (88) with the boundary conditions (74) and the initial condition (75).*

Proof of Theorem 11. We only provide a sketch of the proof reported in.[56] Consider the nonlinear operator

$$A_1 \begin{pmatrix} f \\ g \end{pmatrix} = \begin{pmatrix} g \\ f_{xx} - \mathtt{sat}(ag) \end{pmatrix}$$

with the domain $D(A_1) = (H^2(0,1) \cap H_0^1(0,1)) \times H_0^1(0,1)$. We are want to invoke here a generalization of the Lumer-Phillips theorem, which is the so-called Crandall-Liggett theorem. A precise statement of this theorem can be found;[4] see also[8] and.[49] To apply this theorem, two conditions need to be checked:

(1) A_1 is dissipative, that is for any two elements of $D(A_1)$,

$$\mathbb{R}e \left(\langle A_1 \begin{pmatrix} f \\ g \end{pmatrix} - A_1 \begin{pmatrix} \tilde{f} \\ \tilde{g} \end{pmatrix}, \begin{pmatrix} f \\ g \end{pmatrix} - \begin{pmatrix} \tilde{f} \\ \tilde{g} \end{pmatrix} \rangle \right) \leq 0$$

(2) For all $\lambda > 0$, $D(A_1) \subset \mathtt{Ran}(I - \lambda A_1)$

Let us prove the first item. To do that, given $\begin{pmatrix} f \\ g \end{pmatrix}$ and $\begin{pmatrix} \tilde{f} \\ \tilde{g} \end{pmatrix}$ in $H_0^1(0,1) \times L^2(0,1)$,in $H_0^1(0,1) \times L^2(0,1)$, we denote

$$\Delta = \mathbb{R}e \left(\langle A_1 \begin{pmatrix} f \\ g \end{pmatrix} - A_1 \begin{pmatrix} \tilde{f} \\ \tilde{g} \end{pmatrix}, \begin{pmatrix} f \\ g \end{pmatrix} - \begin{pmatrix} \tilde{f} \\ \tilde{g} \end{pmatrix} \rangle \right) \leq 0$$

. Let us check that $\Delta \leq 0$. Using the definition of A_1 and of the hermitian product in $H_0^1(0,1) \times L^2(0,1)$, we compute

$$\begin{aligned}\Delta &= \mathbb{R}e\left(\int_0^1 (g_x(x) - \tilde{g}_x(x))(\overline{f_x(x) - \tilde{f}_x(x)})\mathrm{d}x + \int_0^1 (f_{xx}(x) - \tilde{f}_{xx}(x))(\overline{g(x) - \tilde{g}(x)})\mathrm{d}x\right)\\ &\quad -\mathbb{R}e\left(\int_0^1 (\mathtt{sat}(a\, g(x)) - \mathtt{sat}(a\, \tilde{g}(x)))(\overline{g(x) - \tilde{g}(x)})\mathrm{d}x\right)\ ,\\ &= -\mathbb{R}e\left(\int_0^1 (\mathtt{sat}(a\, g(x)) - \mathtt{sat}(a\, \tilde{g}(x)))(\overline{g(x) - \tilde{g}(x)})\mathrm{d}x\right)\ .\end{aligned}$$

Note that, for all $a \geq 0$ and for all $(s, \tilde{s})$ in $\mathbb{C} \times \mathbb{C}$,

$$\mathbb{R}e\left((\mathtt{sat}(a\, s) - \mathtt{sat}(a\, \tilde{s}))(\overline{s - \tilde{s}})\right) \geq 0.$$

Thus A_1 is dissipative.

The second item requires to deal with a nonlinear ODE. To be more specific, let $\lambda > 0$ and $\begin{pmatrix} f \\ g \end{pmatrix} \in H_0^1(0,1) \times L^2(0,1)$ be arbitrarily given. Our objective is to find $\begin{pmatrix} \tilde{f} \\ \tilde{g} \end{pmatrix} \in D(A_1)$ such that

$$(I - \lambda A_1)\begin{pmatrix} \tilde{f} \\ \tilde{g} \end{pmatrix} = \begin{pmatrix} f \\ g \end{pmatrix},$$

that is

$$\begin{cases} \tilde{f} - \lambda \tilde{g} = f\ , \\ \tilde{g} - \lambda(\tilde{f}_{xx} - \mathtt{sat}(a\, \tilde{g})) = g\ , \end{cases}$$

Using the first identity to express $\tilde{g}$ in function of f and $\tilde{f}$, we only have to find $\tilde{f}$ such that

$$\begin{aligned} &\tilde{f}_{xx} - \frac{1}{\lambda^2}\tilde{f} - \mathtt{sat}(\frac{a}{\lambda}(\tilde{f} - f)) = -\frac{1}{\lambda}g - \frac{1}{\lambda^2}f\\ &\tilde{f}(0) = \tilde{f}(1) = 0 \end{aligned}$$

holds. The existence of a solution to this nonhomogeneous nonlinear ODE with two boundary conditions is provided by the following lemma.

Lemma 2. *For any $a \geq 0$ and $\lambda > 0$, there exists $\tilde{f}$ solution to*

$$\begin{aligned} \tilde{f}_{xx} - \tfrac{1}{\lambda^2}\tilde{f} - \mathtt{sat}(\tfrac{a}{\lambda}(\tilde{f} - f)) = -\tfrac{1}{\lambda}g - \tfrac{1}{\lambda^2}f\\ \tilde{f}(0) = \tilde{f}(1) = 0 \end{aligned} \tag{90}$$

To prove this lemma, let us introduce the mapping:

$$\begin{aligned} \mathcal{T} : L^2(0,1) &\to L^2(0,1) \ , \\ y &\mapsto z \ , \end{aligned}$$

where $z = \mathcal{T}(y)$ is the unique solution to

$$\begin{aligned} z_{xx} - \tfrac{1}{\lambda^2} z = -\tfrac{1}{\lambda} v - \tfrac{1}{\lambda^2} u + \mathtt{sat}(\tfrac{a}{\lambda}(y-u)) \ , \\ z(0) = z(1) = 0 \ . \end{aligned}$$

It can be proven that $\mathcal{T}$ is a well defined mapping. Then, it is possible to invoke the Schauder fixed-point theorem (see e.g.,[14]) to deduce the existence of y such that $\mathcal{T}(y) = y$. After doing so, we obtain that $\tilde{f} = y$ solves (90) □

After having assessed the well-poseness of the closed-loop system dynamics, we can focus on the study of its stability. The global asymptotic stability of this nonlinear PDE is stated in the following result.

Theorem 12. *For all $a > 0$, the origin of the PDE (88) with the boundary conditions (74) is globally asymptotically stable. More specifically, for all (z^0, z^1) in $(H^2(0,1) \cap H_0^1(0,1)) \times H_0^1(0,1)$, the solution to (88) with the boundary conditions (74) and the initial condition (75) satisfies, $\forall t \geq 0$,*

$$\|z(t,.)\|_{H_0^1(0,1)} + \|z_t(t,.)\|_{L^2(0,1)} \leq \|z^0\|_{H_0^1(0,1)} + \|z^1\|_{L^2(0,1)}$$

together with the attractivity property

$$\|z(t,.)\|_{H_0^1(0,1)} + \|z_t(t,.)\|_{L^2(0,1)} \to 0, \quad \text{as } t \to \infty \ .$$

Proof of Theorem 12. Due to Theorem 11, the formal computation of the time derivative of V_1 previously computed is rigorously justified. Hence we have

$$\dot{V}_1 = -\int_0^1 z_t \mathtt{sat}(a z_t) \mathrm{d}x.$$

This is a weak Lyapunov function because $\dot{V}_1 \leq 0$ which guarantees the stability of the origin. In order to prove the attractivity of the origin, we are going to invoke LaSalle's Invariance Principle [17, Chapter 11] for infinite-dimensional systems. To apply LaSalle's Invariance Principle, we have to check that the set of solutions is precompact. This result can be obtained here by following the approach reported in[19,20] and relies on the following lemma (see below for a sketch of proof).

Lemma 3. *The canonical embedding from $D(A_1)$, equipped with the graph norm, into $H_0^1(0,1) \times L^2(0,1)$ is compact.*

Using the dissipativity of A_1 and Lemma 3, the trajectory $\begin{pmatrix} z(t,.) \\ z_t(t,.) \end{pmatrix}$ is precompact in $H_0^1(0,1) \times L^2(0,1)$. Moreover the ω-limit set $\omega\left[\begin{pmatrix} z(0,.) \\ z_t(0,.) \end{pmatrix}\right] \subset D(A_1)$ is not empty and is invariant with respect to the nonlinear semigroup $T(t)$ (see[66]). We these elements in hand, we can indeed apply LaSalle's Invariance Principle to show that $\omega\left[\begin{pmatrix} z(0,.) \\ z_t(0,.) \end{pmatrix}\right] = \{0\}$. This shows that the origin of the equation (88) with the boundary conditions (74) is attractive. This concludes the proof of Theorem 12. □

Let us now give the main steps of the proof of Lemma 3.

Proof of Lemma 3. Consider a sequence $\begin{pmatrix} f_n \\ g_n \end{pmatrix}_{n\in\mathbb{N}}$ in $D(A_1)$, which is bounded in graph norm, that is there exists $M > 0$ such that, for all $n \in \mathbb{N}$,

$$\left\|\begin{pmatrix} f_n \\ g_n \end{pmatrix}\right\|^2_{D(A_1)} := \left\|\begin{pmatrix} f_n \\ g_n \end{pmatrix}\right\|^2 + \left\|A_1\begin{pmatrix} f_n \\ g_n \end{pmatrix}\right\|^2 \leq M$$

which means that

$$\int_0^1 (|f_n'|^2 + |g_n|^2 + |g_n'|^2 + |f_n'' - a\mathtt{sat}(g_n)|^2)\mathrm{d}x \leq M.$$

From that, we deduce that $\int_0^1 (|g_n|^2 + |g_n'|^2)\mathrm{d}x$ and $\int_0^1 (|f_n'|^2 + |f_n''|^2)\mathrm{d}x$ are bounded. Hence, with compact injection of $H_0^1(0,1)$ in $L^2(0,1)$, and of $H^2(0,1)$ in $H_0^1(0,1)$ we infer the existence of a subsequence of $\begin{pmatrix} f_n \\ g_n \end{pmatrix}_{n\in\mathbb{N}}$ which converges in $H_0^1(0,1)\times L^2(0,1)$, giving the precompactness of the set of solutions to equation (88) with the boundary conditions (74). □

4.1.3. *A boundary linear control*

We now consider the wave equation with a boundary control, as depicted in Figure 9. The system dynamics reads

$$z_{tt}(t,x) = z_{xx}(t,x), \quad \forall x \in (0,1), \quad t \geq 0, \tag{91}$$

with the boundary conditions

$$\begin{aligned} z(t,0) &= 0\ , \\ z_x(t,1) &= u(t)\ , \end{aligned} \tag{92}$$

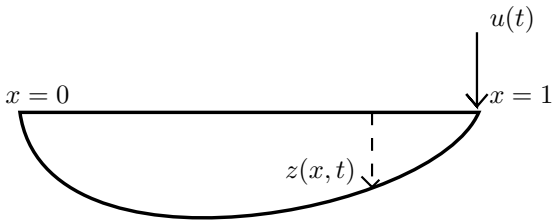

Fig. 9. Wave equation with unbounded control operator

for all $t \geq 0$ and with the initial condition

$$\begin{aligned} z(0,x) &= z^0(x) \ , \\ z_t(0,x) &= z^1(x) \ . \end{aligned} \tag{93}$$

for all x in $(0,1)$.

We define the linear control

$$u(t) = -bz_t(t,1), \ x \in (0,1), \ \forall t \geq 0 \tag{94}$$

and we consider

$$V_2 = \frac{1}{2}\int (e^{\mu x}(z_t + z_x)^2 \mathrm{d}x + \int (e^{-\mu x}(z_t - z_x)^2 \mathrm{d}x.$$

A formal computation of the time derivative along the solutions to (91), (92) and (94) gives

$$\dot{V}_2 = -\mu V_2 + \tfrac{1}{2}\left(e^{\mu}(1-b)^2 - e^{-\mu}(1+b)^2\right) z_t^2(t,1)$$

Assuming that $b > 0$ and letting $\mu > 0$ such that[d] $e^{\mu}(1-b)^2 \leq e^{-\mu}(1+b)^2$, it holds that $\dot{V}_2 \leq -\mu V_2$. Hence V_2 is a strict Lyapunov function and thus the origin of (91) with boundary conditions (92) and command (94) is exponentially stable.

4.1.4. *A boundary saturating control*

Let us consider now the nonlinear control $u(t) = -\mathtt{sat}(bz_t(t,1))$, for all $t \geq 0$. The boundary conditions become:

$$z(t,0) = 0 \ , \quad z_x(t,1) = -\mathtt{sat}(bz_t(t,1)) \ . \tag{95}$$

Inspired by [14, Sec. 2.4], we introduce $H^1_{(0)}(0,1) = \{u \in H^1(0,1), \ u(0) = 0\}$ and $\|u\|_{H^1_{(0)}(0,1)} = \sqrt{\int_0^1 |u'|^2(x)dx}$ for all $u \in H^1_{(0)}$. We are now in

[d]This constraint is always satisfied for $\mu > 0$ small enough by a continuity argument at $\mu = 0$.

position to state the following well-posedness and asymptotic stability result (see[56] for a complete proof).

Theorem 13. *For all $b > 0$, the origin of the PDE (91) with the boundary conditions (95) is globally asymptotically stable. More specifically, for all $(z^0, z^1) \in \{(f,g) \in H^2(0,1) \times H^1_{(0)}(0,1) \ : \ f_x(1) + \mathtt{sat}(bg(1)) = 0, \ f(0) = 0\}$, there exists a unique solution to (91) with the boundary conditions (95) and the initial condition (75). Moreover it satisfies the following stability property, for all $t \geq 0$,*

$$\|z(t,.)\|_{H^1_{(0)}(0,1)} + \|z_t(t,.)\|_{L^2(0,1)} \leq \|z^0\|_{H^1_{(0)}(0,1)} + \|z^1\|_{L^2(0,1)} \ ,$$

together with the attractivity property

$$\|z(t,.)\|_{H^1_{(0)}(0,1)} + \|z_t(t,.)\|_{L^2(0,1)} \to 0, \quad \text{as } t \to \infty \ .$$

Proof of Theorem 13. To prove the well-posedness of the Cauchy problem we can show that A_2 defined by

$$A_2 \begin{pmatrix} f \\ g \end{pmatrix} = \begin{pmatrix} g \\ f'' \end{pmatrix}$$

with the domain $D(A_2) = \{(f,g) \in H^2(0,1) \times H^1_{(0)}(0,1) \ : \ f'(1) + \mathtt{sat}(bg(1)) = 0, \ f(0) = 0\}$ is a semigroup of contraction by applying Lumer-Phillips thereom. The global stability property is immediately inferred from contraction property (consequence of the dissipativity of A_2). Finally, the global attractivity property comes from the following lemma establishing that the origin of the PDE (91) with the boundary conditions (95) is semi-globally exponentially stable. This completes the proof of the theorem. □

Lemma 4. *For all $r > 0$, there exists $\mu > 0$ such that, for all initial condition satisfying*

$$\|(z^0)''\|^2_{L^2(0,1)} + \|z^1\|^2_{H^1_{(0)}(0,1)} \leq r^2 \ , \tag{96}$$

it holds

$$\dot{V}_2 \leq -\mu V_2$$

along the solutions to (91) with the boundary conditions (95).

Proof of Lemma 4. First note that by dissipativity of A_2, it holds that

$$t \mapsto \left\| A_2 \begin{pmatrix} z(t,.) \\ z_t(t,.) \end{pmatrix} \right\| \tag{97}$$

is a non-increasing function. Moreover by continuity of the trace function on $H^1_{(0)}(0,1)$, it holds

$$|z_t(t,1)| \leq \|z_{tx}(t,.)\|_{L^2(0,1)} \leq \left\| A_2 \begin{pmatrix} z(t,.) \\ z_t(t,.) \end{pmatrix} \right\| \leq \left\| A_2 \begin{pmatrix} z(0,.) \\ z_t(0,.) \end{pmatrix} \right\|$$

where the decreasing property of the function in (97) has been used for the last inequality. Thus, for all $t \geq 0$,

$$|z_t(t,1)| \leq \left\| A_2 \begin{pmatrix} z(0,.) \\ z_t(0,.) \end{pmatrix} \right\| . \tag{98}$$

Now, given $r > 0$, for an initial conditions satisfying (96), we have $|z_t(t,1)| \leq r$ and thus there exists $c \neq b$ such that, for all $t \geq 0$,

$$(b-c)|z_t(t,1)| \leq 1$$

and thus, recalling the definition of the deadzone function ϕ in (20), the local sector condition holds $\phi(\phi + cz_t(t,1)) \leq 0$, see (21). Let us now go back to the Lyapunov function candidate V_2. Given $b > 0$, using the previous inequality, we infer that

$$\begin{aligned} \dot{V}_2 &= -\mu V_2 + e^{\mu}(\sigma - \mathtt{sat}(b\sigma))^2 - e^{-\mu}(\sigma + \mathtt{sat}(b\sigma))^2 \\ &\leq -\mu V_2 + e^{\mu}((1-b)\sigma - \phi)^2 - e^{-\mu}((1+b)\sigma + \phi)^2 - 2\phi(\phi + c\sigma) \\ &\leq -\mu V_2 + \begin{pmatrix} \sigma \\ \phi \end{pmatrix}^{\top} \mathcal{M} \begin{pmatrix} \sigma \\ \phi \end{pmatrix} \end{aligned}$$

where

$$\mathcal{M}(\mu, c) = \begin{bmatrix} e^{\mu}(1-b)^2 - e^{-\mu}(1+b)^2 & -e^{\mu}(1-b) - e^{-\mu}(1+b) + c \\ \star & -2 + e^{\mu} - e^{-\mu} \end{bmatrix} .$$

In particular we have at $\mu = 0$ that

$$\mathcal{M}(0, c) = \begin{bmatrix} -4b & -2 + c \\ \star & -2 \end{bmatrix}.$$

We have to select c close to b such that $\mathcal{M}(0,c)$ is symmetric semi-definite negative. Of course, $c = b$ is not convenient since $\mathcal{M}(0,c)$ is not semi-definite negative (moreover the choice $c = b$ would yield the global section condition which does not hold, confirming that the choice $c = b$ is not suitable for c). But $c < b$ and close to b exists such that $\det(\mathcal{M}) > 0$. Thus $\mathcal{M} < 0$.

Given $r > 0$, we consider initial condition such that $\|A_2 \begin{pmatrix} z(.,0) \\ z_t(.,0) \end{pmatrix}\| \leq r$. This implies, for a suitable c ensuring that $(b-c)|z_t(t,1)| \leq 1$ for all $t \geq 0$, that $\dot{V}_2 \leq -\mu V_2$. The semi-global exponential stability follows. □

Note here that the exponential stability is only achieved on bounded sets of initial conditions. An open question is whether we have (or not) the global exponential stability of the origin of the PDE (91) with the boundary conditions (95).

4.2. *KdV equation with a bounded control operator*

In the previous section we reviewed two classes of controllers for the linear wave equation with linear and nonlinear feedback. Different methods for proving asymptotic stability have been reported, one using LaSalle's Invariance Principle and another one establishing semi-global exponential stability based on a local sector condition. In this section, we move to a control problems for a nonlinear PDE. Specifically, let us consider the following nonlinear Korteweg-de-Vries (KdV) PDE:

$$\begin{cases} z_t + z_x + z_{xxx} + zz_x + u = 0, \ x \in [0, L], \ t \geq 0, \\ z(t,0) = z(t,L) = z_x(t,L) = 0, \ t \geq 0, \\ z(0,x) = z^0(x), \ x \in [0,L], \end{cases} \tag{99}$$

where z stands for the state and u for the control.

As shown in,[59] in the uncontrolled scenario ($u = 0$) and for a length L of the spatial domain such that

$$L \in \left\{ 2\pi \sqrt{\frac{k^2 + kl + l^2}{3}} \Big/ k, l \in \mathbb{N}^* \right\}, \tag{100}$$

there exist solutions of the linearized version of (99) for which the $L^2(0,L)$ norm of the state does not decay to zero. This can be observed, for instance, in the particular case for the first critical length $L_1 = 2\pi$ (obtained by letting $k = l = 1$ in (100)) by considering the initial condition $z^0(x) = 1 - \cos(x)$ for all $x \in [0, L]$. Let us denote the second critial by $L_2 = 2\pi\sqrt{\frac{7}{3}}$ (obtained by letting $k = l = 1$ in (100))We refer the reader to the papers[10,11,59] for controllability results of (99) and the role of the so-called critical lengths (100).

In these notes we are interested in the stabilization problem of the origin of the KdV. We refer the reader to[69] for the stabilization of the origin of the linearized KdV equation with anti-diffusion. In[9] and in,[54] localized damping are considered for the linearized KdV equation. Specifically, when setting linear control $u = a(x)z$, for a non-negative continuous function $a : [0,1] \to \mathbb{R}$, we obtain

$$\begin{cases} z_t + z_x + z_{xxx} + a(x)z = 0, \ x \in [0, L], \ t \geq 0, \\ z(t,0) = z(t,L) = z_x(t,L) = 0, \ t \geq 0, \\ z(0,x) = z^0(x), \ x \in [0,L] \end{cases} \tag{101}$$

The following theorem is proven in.[54]

Theorem 14. *The following results hold true for (101).*

- *When L is not a critical length (i.e., (100) does not hold) and $a \equiv 0$, the origin of (101) is asymptotically stable. To be more specific, there exist M and μ such that*

$$\|z(t)\|_{L^2} \leq Me^{-\mu t}\|z(0)\|_{L^2}.$$

- *When $a > 0$ on an non-empty subset of $[0, L]$, then the same conclusion holds.*

Let us now shortly review the stabilization results of the origin of the nonlinear KdV PDE (99) when using a control given by $u = a(x)z$. The papers[13,54,68] consider the following closed-loop dynamics:

$$\begin{cases} z_t + z_x + z_{xxx} + zz_x + a(x)z = 0, \ x \in [0, L], \ t \geq 0, \\ z(t, 0) = z(t, L) = z_x(t, L) = 0, \ t \geq 0, \\ z(0, x) = z^0(x), \ x \in [0, L], \end{cases} \tag{102}$$

The following theorem summarizes some of the contributions contained in these papers (see[13] and[68] for the proof of the first item, respectively for $L = L_1$ and $L = L_2$, and see[54] for the proof of the second item).

Theorem 15. *The following results hold true for (102).*

- *When $L = L_1$ or $L = L_2$ and $a \equiv 0$, the origin of (99) is locally asymptotically stable. More precisely[e], there exist $r > 0$, $M > 0$, and $\mu > 0$ such that the solutions to (102) issuing from $z(0)$ with $\|z(0)\|_{L^2} \leq r$ satisfy*

$$\|z(t)\|_{L^2} \leq Me^{-\mu t}\|z(0)\|_{L^2}$$

- *For all $L > 0$, when $a > 0$ on an non-empty subset of $[0, L]$, then the origin of (102) is globally asymptotically stable. More precisely[f], for all $r > 0$, there exist $M > 0$, and $\mu > 0$ such that*

$$\|z(t)\|_{L^2} \leq Me^{-\mu t}\|z(0)\|_{L^2}$$

4.2.1. *Saturating control for KdV*

Let us now consider the case of a saturating control. To symplify the presentation, we will consider the case where the function $a(x)$ in (102) is a constant denoted by a. The localized control is subject to a saturation

[e]This property is the definition of the global exponential stability of the origin.
[f]This property is the definition of the semi-global asymptotic stability of the origin.

map. To be more specific, let the KdV equation controlled by a saturated distributed control be described by

$$\begin{cases} z_t + z_x + z_{xxx} + zz_x + \mathtt{sat}(az) = 0, \\ z(t,0) = z(t,L) = 0, \\ z_x(t,L) = 0, \\ z(0,x) = z^0(x). \end{cases} \tag{103}$$

where `sat` is the saturation map defined in (17) with $m = 1$, and with level s. The corresponding nonlinear equation (103) is studied in.[45] The case of L^2 saturation, defined in (89), is also considered. In these notes we focus on the nonlinear equation (103), but some numerical simulations will also be performed with the L^2 saturation in the next numerical example.

The well-posedness result is proven in[45] by proving first existence of solution for small time following the approach of,[12,60] and then removing the smallness property of the time existence using *a priori estimates*. It yields the following theorem.

Theorem 16. *For any initial condition $z^0 \in L^2(0,L)$, there exists a unique solution $z \in C([0,T];L^2(0,L)) \cap L^2(0,T;H^1(0,L))$ to (103).*

The global asymptotic stability of the origin, which is also proven in the same paper, can be stated as follows.

Theorem 17. *The origin of (103) is globally asymptotically stable. More precisely there exist $\mu > 0$ and a class $\mathcal{K}$ function[g] $\alpha : [0,\infty) \to [0,\infty)$ such that for any $z^0 \in L^2(0,1)$, any solution z to (103) satisfies, for all $t \geq 0$,*

$$\|z(t)\|_{L^2(0,1)} \leq \alpha(\|z^0\|_{L^2(0,1)})e^{-\mu t}.$$

This result is proved by following the approaches of[9,60] by showing that the origin of (103) is semi-globally exponentially stable.

Proposition 1. *For any given $r > 0$, there exist positive values C and μ such that for all initial condition z^0 satisfying $\|z^0\|_{L^2(0,L)} \leq r$, the solution to (103) satisfies, for all $t \geq 0$,*

$$\|z(t)\|_{L^2(0,L)} \leq C\|z^0\|_{L^2(0,L)}e^{-\mu t}.$$

Proof of Proposition 1. To prove this proposition, a key result is the following claim.

Claim 3. *For all $T > 0$ and $r > 0$, there exists $C > 0$ such that for any solution z to (103) starting from $z^0 \in L^2(0,L)$ with $\|z^0\|_{L^2(0,L)} \leq r$, it*

[g]A class $\mathcal{K}$ function is a continuous and increasing function that is zero at zero.

holds

$$\|z^0\|^2_{L^2(0,L)} \leq C\left(\int_0^T |z_x(t,0)|^2 \mathrm{d}t + 2\int_0^T \int_0^L \mathtt{sat}(az)z \mathrm{d}t\mathrm{d}x\right). \quad (104)$$

Assume Claim 3 holds for the time being. Then with (104) it holds

$$\begin{aligned}\|z(t,.)\|^2_{L^2(0,L)} = \|z^0\|^2_{L^2(0,L)} - \int_0^T |z_x(t,0)|^2 \mathrm{d}t \\ -2\int_0^T \int_0^L \mathtt{sat}(az)z \mathrm{d}x\mathrm{d}t\end{aligned}$$

we get

$$\|z(.,kT)\|^2_{L^2(0,L)} \leq \gamma^k \|z^0\|^2_{L^2(0,L)} \qquad \forall k \geq 0$$

where $\gamma \in (0,1)$. From the dissipativity property, we have $\|z(t,.)\|_{L^2(0,L)} \leq \|z(.,kT)\|_{L^2(0,L)}$ for $kT \leq t \leq (k+1)T$. Thus we obtain, for all $t \geq 0$,

$$\|z(t,.)\|^2_{L^2(0,L)} \leq \frac{1}{\gamma}\|z^0\|_{L^2(0,L)} e^{\frac{\log\gamma}{T}t}$$

We conclude the proof of the semi-global exponential stability, as stated in Proposition 1. □

Let us now prove Claim 3 that has been used in the proof of Proposition 1.

Proof of the Claim 3. We prove (104) by contradiction Assume that there exists a sequence of solution z^n to (103) with

$$\|z^n(.,0)\|_{L^2(0,L)} \leq r \quad (105)$$

and such that

$$\lim_{n\to+\infty} \frac{\|z^n\|^2_{L^2(0,T;L^2(0,L))}}{\int_0^T |z^n_x(t,0)|^2 \mathrm{d}t + 2\int_0^T \int_0^L \mathtt{sat}(az^n(t,x))z^n(t,x)\mathrm{d}t\mathrm{d}x} = +\infty. \quad (106)$$

By dissipativity property, there exists $\beta > 0$ such that

$$\sup_{t\in[0,T]} \|z^n(t,.)\|_{L^2(0,L)} \leq r\,, \quad \sup_{x\in[0,L]} \int_0^T |z^n(t,x)|^2 \mathrm{d}t \leq \beta. \quad (107)$$

Now let us define $\Omega_i := \left\{t \in [0,T],\, \sup_{x\in[0,L]} |z(t,x)| > i\right\} \subset [0,T]$. We have

$$\beta \geq \int_0^T \sup_{x\in[0,L]} |z^n(t,x)|^2 \mathrm{d}t \geq \int_{\Omega_i} \sup_{x\in[0,L]} |z^n(t,x)|^2 \mathrm{d}t \geq i^2 \nu(\Omega_i),$$

Therefore, denoting the Lebesgue mesure by ν, and the complementary set of Ω_i^c) by $\nu(\Omega_i^c)$, we obtain, with (107), $\nu(\Omega_i) \leq \frac{\beta}{i^2}$, and thus $\nu(\Omega_i^c) \geq \max\left(T - \frac{\beta}{i^2}, 0\right)$.

Let us note that denoting, $k(i) = \min(\frac{s}{ai}, 1)$, for each i in $\mathbb{N}$, it holds for all z in Ω_i^c, $|z| \leq i$, and thus[h]

$$(\mathtt{sat}(az) - k(i)az)z \geq 0 \tag{108}$$

Moreover, using again the local sector condition, we have

$$\begin{aligned}\int_0^T \int_0^L \mathtt{sat}(az^n)z^2 \mathrm{d}t\mathrm{d}x &= \int_{\Omega_i} \int_0^L \mathtt{sat}(az^n)z^n \mathrm{d}t\mathrm{d}x + \int_{\Omega_i^c} \int_0^L \mathtt{sat}(az^n)z^n \\ &\geq\ 0 + \int_{\Omega_i^c} \int_0^L ak(i)(z^n)^2 \mathrm{d}t\mathrm{d}x. \end{aligned} \tag{109}$$

where (108) has been used in the last inequality. Thus, with (105), for all i in $\mathbb{N} \setminus \{0\}$,

$$\begin{aligned}\|z^n(t,.)\|^2_{L^2(0,L)} \leq \|z^n(.,0)\|^2_{L^2(0,L)} - \textstyle\int_0^T |z_x^n(t,0)|^2 dt \\ -2\textstyle\int_{\Omega_i^c} \int_0^L ak(i)(z^n)^2 dt\mathrm{d}x.\end{aligned}$$

Let $\lambda^n := \|z^n\|_{L^2(0,T;L^2(0,L))}$ and $v^n(t,x) = \frac{z^n(t,x)}{\lambda^n}$. Due to (105), up to extracting a subsequence, we may assume that $\lambda^n \to \lambda \geq 0$. Due to (106) and (109), we have, for all $i \in \mathbb{N}$

$$\int_0^T |v_x^n(t,0)|^2 \mathrm{d}t + 2\int_{\Omega_i^c} \int_0^L ak(i)(v^n)^2 \mathrm{d}t\mathrm{d}x \to 0 \tag{110}$$

Using Aubin-Lions lemma in,[65] we get $\{v^n\}_{n\in\mathbb{N}}$ converges strongly in $L^2(0,T;L^2(0,L))$. Thus, with (110), we have, for all $i \in \mathbb{N}$

$$v_x(t,0) = 0,\ \forall t \in (t,0) \ \text{ and } \ v(t,x) = 0,\ \forall x \in [0,L], \forall t \in \Omega_i^c.$$

We know that $\nu\left(\bigcup_{i\in\mathbb{N}} \Omega_i^c\right) = T$. We get a contradiction with $\|v\|_{L^2(0,T;L^2(0,L))} = 1$. This concludes the proof of Claim 3. □

Example 7. Let us discretize (103) and illustrate Theorem 17. Moreover we will discretize this equation using the saturation map $\mathtt{sat}_{L2}$ instead of $\mathtt{sat}$ and without any saturation map (the equation becomes (102)).

[h]To prove (108), assume first that $ai \leq s$, then $k(i) = 1$, and $\mathtt{sat}(az) = az$, which gives (108). Second, if $ai > s$ and $\mathtt{sat}(az) = az$, then $1 - k(i) > 0$ and $(\mathtt{sat}(az) - k(i)az) = (1 - k(i))az$, which gives (108). Third, if $ai > s$ and $az > s$, then $(\mathtt{sat}(az) - k(i)az) = s - \frac{s}{ai}az = s(1 - \frac{i}{z}) \geq 0$, which gives (108). The fourth case $ai > s$ and $az < -s$ is studied in a simular way as the third one.

```
"""
Discretizing KdV equation with saturating control.
Use of central difference in space and forward
Euler in time schemes.
Code originally written by S. Marx for
[S. Marx et al, SIAM J. Control Opt., 2017]
"""
import numpy as np
import matplotlib as mpl
import matplotlib.pyplot as plt
from mpl_toolkits.mplot3d import Axes3D

# Parameters of the PDE
L=2*np.pi;
a=1.0

# Space discretization
Nx = 30
x= np.linspace(0,L,Nx+1)
dx = L/Nx;

# Time discretization
dt = 0.06; tfinal=6
Nt= np.floor(tfinal/dt).astype(int)

# Saturation level
s0=0.5

# Set initial condition
z0=[]
for ii in range(Nx+1):
    z0.append(1-np.cos(x[ii]))
```

On line 14, we set the first critical length $L = 2\pi$ and the initial condition $z^0(x) = 1 - \cos(x)$ is chosen on line 32 so that its energy is constant along the linearized KdV equation, without any control. The function a is chosen as the constant value 1 on line 15, and the level of the saturation map is set at 0.5 on line 27. The space and time discretization steps are selected respectively at lines 20 and 23.

```

t = 0 # current time
j = 0 # current time index

# pointwise saturation function
def sat(u):
    m=np.size(u)
    sigma=u
    for i in range(m):
```

```
42          if np.absolute(u[i])>s0:
43              sigma[i]=s0*np.sign(u[i])
44      return sigma
45
46  # L2 saturation function
47  def sat2(u):
48      L2=np.linalg.norm(u)*np.sqrt(dx)
49      sigma=u
50      if not L2<s0:
51          for ii in range(Nx):
52              sigma[ii]=s0*u[ii]/L2
53      return sigma
54
55  L2norm=[] # L2norm of the sol with sat
56  L2normNoSat=[] # L2norm of the sol without sat
57  ztot=np.zeros((Nx+1,Nt+1)) # to save the solution
58  ztotNoSat=np.zeros((Nx+1,Nt+1)) # to save the solution without
        sat
59
60  ztot[:,0]=z0
61  ztotNoSat[:,0]=z0
62  L2norm.append(np.linalg.norm(ztot[:,0])*np.sqrt(dx))
63  L2normNoSat.append(np.linalg.norm(ztotNoSat[:,0])*np.sqrt(dx))
```

The localized saturation `sat` and the L^2 saturation $\texttt{sat}_{L2}$ are defined after line 37 and line 46 respectively. Between lines 55 and 63 the initialization of the state and of its norm for both the linear control (thus with (102)) and the saturated control (thus with (103) with either the saturation map `sat` or with $\texttt{sat}_{L2}$.

```
65  def discretNoSat(z,dx,dt,a):
66      """
67      discretization of the nonlinear KdV using
68      [Pazoto, et al, Numer. Math., 2010]
69      method without saturation
70      """
71      n=len(z)
72      n1=n-1
73      Dm=1/dx*np.identity(n1)
74      Dp=-Dm
75      for i in range(n1-1):
76          Dp[i,i+1]=-Dp[i,i]
77          Dm[i+1,i]=-Dm[i,i]
78      D=1/2*(Dm+Dp)
79      I=np.identity(n1)
80      A=np.dot(np.dot(Dp,Dp),Dm)+D
81      C=I+dt*A
82      NS=np.zeros((n1,n1))
83      NS[n1-1,n1-1]=C[n1-1,n1-1]
84
```

```
    #Fixed-point method
    NIter = 100 # number of iterations
    J =[]
    J.append(z[:-1])
    tmp=J[-1]
    for k in range(NIter):
        tmp=np.linalg.solve(C-NS,z[:-1]-dt/2*np.dot(D,np.
    multiply(tmp,tmp))-np.dot(dt*a,tmp))
        J.append(tmp)
    return tmp

def discret(z,dx,dt,a):
    """
    discretization of the nonlinear KdV using
    [Pazoto, et al, Numer. Math., 2010]
    method with saturation (select sat or sat2 function)
    """
    n=len(z)
    n1=n-1
    Dm=1/dx*np.identity(n1)
    Dp=-Dm
    for i in range(n1-1):
        Dp[i,i+1]=-Dp[i,i]
        Dm[i+1,i]=-Dm[i,i]
    D=1/2*(Dm+Dp)
    I=np.identity(n1)
    A=np.dot(np.dot(Dp,Dp),Dm)+D
    C=I+dt*A
    NS=np.zeros((n1,n1))
    NS[n1-1,n1-1]=C[n1-1,n1-1]

    #Fixed-point method
    NIter = 100 # number of iterations
    J =[]
    J.append(z[:-1])
    tmp=J[-1]
    for k in range(NIter):
        tmp=np.linalg.solve(C-NS,z[:-1]-dt/2*np.dot(D,np.
    multiply(tmp,tmp))-dt*sat(np.dot(a,tmp)))
        J.append(tmp)
    return tmp
```

To discretize (103) and (102), we follow the approach of,[52] and solve, at each time-step, a fixed point problem. No proof of convergence of the numerical scheme is garanteed in the context of (103), since another non-linearity is considered in.[52] In particular the term z_{xxx} is discretized as follows

$$D_+ D_+ D_- z^i$$

where z^i is the discretized version of z, and where Dp and Dm are the matrices defined by

$$Dp = \frac{1}{dx}\begin{bmatrix} -1 & 1 & 0 & \dots & 0 \\ 0 & -1 & 1 & \dots & 0 \\ \vdots & \ddots & \ddots & \ddots & \vdots \\ 0 & 0 & 0 & \dots & -1 \end{bmatrix} \quad Dm = \frac{1}{dx}\begin{bmatrix} 1 & -1 & 0 & \dots & 0 \\ 0 & 1 & -1 & \dots & 0 \\ \vdots & \ddots & \ddots & \ddots & \vdots \\ 0 & 0 & 0 & \dots & 1 \end{bmatrix}$$

It yields two discretizations, for respectively the equations (102) and (103), between lines 66-93 and lines 95-123 respectively. It asks to solved a fixed point problem that is solved using a iteration scheme wit 100 steps (see after lines 85 and 115). The choice of the saturation map (either `sat` or $\texttt{sat}_{L2}$ is made on line 121). In the python code given here, `sat` is considered.

```
125 # making a loop until t > tfinal
126 while t<tfinal-dt:
127     #Forward Euler step
128     ztotNoSat[:-1,j+1]=discretNoSat(ztotNoSat[:,j],dx,dt,a)
129     ztot[:-1,j+1]=discret(ztot[:,j],dx,dt,a)
130     t+=dt
131     j+=1
132     L2normNoSat.append(np.linalg.norm(ztotNoSat[:,j])*np.sqrt(
        dx))
133     L2norm.append(np.linalg.norm(ztot[:,j])*np.sqrt(dx))
134 
135 # plotting the figures
136 space= np.linspace(0,np.pi,Nx+1)
137 t=np.linspace(0,tfinal,Nt+1)
138 
139 fig , ax= plt.subplots()
140 ax.plot(t,L2normNoSat, label='without saturation')
141 ax.plot(t,L2norm, label='with saturation')
142 ax.set_xlabel('t')
143 ax.set_ylabel('L2 norm')
144 ax.legend()
145 plt.savefig('pde-l2norm.png',bbox_inches='tight')
146 
147 mpl.rcParams['legend.fontsize'] = 10
148 fig = plt.figure(); ax = fig.add_subplot(111, projection='3d')
149 SX, ST = np.meshgrid(space, t)
150 ax.plot_surface(SX, ST, ztotNoSat.T, cmap='jet')
151 ax.set_xlabel('x')
152 ax.set_ylabel('t')
153 ax.set_zlabel('z(t,x)')
154 ax.set_title('Solution without saturation')
155 ax.view_init(elev=15, azim=20) # adjust view so it is easy to
        see
156 plt.savefig('pde-3dNoSat.png')
```

```
157
158 mpl.rcParams['legend.fontsize'] = 10
159 fig = plt.figure(); ax = fig.add_subplot(111, projection='3d')
160 ax.plot_surface(SX, ST, ztot.T, cmap='jet')
161 ax.set_xlabel('x')
162 ax.set_ylabel('t')
163 ax.set_zlabel('z(t,x)')
164 ax.set_title('Solution with saturation')
165 ax.view_init(elev=15, azim=20) # adjust view so it is easy to
        see
166 plt.savefig('pde-3d.png')
```

The discretization in time is done after line 125, where an Euler scheme is used. The figures are drawn after line 135. It yields Figures 7 and 7 where the time-evolutions of the solutions to (103) and to (102) are respectively given. It is observed that the solutions converge to the origin, as predicted in Theorem 17 and the second item of Theorem 15.

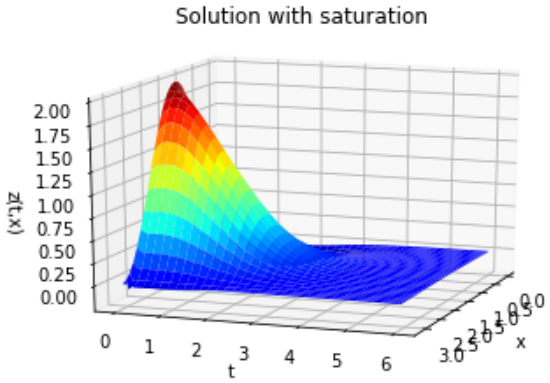

Fig. 10. Solution to (103) with the saturation map `sat`

On Figure 7 the corresponding L^2 norms are compared where it is checked that, as expected, the L^2 norm decreases faster along the solution to (102) than along the solution to (103) with the chosen initial condition.

Selecting the saturaton map $\texttt{sat}_{L2}$ give the Figures 7 and 7 with analoguous conclusions on the time-evolution of the solution to (103) and on

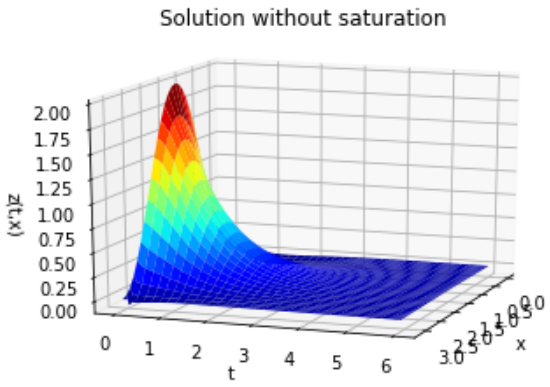

Fig. 11. Solution to (102)

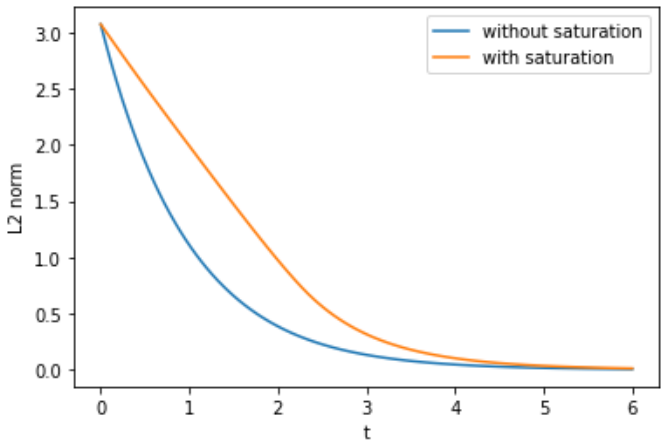

Fig. 12. Comparison of the time-evolutions of the L^2 of the solutions to (103), with the saturation map `sat`, and to (102)

the L^2 norm.

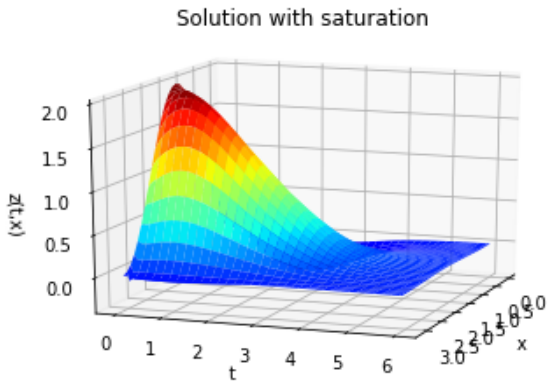

Fig. 13. Solution to (103) with the saturation map $\texttt{sat}_{L2}$

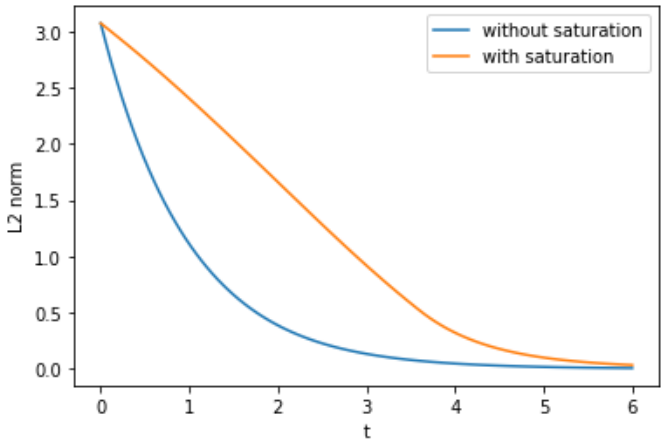

Fig. 14. Comparison of the time-evolutions of the L^2 of the solutions to (103), with the saturation map $\texttt{sat}_{L2}$, and to (102)

4.3. *Conclusion so far*

In this section we have reviewed the well-posedness and the asymptotic stability of the origin of the wave equation and of the Korteweg–de-Vries equation in presence of (possibly saturating) control. Different proofs have

been provided for the attractivity, using either direct Lyapunov method or a LaSalle invariance principle or a contradiction argument.

Let us emphasize that the approaches presented in this section are also useful for certain other classes of equations such as hyperbolic systems. See[5] for the stabilization of linear and quasilinear hyperbolic systems. See also[64] for the stabilization of hyperbolic systems using saturated control.

In[46] an output feedback control has been computed for the linearized KdV equation. It would be relevant to evaluate the impact of the saturation map on the obtained result.

Finally, in addition to the stabilization control problem, the impact of disturbances could be studied. It would be relevant to obtain Input-to-State Stability results in the context of this section (see[28,47] for introductory presentations on this subject for infinite-dimensional systems.)

5. Conclusion

This chapter has reviewed some recent results on stability analysis of distributed parameter systems as those modeled by parabolic partial differential equations, or the wave equation or the Korteweg-de-Vries equation. The suggested approach succeeds to design boundary stabilizing controllers, possibly subject to amplitude constraint, ensuring an asymptotic stability of the closed-loop equation. The constructive approach is based on Lyapunov function, and numerically tractable conditions. Some simulations have illustrated our results and design methods. More recent works follow the present chapter as the control of reaction-diffusion equation coupled with ordinary differential equations (see[35]), or control of such partial differential equation by means of delayed control (see[42]) to cite just a few. As far as hyperbolic system are considered, nonlinear controllers could be also designed as done in.[56,72] Finally, let us cite the papers[36,37] dealing with regulation problems, that could be seen as generalizations of stabilization problems for both the parabolic equations and the wave equation.

References

1. Panos J Antsaklis and Anthony N Michel. *Linear systems*. Springer Science & Business Media, 2006.
2. Andrea Bacciotti and Lionel Rosier. *Liapunov functions and stability in control theory*. Springer Science & Business Media, 2005.
3. Mark J Balas. Finite-dimensional controllers for linear distributed parameter systems: exponential stability using residual mode filters. *Journal of Mathematical Analysis and Applications*, 133(2):283–296, 1988.
4. V. Barbu. *Nonlinear semigroups and differential equations in Banach spaces*. Editura Academiei, 1976.
5. G. Bastin and J.-M. Coron. *Stability and Boundary Stabilization of 1-D Hyperbolic Systems*, volume 88 of *Progress in Nonlinear Differential Equations and Their Applications*. Springer, 2016.
6. S. P. Boyd, L. El Ghaoui, E. Feron, and V. Balakrishnan. *Linear matrix inequalities in system and control theory*, volume 15. SIAM, 1994.
7. Franck Boyer. Controllability of linear parabolic equations and systems. Technical Report hal-02470625, Hal, 2020.
8. H. Brezis. *Opérateurs maximaux monotones et semi-groupes de contractions dans les espaces de Hilbert*. North-Holland, 1973.
9. E. Cerpa. Control of a Korteweg-de Vries equation: a tutorial. *Math. Control Relat. Fields*, 4(1):45–99, 2014.
10. Eduardo Cerpa. Exact controllability of a nonlinear korteweg–de vries equation on a critical spatial domain. *SIAM Journal on Control and Optimization*, 46(3):877–899, 2007.
11. Eduardo Cerpa and Emmanuelle Crépeau. Boundary controllability for the nonlinear korteweg-de vries equation on any critical domain. *Annales de l'IHP Analyse non linéaire*, 26(2):457–475, 2009.
12. Marianne Chapouly. Global controllability of a nonlinear korteweg–de vries equation. *Communications in Contemporary Mathematics*, 11(3):495–521, 2009.
13. Jixun Chu, Jean-Michel Coron, and Peipei Shang. Asymptotic stability of a nonlinear korteweg–de vries equation with critical lengths. *Journal of Differential Equations*, 259(8):4045–4085, 2015.
14. J.-M. Coron. *Control and Nonlinearity*, volume 136 of *Mathematical Surveys and Monographs*. American Mathematical Society, Providence, RI, 2007.
15. J.-M. Coron and E. Trélat. Global steady-state controllability of one-dimensional semilinear heat equations. *SIAM Journal on Control and Optimization*, 43(2):549–569, 2004.
16. J.-M. Coron and E. Trélat. Global steady-state stabilization and controllability of 1D semilinear wave equations. *Commun. Contemp. Math.*, 8(4):535–567, 2006.
17. R. Curtain and H. Zwart. *Introduction to infinite-dimensional systems theory: a state-space approach*, volume 71. Springer Nature, 2020.
18. Ruth Curtain. Finite-dimensional compensator design for parabolic distributed systems with point sensors and boundary input. *IEEE Transactions*

on Automatic Control, 27(1):98–104, 1982.
19. C.M. Dafermos and M. Slemrod. Asymptotic behavior of nonlinear contraction semigroups. *Journal of Functional Analysis*, 13(1):97–106, 1973.
20. B. d'Andréa Novel, F. Boustany, F. Conrad, and B.P. Rao. Feedback stabilization of a hybrid PDE-ODE system: Application to an overhead crane. *Mathematics of Control, Signals, and Systems*, 7(1):1–22, 1994.
21. Etienne De Klerk. *Aspects of semidefinite programming: interior point algorithms and selected applications*, volume 65. Springer Science & Business Media, 2006.
22. Pascal Gahinet, Arkadi Nemirovski, Alan J Laub, and Mahmoud Chilali. LMI control toolbox. *The Math Works Inc*, 1996.
23. J.M. Gomes da Silva Jr and S. Tarbouriech. Anti-windup design with guaranteed regions of stability: an LMI-based approach. *IEEE Transactions on Automatic Control*, 50(1):106–111, 2005.
24. Wolfgang Hahn. *Stability of motion*, volume 138. Springer, 1967.
25. Christian Harkort and Joachim Deutscher. Finite-dimensional observer-based control of linear distributed parameter systems using cascaded output observers. *International journal of control*, 84(1):107–122, 2011.
26. Joao P Hespanha. *Linear systems theory*. Princeton university press, 2018.
27. F.-L. Huang. Characteristic conditions for exponential stability of linear dynamical systems in Hilbert spaces. *Ann. Differential Equations*, 1(1):43–56, 1985.
28. I. Karafyllis and M. Krstic. *Input-to-State Stability for PDEs*. Communications and Control Engineering. Springer, 2019.
29. Rami Katz and Emilia Fridman. Constructive method for finite-dimensional observer-based control of 1-D parabolic PDEs. *Automatica*, 122:109285, 2020.
30. H.K. Khalil. *Nonlinear Systems*. Prentice-Hall, 3rd edition, 2002.
31. Miroslav Krstic and Andrey Smyshlyaev. *Boundary control of PDEs: A course on backstepping designs*. SIAM, 2008.
32. I. Lasiecka and T.I. Seidman. Strong stability of elastic control systems with dissipative saturating feedback. *Systems & Control Letters*, 48(3-4):243–252, 2003.
33. P. Le Gall, C. Prieur, and L. Rosier. Exact controllability and output feedback stabilization of a bimorph mirror. *ESAIM Proc.*, 25:19–28, 2008.
34. H. Lhachemi and C. Prieur. Local output feedback stabilization of a reaction-diffusion equation with saturated actuation. *Arxiv*, page 2103.16523, 2021.
35. H. Lhachemi and C. Prieur. Stability analysis of reaction-diffusion PDEs coupled at the boundaries with an ODE. *Arxiv*, page 2103.04775, 2021.
36. H. Lhachemi, C. Prieur, and E. Trélat. PI regulation control of a 1-d semilinear wave equation. *SIAM Journal on Control and Optimization*, to appear, 2021.
37. H. Lhachemi, C. Prieur, and E. Trélat. PI regulation of a reaction-diffusion equation with delayed boundary control. *IEEE Transactions on Automatic Control*, 66(4):1573–1587, 2021.
38. Hugo Lhachemi and Christophe Prieur. Boundary output feedback stabilization of reaction-diffusion PDEs with delayed boundary measurement. *arXiv*

preprint arXiv:2106.13637, 2021.
39. Hugo Lhachemi and Christophe Prieur. Global output feedback stabilization of semilinear reaction-diffusion PDEs. *arXiv preprint arXiv:2111.12649*, 2021.
40. Hugo Lhachemi and Christophe Prieur. Nonlinear boundary output feedback stabilization of reaction diffusion PDEs. *arXiv preprint arXiv:2105.08418*, 2021.
41. Hugo Lhachemi and Christophe Prieur. Finite-dimensional observer-based boundary stabilization of reaction–diffusion equations with either a Dirichlet or Neumann boundary measurement. *Automatica*, 135:109955, 2022.
42. Hugo Lhachemi and Christophe Prieur. Predictor-based output feedback stabilization of an input delayed parabolic PDE with boundary measurement. *Automatica*, to appear, 2022.
43. Hugo Lhachemi, Christophe Prieur, and Robert Shorten. An LMI condition for the robustness of constant-delay linear predictor feedback with respect to uncertain time-varying input delays. *Automatica*, 109:108551, 2019.
44. Hugo Lhachemi and Robert Shorten. Boundary output feedback stabilization of state delayed reaction-diffusion pdes. *arXiv preprint arXiv:2105.15056*, 2021.
45. S. Marx, E. Cerpa, C. Prieur, and V. Andrieu. Global stabilization of a Korteweg–De Vries equation with saturating distributed control. *SIAM Journal on Control and Optimization*, 55(3):1452–1480, 2017.
46. Swann Marx and Eduardo Cerpa. Output feedback stabilization of the Korteweg–de Vries equation. *Automatica*, 87:210–217, 2018.
47. A. Mironchenko and C. Prieur. Input-to-state stability of infinite-dimensional systems: recent results and open questions. *SIAM Review*, 62(3):529–614, 2020.
48. Andrii Mironchenko, Christophe Prieur, and Fabian Wirth. Local stabilization of an unstable parabolic equation via saturated controls. *IEEE Transactions on Automatic Control*, 66(5):2162–2176, 2021.
49. I. Miyadera. *Nonlinear Semigroups*. Translations of mathematical monographs. American Mathematical Society, 1992.
50. Yuri V Orlov. Discontinuous unit feedback control of uncertain infinite-dimensional systems. *IEEE Transactions on Automatic Control*, 45(5):834–843, 2000.
51. Yury Orlov. On general properties of eigenvalues and eigenfunctions of a Sturm–Liouville operator: comments on "ISS with respect to boundary disturbances for 1-D parabolic PDEs". *IEEE Transactions on Automatic Control*, 62(11):5970–5973, 2017.
52. Ademir Fernando Pazoto, Mauricio Sepúlveda, and O Vera Villagrán. Uniform stabilization of numerical schemes for the critical generalized korteweg-de vries equation with damping. *Numerische Mathematik*, 116(2):317–356, 2010.
53. A. Pazy. *Semigroups of linear operators and applications to partial differential equations*. Applied mathematical sciences. Springer-Verlag, 1983.
54. G Perla Menzala, Carlos F Vasconcellos, and Enrique Zuazua. Stabilization of

the korteweg-de vries equation with localized damping. *Quarterly of applied Mathematics*, 60(1):111–129, 2002.
55. C. Prieur and J. de Halleux. Stabilization of a 1-D tank containing a fluid modeled by the shallow water equations. *Systems & Control Letters*, 52(3-4):167–178, 2004.
56. C. Prieur, S. Tarbouriech, and J. M. Gomes da Silva Jr. Wave equation with cone-bounded control laws. *IEEE Transactions on Automatic Control*, 61(11):3452–3463, 2016.
57. Christophe Prieur and Emmanuel Trélat. Feedback stabilization of a 1D linear reaction-diffusion equation with delay boundary control. *IEEE Transactions on Automatic Control*, 64(4):1415–1425, 2019.
58. J. Prüss. On the spectrum of C_0-semigroups. *Trans. Amer. Math. Soc.*, 284(2):847–857, 1984.
59. Lionel Rosier. Exact boundary controllability for the korteweg-de vries equation on a bounded domain. *ESAIM: Control, Optimisation and Calculus of Variations*, 2:33–55, 1997.
60. Lionel Rosier and Bing-Yu Zhang. Global stabilization of the generalized Korteweg–de Vries equation posed on a finite domain. *SIAM Journal on Control and Optimization*, 45(3):927–956, 2006.
61. D. L. Russell. Controllability and stabilizability theory for linear partial differential equations: recent progress and open questions. *SIAM Review*, 20(4):639–739, 1978.
62. Yoshiyuki Sakawa. Feedback stabilization of linear diffusion systems. *SIAM Journal on Control and Optimization*, 21(5):667–676, 1983.
63. R. Sepulchre, M. Janković, and P. V. Kokotović. *Constructive nonlinear control*. Communications and Control Engineering Series. Springer-Verlag, Berlin, 1997.
64. Suha Shreim, Francesco Ferrante, and Christophe Prieur. Design of saturated boundary control for hyperbolic systems. In *1st Virtual IFAC World Congress*, Berlin, Germany, 2020.
65. Jacques Simon. Compact sets in the space $l^p(o,t;b)$. *Annali di Matematica pura ed applicata*, 146(1):65–96, 1986.
66. M. Slemrod. Feedback stabilization of a linear control system in Hilbert space with an a priori bounded control. *Mathematics of Control, Signals, and Systems*, 2(3):265–285, 1989.
67. E.D. Sontag, H.J. Sussmann, and Y.D. Yang. A general result on the stabilization of linear systems using bounded controls. *IEEE Trans. Automat. Control*, 39(12):2411–2424, 1994.
68. Shuxia Tang, Jixun Chu, Peipei Shang, and Jean-Michel Coron. Asymptotic stability of a korteweg–de vries equation with a two-dimensional center manifold. *Advances in Nonlinear Analysis*, 7(4):497–515, 2018.
69. Shuxia Tang and Miroslav Krstic. Stabilization of linearized korteweg-de vries systems with anti-diffusion. In *2013 American Control Conference*, pages 3302–3307. IEEE, 2013.
70. S. Tarbouriech, G. Garcia, J.-M. Gomes da Silva Jr, and I. Queinnec. *Stability and Stabilization of Linear Systems with Saturating Actuators*. Springer,

London, 2011.

71. André L Tits and Yaguang Yang. Globally convergent algorithms for robust pole assignment by state feedback. *IEEE Transactions on Automatic Control*, 41(10):1432–1452, 1996.
72. N. Vanspranghe, F. Ferrante, and C. Prieur. Velocity stabilization of a wave equation with a nonlinear dynamic boundary condition. *IEEE Transactions on Automatic Control*, to appear, 2022.
73. W Wonham. On pole assignment in multi-input controllable linear systems. *IEEE Transactions on Automatic Control*, 12(6):660–665, 1967.
74. L. Zaccarian and A.R. Teel. *Modern Anti-windup Synthesis: Control Augmentation for Actuator Saturation*. Princeton Series in Applied Mathematics. Princeton University Press, 2011.
75. Liguo Zhang and Christophe Prieur. Stochastic stability of Markov jump hyperbolic systems with application to traffic flow control. *Automatica*, 86:29–37, 2017.